Filip Marjan Gallob, BSc

Functional assessment of novel molecularly targeted drug combinations in pediatric acute myeloid leukemia (AML)

A study on the effects of novel drug combinations in a 3D, long-term setting *ex vivo*.

MASTER'S THESIS

to achieve the university degree of

Master of Science

Master's degree programme:

Biochemistry and Molecular Biomedicine

submitted to

Graz University of Technology

Supervisor:

Assoz. Prof. Priv.-Doz. Dr.techn, Andreas Prokesch

Medical University of Graz

Co-Supervisor:

Univ.-Doz. Dr. Michael Dworzak (MD)

Vienna, November 2020

AFFIDAVIT

I declare that I have authored this thesis independently, that I have not used other than the declared sources/resources, and that I have explicitly indicated all material which has been quoted either literally or by content from the sources used. The text document uploaded to TUGRAZonline is identical to the present master's thesis.

Date, Signature

Kurzfassung

Die akute myeloische Leukämie (AML) im Kindes- und Jugendalter ist eine seltene Krebserkrankung des hämatopoetischen Systems. Das wesentliche Merkmal der AML ist die unkontrollierte, klonale Vermehrung unreifer myeloischer Vorläuferzellen. Sie umfasst rund 20% aller akuten Leukämien in dieser Altersgruppe und der oft rapide Verlauf führt ohne entsprechende Behandlung binnen weniger Wochen zum Tod. In den vergangenen Jahrzehnten konnten wesentliche Fortschritte in der therapeutischen Behandlung der AML erzielt werden. Durch standardisierte Verfahren in Diagnostik und Kombinationschemotherapie liegt die aktuelle 5-Jahres-Überlebensrate bei 70%. Hingegen erleiden 30% der AML-Patienten einen Krankheitsrückfall mit einer wesentlich schlechteren Prognose. Die hohe Inzidenz an Rezidiven und das beobachtete Stagnieren der Überlebensrate, zeigen, dass Vorteile einer weiteren Intensitätssteigerung der Kombinationschemotherapie nicht zu erwarten sind. Dies unterstreicht die Notwendigkeit für den Einsatz von neuen, individualisierten und zielgerichteten Therapieansätzen. Basierend auf den zugrundeliegenden AML-typischen genetischen Aberrationen wurde bereits eine Vielfalt an potentiellen Angriffspunkten identifiziert, jedoch resultierten diese Erkenntnisse bisher noch nicht in neuen klinischen Interventionen. Folglich ist ein komplementärer, funktioneller Ansatz notwendig, um die Effekte von neuen niedermolekularen Verbindungen auf diese Angriffspunkte zu erforschen. Da Plattformen, welche funktionelle Effekte neuer Substanzen charakterisieren, sich zunehmend auf Kurzzeit- und Hochdurchsatzmethoden beschränken, bleiben sowohl Langzeit- als auch Kombinationseffekte solcher Substanzen weitgehend unerforscht. Ziel dieser Masterarbeit war es, bereits FDA-zugelassene Substanzen zu kombinieren und deren Effekte an primären AML-Zellen in Langzeitkulturen zu untersuchen. Um eine potenzielle klinische Umsetzung synergistisch wirkender Kombinationen zu beschleunigen, wurden sowohl eine Vorauswahl FDA-zugelassenen Substanzen für Kombinationstestungen getroffen, als auch die getesteten Konzentrationsbereiche auf physiologisch erreichbare Konzentrationen beschränkt. Um synergistisch wirkende Kombinationen zu identifizieren, wurden diese vorab an AML-Zelllinien getestet und deren Effizienz durch das Bliss-Independence Model erfasst. Die Kombinationen wurden basierend auf den von ihnen inhibierten Signaltransduktionen ausgewählt. Insgesamt wurden 15 Kombinationen an drei AML-Zelllinien getestet. Basierend auf den vorab festgelegten Kriterien zeigten zwei Kombinationen synergistische Effekte: Dasatinib + Venetoclax und Ruxolitinib + Venetoclax. In parallel laufenden Experimenten wurden Kulturbedingungen untersucht, die ein langfristiges Überleben und Proliferieren von primären AML-Zellen ermöglichen. Hier wurde etabliert, dass 3D-Methylzellulosemedium sich für einen Langzeiteffekt- und phänotyp orientierten Sensitivitätstest für niedermolekulare Verbindungen eignet. Primäre AML-Zellen überlebten im Durschnitt 14 Tage unter den *ex vivo* Bedingungen und konnten teils bis zum Tag 24 expandiert werden. Die 3D-Kulturbedingungen führten in einigen Zellen zu einer aberranten monozytären Teildifferenzierung der Blasten, welche sich jedoch nicht inhibierend auf die proliferativen Eigenschaften der Blasten auswirkte. Zuletzt wurde die in AML-Zelllinien etablierte Medikamentenkombination Ruxolitinib + Venetoclax an vier primären AML-Proben getestet. Obwohl ein heterogener Effekt zu beobachten war, zeigte die Kombination im Durschnitt eine stärkere antiproliferative Wirkung als ein einfacher additiver Effekt der einzelnen Komponenten. Zusammenfassend betrachtet, konnte im Rahmen dieser Masterarbeit ein Langzeitkultursystem etabliert werden, welches sich für die Feststellung multipler Medikamentsensitivitätsparameter über einen therapierelevanten Zeitraum eignet. Basierend auf solch einem System könnten in Zukunft die Empfindlichkeiten leukämiescher Blasten festgestellt werden und somit Therapierelevante Entscheidungen beeinflussen.

Abstract

Pediatric acute myeloid leukemia (AML) is a rare hematopoietic cancer that accounts for about 20% of pediatric acute leukemias. It is characterized by the clonal expansion of myeloid precursor cells and without treatment, the disease leads to a fatal outcome within weeks. In the past decades refinements in standard chemotherapy have yielded immense improvements regarding disease outcome and current 5-year survival rates have plateaued at 70%. However, 25 to 35% of patients relapse with a considerable worse prognosis and the need for a more targeted approach has become apparent. So far, several targetable genetic aberrations have been identified but the lack of progress in AML therapy based on these insights has only underscored that in addition to genetic data a functional approach is needed. Since most functional drug discovery programs in this field are focused on short-term high throughput single drug screens there is a lack of understanding for non-immediate cytotoxic effects as well as for effects of drug combinations. Therefore, this thesis aimed to identify drug combinations of promising FDA-approved drugs and study their effects on primary AML cells *ex vivo* in a long-term setup using a functional approach. To that end, we first screened AML cell lines for susceptibility to combinations from a preselection of agents and quantified synergistic effects by using the bliss-independence model. To maximize clinical translation, we only used FDA approved drugs in concentrations not surpassing their respective C_{max}. In total, we tested 15 different combinations that were chosen based on the non-interaction of the targeted pathways. The two combinations displaying the strongest synergistic effect by our metrics were Dasatinib + Venetoclax and Ruxolitinib + Venetoclax. In parallel we assessed culturing conditions for long-term survival of primary AML cells *ex vivo* so we could establish a long-term, functional, phenotype-driven drug sensitivity assay. We established that 3D methylcellulose medium was superior to the corresponding 2D suspension culture model in supporting *ex vivo* maintenance and expansion of primary AML cells. The average time that primary AML cells survived in culture was 14 days and culturing conditions supported cellular survival and proliferation up to 24 days. We observed that 3D culturing conditions triggered changes in immunophenotype of AML blasts after long-term culturing. Although the changes in immunophenotype indicated a partial monocyctic differentiation, the immunophenotype was aberrant and cells did not stop proliferating. Finally, we assessed the effectiveness of the drug combination Ruxolitinib + Venetoclax in four different patient samples. Although the effect of single agent and combination treatment on AML cells varied across patients, on average the effect on total cell number and live cell number suggests a stronger response than a simple additive effect. We demonstrate that our long-time screening assay with multi parameter readouts can be used to assess vulnerabilities of leukemic cells and may help guiding clinical decision making in the future.

Acknowledgments

I would first like to thank Univ.- Doz. Dr. Michael Dworzak (MD) for giving me the opportunity to work on my master thesis at the CCRI under his supervision. His enthusiasm and commitment proved to be a valuable source of inspiration. Especially his active encouragements and input regarding the clinical aspects of this thesis were a great help throughout. In this regard, I would also like to thank Angela Schumich and Susanne Suhendra MSc, who were always generous with their time when it came to sharing their knowledge and expertise regarding the applied aspects of this thesis. I am also especially thankful to Margarita Maurer-Granofszky PhD. Throughout my time at the CCRI, Margarita has provided me with invaluable support and mentorship while always respecting my knowledge in this field. I also appreciate greatly her trust, patience and calm when handling my naïve questions.

To my supervisor at the Medical University of Graz Assoz. Prof. Priv.-Doz Dr. Andreas Prokesch, thank you for the straightforward supervision of this thesis. The provided input and fast corrections were incredibly helpful.

To Mami, Atek, Lara, Lena and Pepca, your unconditional support and encouragements made a big difference throughout my time as a student. Hvala vam za podporo in potrplenje. Lo apprezzo davvero.

Since finishing a master´s degree can be a tedious affair, I greatly appreciate the help and moral assistance provided by Franz Kuchler, Jakob Prömer and Astrid Radkohl, who know exactly how obscure this process can be. Your empathy, humor and readily provided distractions are greatly appreciated

Last, but certainly not least, I would like to thank Katarina Stefaner. I struggle to put into words not only my gratitude for your academic and professional support but also for the endless stream of encouragements and the “occasional” kicks I needed to be prompted into action. Your exemplary academic commitment and special brand of pragmatism continue to be a catalyst for my own progress.

Table of Contents

1. Introduction 1

1.1. Cancer 1

1.2. Precision cancer medicine and anti-cancer drugs 2

1.2.1. Small Molecule Inhibitors in cancer therapy 3

1.2.2. Drug combinations 4

1.3. Clinical aspects and molecular landscape of pediatric AML 7

1.3.1. Molecular landscape of pediatric AML 8

1.3.2. Diagnosis and Classification of pediatric AML 9

1.3.3. Risk stratification and prognostic factors 13

1.3.4. Current treatment and outcome 15

1.3.5. Targeted therapy in pediatric AML using SMIs 16

2. Hypothesis and aims 17

2.1. Hypothesis 17

2.2. Aims 18

3. Methods 19

3.1. Assessment of current drug application in literature 19

3.1.1. Devising single drug catalog 19

3.1.2. Assessment of drug combination potential 19

3.2. Cell line experiments and cell culture assays 20

3.2.1. Thawing and freezing procedure 20

3.2.2. Mycoplasma test 21

3.2.3. Apoptosis assay and cell number 21

3.2.4. Cell cycle distribution 22

3.2.5. Single-drug dose-response assay 23

3.2.6. Cross-validation of dose response data with PharmacoDB dataset 24

3.2.7. Drug combination testing on cell lines 25

3.3. Primary cells experiments 26

3.3.1. Determination of culture conditions that support long-term survival of primary AML blasts 26

3.3.2. Patient samples and preparation of AML cells 27

3.3.3. Cell sorting of primary AML cells 28

3.3.4. Comparison of 2D versus 3D culture conditions 28

4. Materials 31
4.1. Solutions and Media 31
4.2. Lab equipment 32
4.3. Antibodies 33
4.4. Cytokines 34
4.5. Inhibitors 35
4.6. Cell lines and primary cells 36
4.7. Patient Samples 36
5. Results 37
5.1. Assessment of current drug application in literature 37
5.1.1. Catalogue of selected single agents 37
5.1.2. Assessment of drug combination potential 38
5.2. Efficacy assessment of single drugs and drug combinations on cell lines 39
5.2.1. Single agent IC_{50} assessment on cell lines 39
5.2.2. Cross-validation of dose response data with PharmacoDB dataset 40
5.2.3. Drug combination testing using AML cell lines 42
5.2.4. Further analysis of drug combinations on HL-60 cell line 44
5.3. Primary cells 47
5.3.1. Primary cells and sorting data 48
5.3.2. Long-term cell cultures of primary AML cells in 2D and 3D conditions 50
5.3.3. Effects of long-term culturing conditions on the immunophenotype of primary AML cells 52
5.3.4. Impact of lowering GM-CSF concentrations in sample P4 55
5.3.5. Validation of drug combination on primary cells 56
6. Summary of experiments and results 61
7. Discussion 63
7.1. Identifying drug combinations based on nonoverlapping of targeted pathways 63
7.2. Long-term cell culture of primary AML cells 65
7.3. Drug combinations in primary cells 67
8. Conclusion and outlook 69
9. References 72

List of tables

Table 1: FAB classification. Modified from [31,64]. 11
Table 2: Risk stratification of pediatric AML. 14
Table 3: Cytokine concentration for primary cells. 29
Table 4: Duraclone^{Tm} LAIP-tube flow cytometry panel. 30
Table 5: Solutions and Media. 31
Table 6: Lab equipment. 32
Table 7: Antibodies. 33
Table 8: Cytokines. 34
Table 9: Inhibitors. 35
Table 10: Cell lines. 36
Table 11: Patient Samples. 36
Table 12: SMI´s selected for single drug- and combination testing. Main targets are kept in bold characters. 37
Table 13: IC_{50} values determined through dose-response assay. 40
Table 14: Location parameters of deviation from bliss values across AML cell lines. 43
Table 15: Sorting data of primary cells and LAIP drop-ins 49
Table 16: Long term survival and expansion of primary AML cells in 3D culturing conditions. 52

Table of figures

Figure 1: Precision cancer medicine. 3
Figure 2: Mechanisms of drug resistance. 5
Figure 3: Heterogeneity of pediatric AML. 7
Figure 4: FACS apoptosis and cell cycle analysis. 22
Figure 5: Flowchart of dose-response analysis and drug combination testing. 24
Figure 6: Drug dilution scheme for combination testing. 25
Figure 7: Flowchart of primary cell experiments. 27
Figure 8: Heuristic combination matrix. 38
Figure 9: Cross-validation of dose response curves with PharmacoDB dataset. 41
Figure 10: Combinations tested on cell lines. 42
Figure 11: Heatmap of drug combinations. 43
Figure 12: Heatmap of cumulative bliss data. 44
Figure 13: Effects of Venetoclax and Dasatinib on HL-60 cell line. 45
Figure 14: Effects of Venetoclax and Ruxolitinib on HL-60 cell line. 46
Figure 15: Comparison of 2D versus 3D culturing conditions of samples P1, P2 and P3. 51
Figure 16: Immunophenotype tracking in long-term cell culture in sample P4. 53
Figure 17: Immunophenotype tracking in long-term cell culture in sample P5. 54
Figure 18: Reduction of GM-CSF in long-term cell cultures of primary cells in sample P4. 56
Figure 19: Cell number and cell viability of P5 when treated with Ruxolitinib + Venetoclax after 17 days. 57
Figure 20: Cell number and cell viability of P8 when treated with Ruxolitinib + Venetoclax after day 7 and 14. 58
Figure 21: Cell number and cell viability of sample P9 and P10 on day 9 after combination treatment. 59
Figure 22: Sensitivity of patient samples P8, P9 and P10 to Ruxolitinib and Venetoclax combination treatment. 60
Figure 23: Hypothetical synergy dynamics. 64

List of Abbreviations

Abbreviation	Description
.csv	Comma Separated Value (file type)
AB	Antibody
ABB	Annexin Binding Buffer
ALL	Acute Lymphoblastic Leukemia
AML	Acute Myeloid Leukemia
APL	Acute Promyelocytic Leukemia
ARA-C	Cytarabine
AUC	Area Under the Curve
AYA	Adolescents and Young Adults
BCL-2	B-Cell Lymphoma 2
BH-3	B-Cell Lymphoma 2 Homology 3
BM	Bone Marrow
CD	Cluster of Differentiation
C_{max}	Maximum Serum Concentration
CML	Chronic Myeloid Leukemia
CNS	Central Nervous System
CR	Complete Remission
DMSO	Dimethyl Sulfoxide
EFS	Event Free Survival
F	Female
FAB	French American British
FCM	Multicolor Flow Cytometry
FCS	Fetal Calf Serun
FDA	Food and Drug Administration
FISH	Fluorescence In Situ Hybridization
FLT-3	FMS like Like Tyrosine kinase 3
FSC	Forward Scatter
HR	High Risk
HSCT	Hematopoietic Stem Cell Transplantation
IMDM	Iscove Modified Dulbeccos Media
IR	Intermediate Risk
LAIP	Leukemia Associated Pheotype

LR	Low Risk
M	Male
MB	Mega Base
MDF	Multiparameter Flow Cytometry
MNC	Mononuclear Cells
MRD	Minimal Residual Disease
NK	Normal Karyotype
NOS	Not Otherwise Specified
OS	Overall Survival
PB	Peripheral Blood
PB	Peripheral Blood
PBS	Phosphate Buffered Saline
PDB	*PharmacoDB*
PPI	Protein-Protein Interaction
RPMI	Roswell Park Memorial Institute
RT-PCR	Real Time Polymerase Chain Reaction
SCT	Stem Cell Transplantation
SD	Standard Deviation
SMI	Small Molecule Inhibitor
SSC	Side Scatter
STAT	Signal Transducer and Activator of Transcription protein
TARGET	Therapeutically Applicable Research to Generate Effective Treatments
TK	Tyrosine Kinase
TKI	Tyrosine Kinase Inhibitor
WBC	White Blood Cell Count
WHO	World Health Organization

1. Introduction

1.1. Cancer

The global incidence of cancer has been documented to have risen to 18.1 million cases in 2018, causing 9.6 million deaths worldwide[1,2]. Moreover, cancer incidence is estimated to increase over 50% in the coming decades and is projected to establish itself as the leading cause of death in humans[3,4].

The term ´Cancer´ refers to a wide variety of heterogeneous malignancies, the underlying cause of which is the uncontrolled, autonomous proliferation and clonal expansion of distinct cells in an organism. It results from the acquisition of somatic genetic alterations. The abnormal growth patterns caused by recurrent driver oncogene and/or tumor suppressor gene mutations are the product of an incremental process, involving multiple aberrations in cellular pathways accumulating over time. On average, genomes of human cancer cells harbor 30-60 mutations influencing protein interactions[5]. The emergence of the cancer cell follows the acquisition a variety of hallmark capabilities including but not limited to: resisting cell death, deregulation of cellular energetics, sustaining proliferative signaling, evading growth suppression, avoiding immune destruction, tumor-promoting inflammation, activating invasion and metastasis, enabling replicative immortality, genome instability and mutation, inducing angiogenesis[6]. There is no single underlying master regulator of theses cellular processes. Instead, the complex interplay of underlying genetic heterogeneity and distinct tumor microenvironments enables the emergence and maintenance of the neoplastic state.

Only a small portion of diagnosed cases annually occur in children from infancy to age 14, around 300,000 cases per year globally. Several cancer types found throughout the pediatric population also display prevalence in adolescents and young adults (AYA). These however, display different biological and clinical characteristics[7]. Types of cancers occurring in that age group can be broadly classified into leukemias, brain-tumors and non-central nervous system (CNS) solid tumors[8,9].

Since genetic changes largely facilitate carcinogenesis, efforts in genomic analyses by sequencing have elucidated clinically relevant subtypes of pediatric cancers. One key insight is, that the mutational burden in pediatric cancers is considerably lower when compared to

adult cancers, with the exception of germline mutations affecting DNA damage repair[5,8,10]. This however, should not convey the notion of reduced disease complexity.

1.2. Precision cancer medicine and anti-cancer drugs

Precision cancer medicine has been defined as the process of matching a specific therapy with a particular subtype of any cancer. In an ideal scenario, this approach would yield an ideal and specific treatment option for every cancer subtype, with superior benefits in regard to toxicity and outcome[11].

So far, this effort has been largely based on genetic insights, producing therapeutic improvements with varying degrees of success in terms of specificity. A stellar example of moving from identified aberration in a cancer subtype to a matching therapy, is the development of the tyrosine kinase inhibitor (TKI) Imatinib for the treatment of chronic myeloid leukemia (CML) patients carrying the t(9;22) translocation[12].

However, the relationship between the identification of a genetic predictive biomarker and a cancer specific vulnerability is not a linear one, i.e. a somatic mutation present does not constitute a somatic vulnerability[11,13]. The advent of massive parallel sequencing has illuminated the enormous heterogeneity of mutations occurring in tumors[14]. Efforts have shown that, so far, only a small number of canonical driver mutations have been therapeutically addressed. The majority of cancers meanwhile, display a more complex pattern of genetic aberrations and are thus increasingly difficult to match to a single type of treatment[11,14,15].

Hence, it has been recognized that in addition to genomic data a functional component is needed to augment the notion of precision cancer medicine. At the core of functional testing, is the principle of assessing the response of a tumor cell to an exogenous perturbation. Evaluating outcomes in a simple system allows for the prediction of outcomes when initial conditions are known (e.g. a specific cancer geno- or phenotype). Thus, there is the possibility to retrospectively assign sensitivities of a cancer cell to a specific chemical and by comparing them to normal cells cancer vulnerabilities might become apparent[11,16].

Historically, functional screenings managed to produce immediate and valuable results without the elucidation of underlying molecular mechanisms and pathways. This, however, still dramatically improved existing therapies for a variety of cancers. Molecular mechanisms in curative regimens for acute lymphoblastic leukemia (ALL), acute promyelocytic leukemia

(APL) and testicular cancer for instance remained little-known, while the benefit of these therapies was undisputable[11,16–18]. This clearly demonstrates, that the term precision cancer medicine as understood at the time of writing, will be a highly interdisciplinary challenge with necessary contributions from multi-omics platforms, functional platforms and clinical experiences to augment the shortcomings of the individual disciplines (see Figure 1).

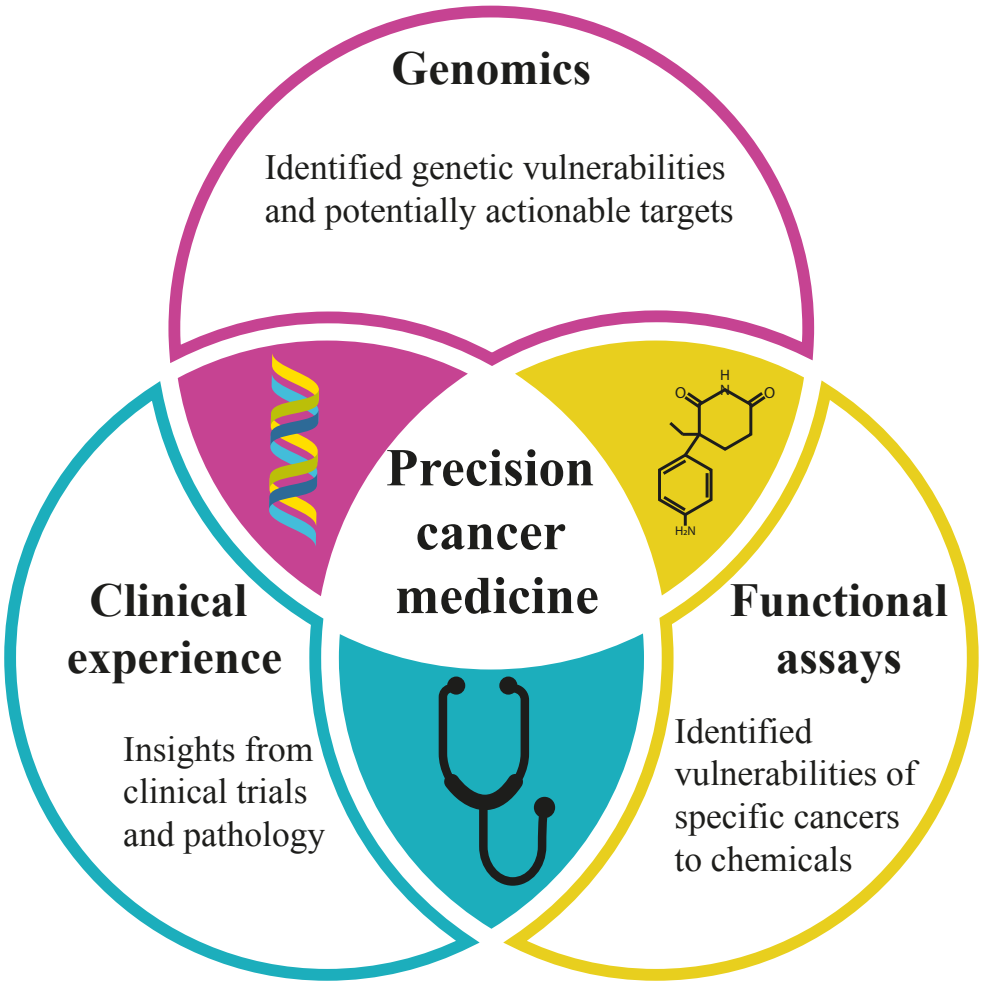

Figure 1: Precision cancer medicine.

Integrative analysis across multiple scientific disciplines will be required to rationally determine novel and effective therapeutic regimens that specifically target unique vulnerabilities of a cancer cell and/or patient. The current cancer models therefore, need to augment their genomic data with clinical experiences, data from functional platforms as well as with data from multi-omics studies.

1.2.1. Small Molecule Inhibitors in cancer therapy

Due to the early recognition of the crucial role TKI play in cancer therapy and oncology, current research is heavily invested in their therapeutic indication among a wide variety of cancers[19,20]. After the initial success of Imatinib (Gleevac®, Novartis) as the first TKI with Food and Drug Administration (FDA) approval in 2001, the number of FDA approved TKI surged, with currently

52 therapeutics targeting around 20 different protein kinases[21]. A minimum of 21 TKIs are multi kinase inhibitors, which endows them with therapeutic flexibility when considering drug combinations but this can also be considered a potential drawback when considering off-target effects. Based on the crucial functions of tyrosine kinases (TK) in cellular activities, an increase in TKI identification and subsequent indication during therapies can be expected. This argument is augmented by the notion, that 244 protein kinases have been mapped to cancer related amplicons[22].

Even though advantages and versatility of TKI have been recognized, the vast majority of the protein kinase superfamily remains underrepresented in cancer research[22]. Furthermore, TKI are considered part of the small molecule inhibitor (SMI) family, which extends beyond KI and also includes molecules targeting protein-protein interactions (PPI)[23,24]. Theses have been more difficult to identify, because of the more complicated way they interact with their target[25]. So far, the FDA has approved one single drug targeting PPIs in cancer treatment.

Of particular relevance for hematopoietic cancers is the absence of a SMI specifically targeting the different members of the *signal transducer and activator of transcription protein* (STAT) family in the current FDA lineup[21]. Aberrancies in this pathway have shown to be a prominent feature in many hematopoietic cancers[21,26–28]. SMIs are utilized more and more in the treatment of AML and cancer therapy. Either they are used complementary to standard chemotherapy regimens or even as single treatment in particular cases[29,30]. Especially in elderly patients afflicted with AML, disease outcome is often affected negatively by the fact, that they are unable to receive intensive chemotherapy[31,32]. The current scope of agents in AML includes but is not limited to: Epigenetic modifiers such as IDH inhibitors, BET inhibitors, HDAC inhibitors, LSD1 inhibitors and DOTL Inhibitors; Cell cycle and signaling inhibitors such as CDK inhibitors, Plk inhibititors, Wee1 inhibitors, MDM2 inhibitors, Aurora kinase inhibitors, Hedgehog pathway inhibitors; Other agents such as *B-cell lymphoma 2* (BCL-2) *Homology* (BH-3) mimetics, Neddylation inhibitors, Aminopeptidase inhibitors[33–35].

1.2.2. Drug combinations

Although targeting pathway dysregulations by SMIs is emerging as a promising new treatment option, responses vary among patients and development of drug resistance is not uncommon. In part, this can be attributed to initial disease heterogeneity among patients, rescue signaling from the tumor microenvironment, as well as selection for genetically heterogeneous sub-clones during therapy. Resistance to single agents can also be attributed to activation of downstream targets, which renders the upstream inhibition meaningless(see Figure 2)[36].

Despite constant progress in identifying actionable targets, there is increasing evidence that single drug treatment will most likely not suffice to overcome those barriers. Since a plethora of genes and pathways not intrinsically oncogenic are involved in tumor progression and maintenance, rationale drug combinations could act in a synergistic way by expanding their respective range of targets. The potentiating effect of two agents is believed to impact the cancer cell in two major ways: 1) By inhibiting a driver event (e.g. the inhibition of the "driver" *FMS like like tyrosine kinase 3* (FLT-3)) and 2) Increasing oncogenic stress (e.g. Increasing cells susceptibility to apoptotic signals)[33,37]. Other beneficial effects in drug combination treatments are dose and toxicity reduction and increased chances of evading resistance at induction[38]. Essentially there are currently two distinct approaches how drug combinations are used in a clinical setting: 1) combining novel agents with standard-of-care treatment and 2) combining novel agents with each other to generate a distinct response[33,37,39].

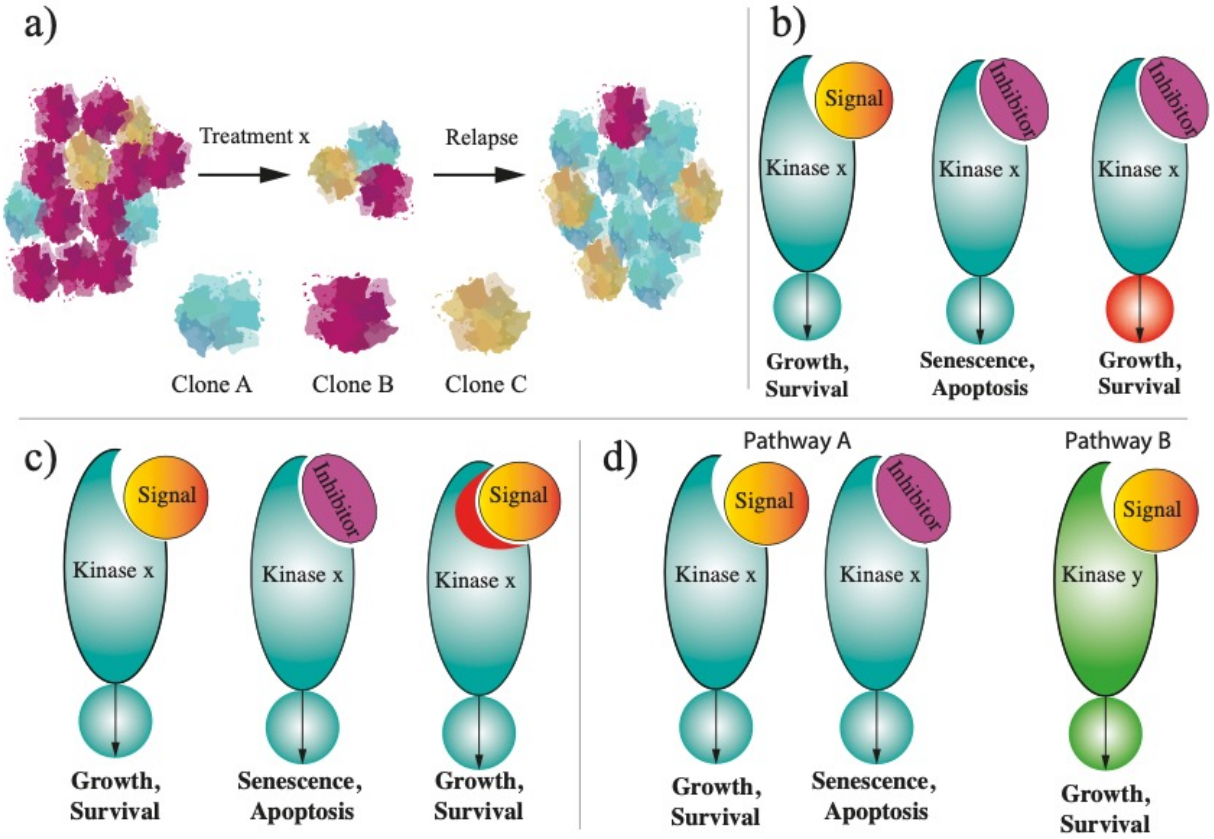

Figure 2: Mechanisms of drug resistance. Modified from[36]

a) Drug resistance can be caused by the selection for a resistant clone present at induction or emerging during treatment. **b)** Mutations in downstream effectors (indicated in red) can reactivate signaling through a pathway despite an effective inhibitor present. **c)** Second-site mutations (indicated in red) can preclude the inhibitor of acting on the target and oncogenic signaling is reinstated. **d)** Oncogenic signaling can be channeled through an alternative pathway (Pathway B) even though the agent is able to inhibit signaling through Pathway A.

The most plausible principle to circumvent the occurrence of resistance is to simultaneously intercept signaling of the "driver" signal (e.g. FLT-3 signaling) as well as a parallel pathway providing an intercellular survival signal. This principle has previously shown to be effective in other cancers[33,40].

The effect of two drugs generating a greater response in targeted cells than a simple addition of their effects, is said to be synergistic. A synergistic relationship of two drugs is often summarized by the illustrative equation*: 1+1=3*. However, the underlying principles are vastly more complex and there is considerable variation amongst definitions of synergism. The common denominator of these definitions is, put simply: Synergism is more than an additive effect and antagonism is less than an additive effect. Eventually a unifying definition has to be declared, since the term is often misused and this could potentially have an impact on FDA approval, patent claims and grant applications[38,39,41].

Quantitative predictions of a combinations synergism extend in clinical models are still limited. Hence, novel combinations are still subject to rigorous scrutiny in preclinical models since this is currently the most effective way to assess their mode of action, which means retrofitting the affected cellular mechanisms to observed impact on biomarkers. However, this effect-based strategy has so far proven to be capable of producing quicker results rather than using a mechanism-based strategy. Also, critical shortcomings in current drug screening efforts include long-term effects of combinations on cells (>72h) and the duration of inhibition are rarely defined clearly. These obstacles clearly underscore the value and potential of functional testing to clinical translation of novel drug combinations[16,39].

One of the most relied upon methods to determine synergism in preclinical setups is the *Bliss Independence model*. In this model, synergy is determined by comparing the observed value of any given combination to a predicted response which implements additivity. The deviation between the prediction and the observed value is interpreted as synergism or antagonism. In this model it is assumed, that there is no effect based on interactions between used agents[38,42,43].

1.3. Clinical aspects and molecular landscape of pediatric AML

AML represents a subcategory of acute leukemias, which in turn is classified as a type of cancer that affects the peripheral blood (PB) and bone marrow (BM). Hallmarks of this disorder include the infiltration of the BM, PB and other extramedullary tissues by clonally expanding leukemic cancer cells, or blasts. Leukemic blasts are a clonally proliferative, abnormally- or undifferentiated group of cells originating in the myeloid system (see Figure 3). The accumulation and enrichment of leukemic blasts results in the displacement and reduced production of other normal hematopoietic cells, which consequently leads to a diminished function and/or failure of said organs[31,44,45]. Without diagnosis or treatment, the disease develops rapidly and leads to a fatal outcome within weeks or months[46].

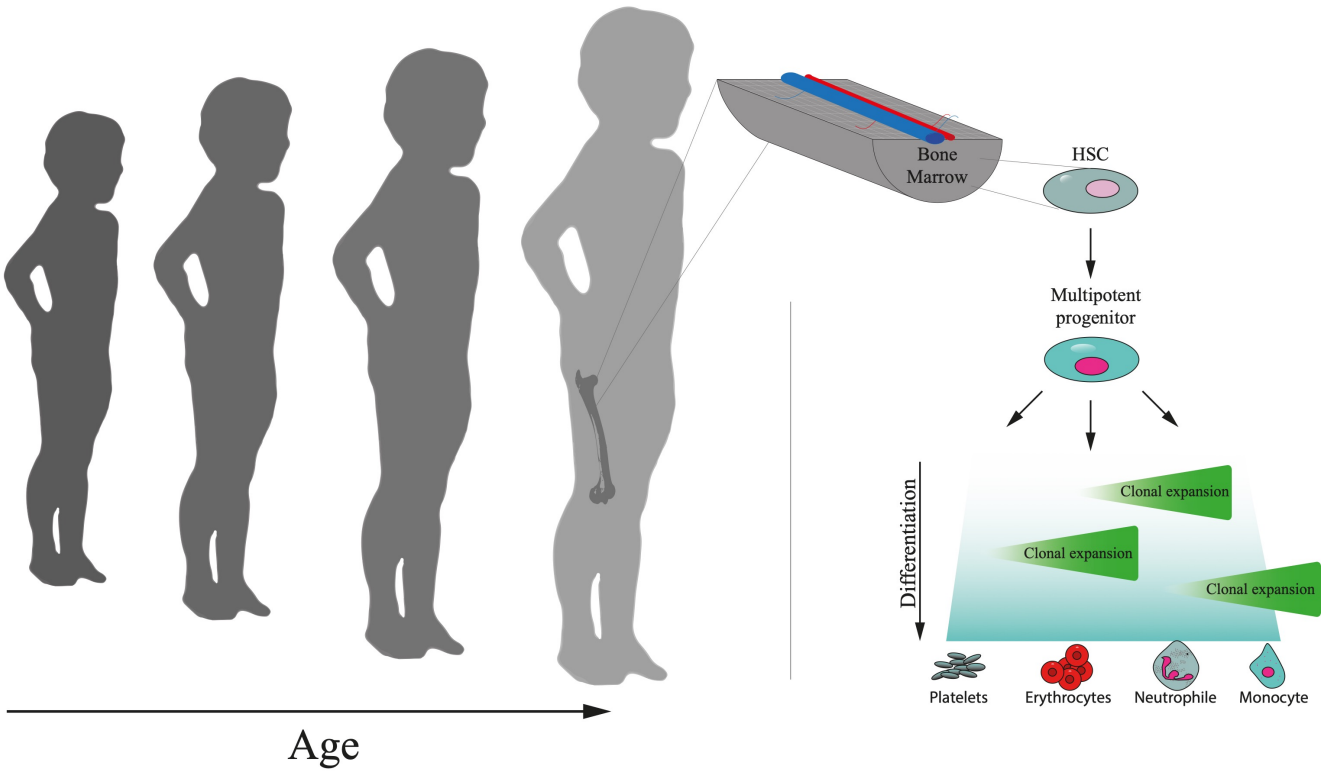

Figure 3: Heterogeneity of pediatric AML.

Heterogeneity of pediatric AML occurs at multiple levels. Underlying is a genetic heterogeneity which so far has shown, that specific genetic aberrations appear more frequently at certain ages, e.g. overall mutational burden increases with age, while fusions and focal copy number aberrations are more common in younger patients. Consequently, there is also phenotypic heterogeneity, which varies considerably between patients.

50 years ago, AML intervention largely consisted of palliative measures and was largely considered incurable. With the advent of modern chemotherapy however, adult AML is now cured in 35 to 40% of patients 60 years of age or younger. Nevertheless, good prognosis plummet with increasing age (>60 yrs.), where outcomes change radically to a median survival of 5 to 10 months and curing rates drop to 5 to 15%[31]. The drastic change in outcome is mainly attributed to the fact that high-dose chemotherapy is not suited for this subgroup of patients, which after all account for over 50% of AML cases in the US alone[47,48].

With a prevalence of 0.7 cases per 100.000 inhabitants younger than 15 years of age, pediatric AML accounts for about 20% of all acute leukemias. The median age of disease onset lies at 6.3 years, with incidence slightly peaking during the first two years of live as well as at 13 years for children <15 years. Pediatric AML affects both genders equally in a ratio close to 1:1[49,50]. The incidence of pediatric AML is substantially lower when compared to adult AML with seemingly better outcomes on long-term survival[51].

Risk adapted high dose chemotherapy promoted 5-year survival rates in pediatric AML to surge and plateau at 70% in the past decade alone[52]. Due to the aggressive nature of the treatment however, high toxicity and the potential of developing a secondary malignancy are common amongst patients. The nuances of pediatric AML therapy remain subject of discussion[31]. Although corresponding clinical trials show areas of consensus, common ground is yet to be found on topics such as number and type of drugs utilized, duration and intensity of treatment as well as indications for hematopoietic stem cell transplantation (HSCT)[55,56].

Ongoing improvements of therapeutic approaches in pediatric AML are facing the major challenge of developing novel compounds, which are targeted at actionable molecular aberrations and are aimed at minimizing toxicity yet maximizing antileukemic effect. Also, innovations in supportive care as well as the improvement of risk stratification and subsequent risk-directed therapy will be crucial in improving disease outcome.

1.3.1. Molecular landscape of pediatric AML

Cytogenetic and molecular heterogeneity of pediatric AML is vast and new subtypes are constantly emerging. Generally speaking, AML development is a gradual process involving at least two genetic aberrations: a type 1 mutation (giving hematopoietic cells a proliferative advantage) and a type 2 mutation (hindering the cells from maturing)[57].

Several studies so far have confirmed and extended observations on unique molecular aspects of this disease. The most extensive and comprehensive study performed on this matter was performed by the Children´s Oncology Group - National Cancer Institute Therapeutically Applicable Research to Generate Effective Treatments (TARGET) AML initiative. It demonstrates that, similar to adult AML it is the result of a small number of cooperatively acting mutations affecting differentiation and self-renewal properties as well as signaling mediators. Also, provided data highlights key genetic lesions occurring preferentially or exclusively in pediatric AML[58–60].

Pediatric AML has a lower somatic mutation frequency than adult AML, with less than one somatic aberration in a protein-coding region per megabase (MB). Overall mutational burden increases with age while cytogenetic aberrations occur less frequent in older patients. Smaller sequence-variations are also a feature of increasing age. Meanwhile, fusion genes and aberrations in focal copy number are a prominent feature in younger age groups. Notably, presence of CBFA2T3-GLIS2, KMT2A and NUP98 fusion events are associated with fewer overall mutations while correlating with inferior outcome. Also, recurrent focal deletions are a uniquely pediatric feature[58–60].

Due to their frequency among afflicted patients the co-occurrences of distinctive alterations bare special clinical significance. For instance, FLT3-ITD accompanied by NPM1 mutations are associated with favorable outcome, while in co-occurrence with WT1 mutations and or NUP98-NSD1fusions the resulting outcomes are adverse[58–60].

Pediatric specific variants and hotspots are also found in cellular signaling molecules. Signaling mediators NRAS and KRAS are unproportionally dysregulated, particularly in patients harboring KMT2A fusions. Other notable signaling aberrations include mutations in receptor tyrosine kinases FLT3 and KIT[58–60].

1.3.2. Diagnosis and Classification of pediatric AML

The immense heterogeneity of pediatric AML poses a challenge to standard diagnostic procedures. A definitive diagnosis therefore has to incorporate multiple factors acquired from a spectrum of diagnostic tests. Initial diagnostic tests can be performed on PB (in case of a sufficient number of blasts) if a BM aspirate is contraindicated due to the patient´s condition. The standard diagnostic procedure is based on data acquired from morphology, cytochemistry, immunophenotyping, karyotyping, fluorescence in situ hybridization (FISH) as well as genetic markers of cells acquired from the BM and PB[51]. Since AML constitutes a liquid cancer,

standard cancer-stage classifications do not apply easily. Instead the outcome for a patient with AML is influenced by factors such as genetic AML subtype, age and other diagnostic data determined at diagnosis[31].

Cytochemistry and immunophenotyping represent the most common tools to distinguish between the most common types of leukemia in children at diagnosis, which are ALL and AML. Based on this initial assessment of the cancers get subdivided in specific subtypes based on genetic and phenotypic data and treatment is assigned accordingly[51]. Still the majority of genetic and chromosomal abnormalities are detected by conventional karyotyping, FISH and additional real time quantitative polymerase chain reaction (RT-PCR). Relevant translocations, fusions, losses or gains of chromosomal material and specific mutations are determined thusly[61].

Based on morphology and their unique molecular signature, AML is classified into different subtypes. Prognosis of different subtypes varies, depending on factors such as age, presence of prior hematological disorders, white blood cell count (WBC) and molecular and genetic aberrations[62]. Historically AML can be classified according to two major systems: the French-American-British (FAB) classification and the classification according to the World Health Organization (WHO), *The WHO Classification of Tumours of Hematopoetic and Lymphoid Tissues.* The FAB classification was founded several decades ago and defined subgroups of AML largely based on morphological and cytochemical characteristics (see Table 1). The objective was to create an objective platform for the diagnosis of AML and to facilitate comparison between cases[63,64]. However, once the importance of cytogenetic data became apparent it was unclear whether the FAB-classification would be able to obtain diagnostic value beyond the information it was based upon.

The mounting cytogenetic evidence of AML´s diversity highlighted the necessity for an updated classification scheme, which would be able to integrate the information provided by genetic studies and fluently adapt to AML´s changing landscape. Guided by a panel of experts, the WHO devised a new classification, which blends genetic, immunophenotypic, clinical and biological information to discriminate between discrete disease entities[45,62,65–67]. Rather than definitely replacing the old FAB system, the WHO classification embedded the FAB classification in the “AML, not otherwise specified (NOS)” category, which consists of non-classifiable cases.

The major advantage of the WHO classification scheme is underpinned by the fact that it is open to revisions. This facilitates the constant integration of scientific and clinical data in new editions, the latest of which was published in 2016. Even though, the WHO classification essentially replaced the FAB scheme, it still is installed in the latest revision. Data on the prognostic value of the FAB relict remains controversial[64,66].

Table 1: FAB classification. Modified from [31,64].

FAB type	Name	Relationship with cytogenetics
M0	minimally differentiated acute myeloblastic leukemia	
M1	acute myeloblastic leukemia, without maturation	
M2	acute myeloblastic leukemia, with granulocytic maturation	t(8;21)(q22;q22), t(6;9)(p23:q34)
M3	promyelocytic, or acute promyelocytic leukemia (APL)	t(15;17)(q22;q21)
M4	acute myelomonocytic leukemia	
M4Eo	myelomonocytic together with bone marrow eosinophilia	inv(16)(p13.1q22) or t(16;16)(q13.1;q22)
M5	acute monoblastic leukemia	MLL-gene rearrangements
M6	acute erythroid leukemias	
M7	acute megakaryoblastic leukemia	t(1;22)(p13;q13)

Acute myeloid leukemia and related neoplasms according to the 2016 updated WHO classification[62,65–67]

AML with recurrent genetic abnormalities

- AML with t(8;21)(q22;q22.1);RUNX1-RUNX1T1
- AML with inv(16)(p13.1q22) or t(16;16)(p13.1;q22);CBFB-MYH11
- APL with PML-RARA
- AML with t(9;11)(p21.3;q23.3);MLLT3-KMT2A
- AML with t(6;9)(p23;q34.1);DEK-NUP214
- AML with inv(3)(q21.3q26.2) or t(3;3)(q21.3;q26.2); GATA2, MECOM
- AML (megakaryoblastic) with t(1;22)(p13.3;q13.3);RBM15-MKL1
- Provisional entity: AML with BCR-ABL1
- AML with mutated NPM1AML with biallelic mutations of CEBPA
- Provisional entity: AML with mutated RUNX1

AML with myelodysplasia-related changes
Therapy-related myeloid neoplasms
AML, NOS

- AML with minimal differentiation
- AML without maturation
- AML with maturation
- Acute myelomonocytic leukemia
- Acute monoblastic/monocytic leukemia
- Pure erythroid leukemia
- Acute megakaryoblastic leukemia
- Acute basophilic leukemia
- Acute panmyelosis with myelofibrosis

Myeloid sarcoma
Myeloid proliferations related to Down syndrome

- Transient abnormal myelopoiesis (TAM)
- Myeloid leukemia associated with Down syndrome

1.3.3. Risk stratification and prognostic factors

Each AML-patient can be classified according to the above-mentioned classification scheme. In turn, each clinically relevant subgroup carries prognostic value and may influence the choice of treatment for the patient. Risk-group stratification in pediatric AML patients is therefore largely based on genetic abnormalities of the leukemic blasts. According to Creutzig et.al., pediatric AML can be divided into three risk groups: Favorable, Intermediate and Adverse (see Table 2). Despite the stratification of patients into low (LR), intermediate (IR) and high risk (HR), their clinical outcome as well as relapse risk vary considerably even within the respective groups[47,68–70]. In addition to cytogenetic and molecular genetic aberrations at diagnosis, assessment of therapy response via monitoring of minimal residual disease (MRD), by RT-PCR or by multicolor flow cytometry (FCM) during and after therapy has been demonstrated useful for refined identification of AML patients at high risk of relapse by some research groups[71–73].

Table 2: Risk stratification of pediatric AML.

Prognosis	Genetics
Favorable	t(8;21)(q22;q22)/*RUNX1-RUNX1T1* inv(16)(p13.1q22) or t(16;16)(p13.1;q22)/*CBFB-MYH11* t(15;17)(q22;q21)/*PML-RARA* Molecular (in CN-AML) *NPM1-mutated AML* *CEBPA* double mutation t(1;11)(q21;q23)/*KMT2*A-*MLLT11(AF1Q)* *GATA1s*
Intermediate	Cytogenetic aberrations that can´t be classified either as high or low risk
Adverse	-7, -5 or del(5q) inv(3)(q21q26.2) or t(3;3)(q21;q26.2)/*RPN1-MECOM(EVI1-MDS1-EAP)* t(6;9)(p23;q34)/*DEK-NUP214* t(7;12)(q36;p13)/*ETV6(TEL)-HLXB9(MNX1)* t(4;11)(q21;q23)/ *KMT2-MLLT2(AF4)* t(6;11)(q27;q23)/ *KMT2-MLLT4(AF6)* t(5;11)(q35;p15.5)/*NUP98-NSD1* t(10;11)(p12;q23)/ *KMT2-MLLT10(AF10)* 12p/ t(2;12) complex karyotype *WT1*mut/*FLT3*-ITD t(9;22)(q34;q11.2)

The predictive value of MRD measuring has been verified by multiple independent study groups[71,74,75]. Therefore, assessment of both, genetic features at diagnosis and assessment of MRD have become routine for risk stratification of pediatric patients with AML in most clinical trials nowadays and guide clinical decision making [73].

1.3.4. Current treatment and outcome

A high dose polychemotherapy is the current standard first line treatment for pediatric AML. The current treatment model is split into three distinct treatment phases: Induction, consolidation and interim maintenance.

The therapeutic backbone of AML induction therapy is formed by the combination of the cytostatic drugs cytarabine (Ara-C) and anthracyclines. The objective of the induction phase is the extermination of leukemic blasts and the restoration of normal hematopoiesis. While the effectiveness and dosage of Ara-C has been uniformly accepted, there are still ongoing trials to determine the most effective anthracycline and its application[52]. However, idarubicin and liposomal daunorubicin have been identified as promising agents, due to lower toxicity and lower treatment-related mortality and morbidity[76,77].

Generally, two courses of induction therapy are recommended, followed by two (in favorable-risk patients) or three courses of consolidation therapy. A remission is achieved in 2/3 of patients in the 4-6 weeks of induction therapy. Following the second block of therapy, the number of remission increases up to 90%[53,54,78]. Evan if a complete remission is not achieved, a resumption of therapy is recommended. Post-remission therapy also comprises multiple therapy blocks of high-dose chemotherapy, often containing the same antileukemic drugs[79].

A special form of therapy intensification represents the HSCT. The antileukemic effect that is underlying this approach is based on the Graft-versus-leukemia-effect of the transplanted cells[80]. Although relapse incidence is lower than in conventional chemotherapy treated patients, it is difficult to evaluate HSCT benefits. Differences in prior treatment and the high rates of HSCT related morbidity and mortality add to the difficulty of HSCT indication[81,82].

With currently available high-intensity chemotherapy, 5-year overall survival (OS) have stagnated at 60-75%[51]. Meanwhile event free survival (EFS) is still only at 50% and relapse rates are currently at around 25-35%. Relapsed patients have a considerable worse prognosis with 5-year OS around 30%[83]. Since toxicity and mortality of treatment related complications by standard chemotherapy alone are still very high, therapy outcome is unlikely to be boosted by the means of chemotherapy alone.

1.3.5. Targeted therapy in pediatric AML using SMIs

The conspicuous lack of tumor specificity from current treatment options stems mainly from an inadequate understanding of AML biology, thus justifying the continuous usage of chemotherapy. However, at present, the focus of investigation finally has shifted away from developing and refining chemotherapy for curative purposes. A targeted approach, based on actionable molecular aberrations is slowly loosening the therapeutic stagnation of the past decades. Targeted therapy bears the prospect of decreased treatment related morbidity and mortality as well as increased EFS and OS rates. As described previously, inactivation of oncogenic signaling is a viable approach if, however, a driver has been identified. Pediatric AML offers few if any such obvious targets such as the BCR-ABL fusion kinase[12,33,84].

An instructive example is the deployment of FLT3 inhibitors. One type of FLT3 mutations (FLT3-ITD) is prominent in adult and pediatric AML and successes in treatment of adult AML have reinforced the notion that the same inhibitor might be effective in the pediatric form as well. However, the success of the FLT3 inhibitor Midostaurin in adult AML only produced modest results in pediatric AML[85]. In fact, no sooner than second and third generation FLT3 inhibitors like Quizartinib were introduced, targeted therapies started to show improved results in relapsed cases in combination with salvage chemotherapy[86].

However, so far FLT3 inhibitors are the only SMIs used to target a specific genetic subgroup, even though recent studies have extensively added to the list of potential targets[58,84]. More general targets are made available by mutations in the RAS family (HRAS, KRAS, NRAS) which are collectively found in about 30% of cases in pediatric AML[58]. Agents targeted at RAS/MAPK signaling have been investigated in adult AML but their effectiveness has yet to be determined in the pediatric form[87]. In addition, inhibition of the PI3K/AKT/mTOR pathway serves as a potential target and agents have been proven to be tolerable in other pediatric leukemias[88]. In terms of pathway dysregulation there are still several options to explore, such as inhibition of STAT signaling or the Hedgehog pathway[28,89]. Also, due to the outstanding anti-leukemic effect in adult AML, targeting epigenetic regulators such as the BET protein family is considered as an option[84,89].

2. Hypothesis and aims

2.1. Hypothesis

Most current drug testing platforms are focused on high throughput, single drug, screening efforts thereby neglecting the potential of drug combinations (i.e. synergism) as well as effect not inherently linked to immediate cytotoxic effects (e.g. cellular differentiation). Therefore, it is hypothesized that a long-term functional phenotype-driven drug sensitivity assay using novel drug combinations of promising FDA-approved drugs may yield critical insights into potential novel options for targeted therapy.

Pediatric AML is a low incidence malignancy with an enigmatic disease profile. Efforts are being made in deciphering pediatric AML biology, however genetic studies alone have not yet proven to facilitate a change in therapeutic dogma[11,90]. A disease profile has yet to be established, that incorporates data beyond genetic studies. Assessment of actionable functional information by exogenous perturbation of primary cells may offer further insights into disease behavior and spur therapeutic efforts and success[11]. Also, adult AML and pediatric AML should be considered two distinct disease entities. Insights in adult AML should therefore not be extrapolated towards the pediatric form.

Effects of aberrant pathway inhibition by novel SMIs and combinations thereof could provide valuable data concerning drug sensitivity of leukemic blasts. Therefore, it is hypothesized that functional, multi parameter ex vivo drug screens of novel drug combinations, may be offering further insights into drug response profiles of pediatric AML [11,16,33,91]. By testing the efficacy of FDA approved drugs or drugs with pending FDA approval, not yet employed for pediatric AML therapy, potential sensitivities could be identified.

Also, ideal culturing conditions for primary pediatric AML cells are not yet agreed upon, especially for drug screening assays lasting longer than the 72h golden standard to assess the duration of pathway inhibition in future studies. Additionally, established pharmacokinetic and pharmacodynamics (C_{max} and AUC) data of different agents will be considered to maximize clinical translation[92].

2.2. Aims

The main aims are (I) the development of an ex-vivo long-term cell culture model for primary AML cells and (II) to use this model for functional testing of a thoroughly selected set of FDA approved drugs, either alone or in combination.

The specific aims were to:

- Compile a comprehensive catalogue of FDA approved drugs with potential efficacy against pediatric AML
- Compile a catalogue of useful drug combinations of agents in established catalogue, based on current understanding of drug interactions on a molecular level
- Perform drug screens to determine dose-response curves with single drugs on AML cell lines
- Screen potential drug combinations for synergistic effects using AML cell lines
- Assess impact of effective drug combinations on AML cell lines in an upscaled setup
- Establish basic culture conditions for primary AML samples for long-term in vitro survival
- Compare viability of primary AML cells in 2D versus 3D culture conditions
- Make a phenotypical assessment of primary pediatric AML cells after long-term culture
- Assess the effects of established drug combinations on primary AML cells

3. Methods

3.1. Assessment of current drug application in literature

Novel cancer therapy is guided by insights into the genomic landscapes of individual cancer patients and the understanding that the disease is a result of pathway dysregulation [5,58,90]. Inhibition of abnormal pathway activity by SMIs has proven to be an auspicious therapeutic approach and effects of novel SMIs need to be explored. Due to a plethora of agents displaying antineoplastic activity, we assessed clinically relevant drugs interfering with pertinent pathways from literature. In addition, we chose agents on grounds of compatibility in terms of drug combinations.

3.1.1. Devising single drug catalog

Due to the constantly expanding inventory of anti-cancer drugs, a small but comprehensive catalogue of SMIs needed to be devised. The goal was to create a small but thorough catalog fulfilling five major requirements: 1. Compounds should have FDA approval or FDA approval pending 2. It should reflect current trends in leukemia therapy 3. Combination of the single agents should be feasible 4. They should target a variety of different pathways 5. All experiments should be performable in a constricted time frame, thus limiting the number of agents.

Abnormal pathway activity in pediatric AML has been independently established in multiple studies [28,58]. SMIs targeting well established aberrations, such as first and second generation FLT3 inhibitors, were included. Furthermore, common genetic aberrations identified by *Bolouri et.al.* were cross referenced with the actionable-gene-application from the *oncogene* database [93]. Additionally, expert opinions on current clinical practices were taken into account to exclude agents with unfavorable pharmacokinetics, as well as including agents applicable for next generation functional diagnostics [16]. The final selection of drugs included 14 compounds (see Table 12)

3.1.2. Assessment of drug combination potential

Due to the complex nature of pediatric and adult AML it has been proposed that combinations of targeted agents are an effective way to increase antineoplastic effect of current therapies [16,38]. So far, this approach has proven to be effective in a number of different proliferative

malignancies and trials [94,95]. Therefore, we tested a combination of agents targeting nonoverlapping signaling pathways and belonging to different classes of inhibitors using AML cell lines.

We conceived a list of potentially synergistic drug combination, building on the previously established single drug catalogue and the non-interaction premise. To that end, common genetic alterations and pathways in pediatric AML according to the *TARGET* dataset and Bolouri, H., Farrar, J., Triche, T. et al. were cross referenced with open source applications such as *Pathway Commons, The Drug Gene Interaction Database, Vizome* and *ChEMBL* to identify actionable targets [96–98]. Also, to determine nonoverlapping pathways, said applications were used to get a basic view on known and/or suspected interactions. Based on the insights, combinations were deemed feasible if there was published data available (e.g. MDM2 + BCL2), or if there was minimal pathway interaction (e.g. BCL2 + Ruxolitinib). We devised a combination matrix, which visualizes the identified advantageous combinations based on the minimal interaction assumption. We assigned more or less relevance to a combination based on the number of interactions of the cardinal pathway components targeted by a drug, identified by the open source online applications (e.g. the significance of a particular combination pair is exemplified by the color and size of a circle in Figure 8). The combination matrix served as a template to determine which combinations could be omitted based on the minimal interactions assumption.

3.2. Cell line experiments and cell culture assays

Primary cells of pediatric AML patients are a valuable and bounded resource. Therefore we tested SMIs and SMI combinations initially on 3 different AML cell lines before moving to primary cells[11]. Cell lines with leukemia associated genetic aberrations were chosen and obtained in house[99–101]. Cell lines and their respective aberrations are listed in Table 10.

3.2.1. Thawing and freezing procedure

Frozen cell lines were thawed rapidly using a water bath pre-heated to 37°C. Vials were left floating in a rubber rack, till only a small ice clump remained. Next, pre-warmed RPMI containing 10% fetal calf serum (FCS) was pipetted on top of the frozen sample and gently pipetted up and down. The mixture was then immediately transferred into a 15ml falcon tube and filled up to 10ml with RPMI 10% FCS. The cells were then spun down at 300g for 10 min.

Subsequently the medium was discarded and the cells were resuspended in RPMI with the appropriate percentage of FCS, which was 10% FCS for MV4-11, THP-1 and HL-60. The cells were then immediately transferred into appropriate culture flasks and incubated at 37°C and 5% CO_2.

For long time storage, cells were diluted to a concentration of 1-10 x 10^6 cells/ml in RPMI 10% FCS and transferred into cryotubes. *CryoSure-DMSO* was then added according to the manufacturers manual and cells were rapidly transferred into a -80° Mr.Frosty container for long time storage.

3.2.2. Mycoplasma test

To avoid a negative impact on reliability and reproducibility in the cell line experiments, the cultures were tested for mycoplasma contamination. Hence MycoAlert™ Mycoplasma Detection Kit by Lonza was used according to the manufacturers instructions.

3.2.3. Apoptosis assay and cell number

To assess apoptosis, we used a Annexin V/7-AAD staining (see Figure 4). Cells were harvested, counted and washed once with cold phosphate buffered saline (PBS). The cell-pellet was then resuspended in 100 µl 1x Annexin Binding Buffer (ABB) and stained with Annexin V (1 µl per 1-5x10^5 cells) and 7-AAD. Cells were vortexed and incubated for 15 min at room temperature. Afterwards cells were toped up with 400 µl 1x ABB and transferred into Trucount tubes. Trucount tubes were used to determine absolute cell numbers in samples rather than relative frequencies. Trucount tubes contain a known number of fluorescent beads and the acquired number of beads is reflective of the total cell count of acquired cells. Afterwards we acquired samples instantly on a LSRII the flow cytometer (Becton Dickinson) and analyzed the data using BD FACS DiVa ™.

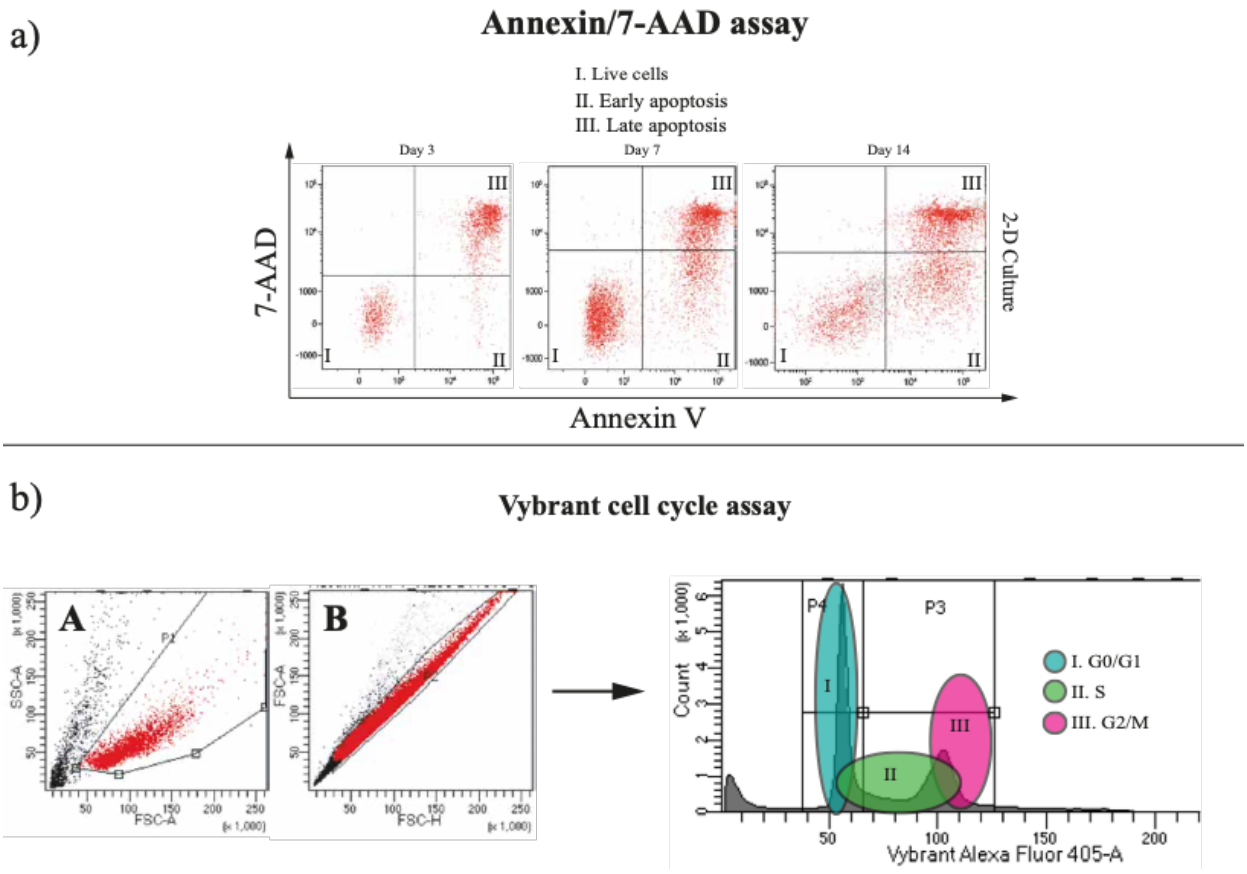

Figure 4: FACS apoptosis and cell cycle analysis.

a) Cells were stained with Annexin/7-AAD, which is used to display dead and apoptotic cells. Cells were then acquired and displayed in a four-chamber dot plot, showing viability of cells (e.g. cells positive for both, Annexin V and 7-AAD are in a late apoptotic state). **b)** Cells were stained with Vybrant cell cycle dye. Dot plots (bottom left) are showing basic gating strategy for removal of debris and gating on singlets. These populations served for the generation of a histogram (bottom right), displaying the distribution of cells across the cell cycle.

3.2.4. Cell cycle distribution

Cell cycle status of cells was determined through flow cytometry, using Vybrant™ DyeCycle™ staining. Cells were harvested, counted, washed once with cold PBS and then diluted to $1x10^6$ cells/mL. 1 mL of cells was than stained with 1 µl Vybrant™ DyeCycle™ to a final concentration of 5 µM. Cells were then incubated at 37°C for 1h and measured immediately after incubation without washing.

3.2.5. Single-drug dose-response assay

To identify drugs and doses suitable for clinical translation, we established IC_{50} values of single compounds through cell line experiments. Generated data on single drug dosage obtained through dose-response curves, was also essential to guide combination testing. We aimed to keep the concentrations of single agents in a combination under their respective C_{max} values, to ensure that these concentrations were of clinical relevance and would be achievable in patients[92,102,103]. Furthermore, we compared results to public available drug screening platforms to confirm accuracy. To that end, we tested compounds using AML cell lines and a 72h drug screen, to determine single-drug efficacy IC_{50} values. Figure 5 provides a graphical abstract of the experiment. SMIs were purchased from *Santa Cruz*, *Selleckchem* and *TargetMol* and reconstituted in dimethyl sulfoxide (DMSO) and stored at -80°C. Aliquots were stored at -20°C.

To generate a dose response curve, we cultured cell lines in RPMI 1640 complemented with 10% FCS. Using a hemocytometer, cell number was determined to confirm that cells were in the exponential growth face before seeding. Afterwards cells were diluted with prewarmed RPMI 1640 and placed into a 96 well plate at a concentration of 5000 cells/well. Every experiment was performed in triplicates. The outermost wells were filled with sterile H_2O to avoid edge effect[104]. 96-well plates were then placed into an incubator at 37°C and 5% CO_2 for 24h. Subsequently, drugs in serial dilutions were added to the cells to a final volume of 200ul. Extra wells for Blank and DMSO controls were considered. The 96-well plate was put on a plate shaker for 5 min and was then transferred back into the incubator for 72h. Cells were then spun down for 5 min at 300g to remove 100 ul of medium. The Cell Titer Glo (*Promega*) assay was performed according to the manufacturers protocols. After cell lysis, the cell lysate was transferred into opaque-walled multiwall plates. Subsequently luminosity was determined by means of a luminometer. The data was exported in .csv file format.

Blank was subtracted from all values using the *Microsoft Excel* software. The data was then imported into *Graphpad Prism 8.* First, concentrations were log transformed before luminometer raw data was normalized, using 0 as 0% and setting 100% to the largest mean in each dataset. Thus, drug response was expressed in %. Subsequently the nonlinear regression function “log(inhibitor) vs. response – Variable slope (four parameters)” with constraints set with 0 for *Bottom* and 100 for T*op* was performed. The resulting graph plotted cell viability data against transformed drug concentration value. The cell line specific IC_{50} values were derived from the respective survival curves. IC_{50} was defined as the concentration at which the measured viability signal was reduced to 50% of the vehicle (DMSO) control[38].

3.2.6. Cross-validation of dose response data with *PharmacoDB* dataset

To validate the dose-response data and the IC_{50} values of SMIs in cell lines, the results were compared to the open source *PharmacoDB* (PDB) dataset. This dataset contains dose-response data for a variety of cell lines and compounds from different laboratories in .csv file format. This permits comparison of different datasets in *Excel* and *Prism Graphpad* across different laboratories.

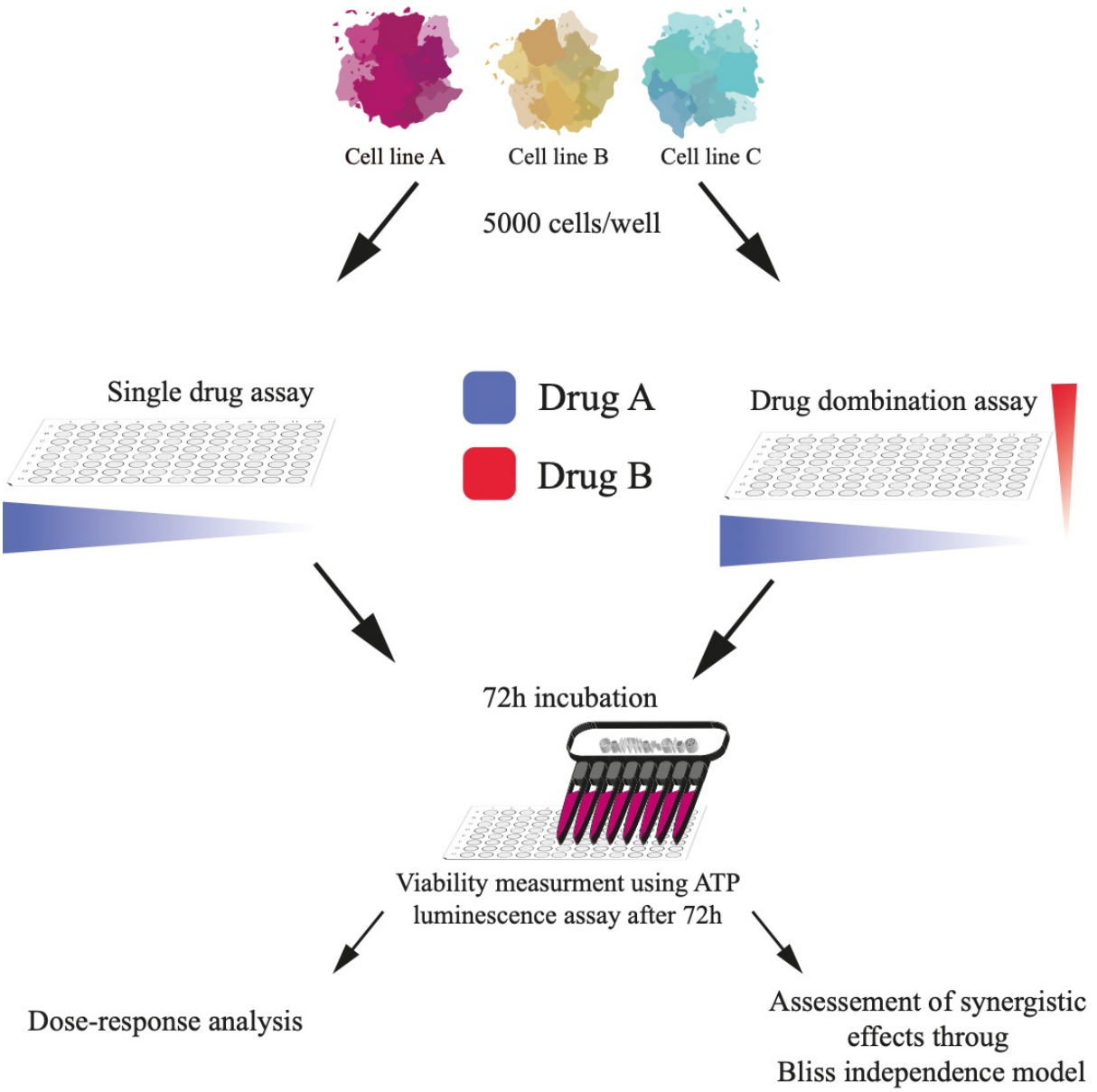

Figure 5: Flowchart of dose-response analysis and drug combination testing.

Single agents and drug combinations were tested on 3 different AML cell lines (HL-60, MV4-11 and THP-1, exemplified by the colored spheroids) with ATP levels (viability surrogate) as readout. Single drug assays and drug combination assays were performed under identical parameters. Drug combination assays were composed to include every permutation of concentrations in a given range.

3.2.7. Drug combination testing on cell lines

Through the constructed combination matrix (see Figure 8), it was determined which combinations were going to be tested in the preclinical model on cell lines. In order to assess the effectiveness of compounds in combination, essentially the same experimental setup as for IC_{50} determination was used. After cell seeding and a 24h incubation period, the individual compounds were dispensed in serial dilutions as well as in combination in a checkerboard fashion to include all possible permutations of the two serially diluted drugs. To identify synergistic or antagonistic effects of combinations, concentrations clustering around the IC_{50} value of the respective compounds were employed, using serial dilutions (log-steps and log-steps of $IC_{50}/2$). The IC_{50} value was calculated from a dose response curve and therefore it is more accurate to consider the IC_{50} value as the representation of a range[105]. The concentration range for every agent always included values under, above and around the IC_{50} value of every agent(see Figure 6)[38,106].

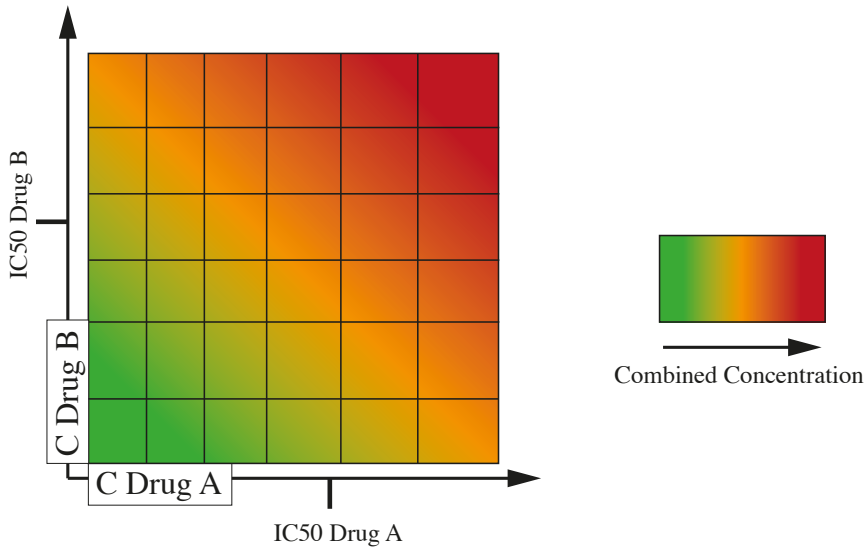

Figure 6: Drug dilution scheme for combination testing.

Compounds were serially diluted and combined in a checkerboard fashion. The concentration ranges included values above and under each drug respective IC_{50} value.

As in the single dose experiments the read out used was viability, detected through ATP levels via the *Cell Titer Glo* assay after a 72h incubation period. To identify a synergistic relationship between compounds, the bliss independence model was implied. To that end the equation $E(x,y) = E(x) + E(y) - E(x) * E(y)$ was used, where E is the effect and x and y the respective doses of the two compounds used in the combination, to determine a predictive value for an additive effect[38,43,107]. The deviation of said predicted value was subsequently determined by

subtracting the predicted value from the actual value. The results were then converted into bar charts for visualization.

Combinations displaying synergistic effects in the bliss independence model, were then tested in an upscaled setup, to further investigate their effects on cellular growth and apoptosis in cell lines. Except for the dish (24-well-plate), starting cell number (25000 cells/ml), and number of concentrations tested, assay conditions stayed identical to the previous combination screens. As readout, total cell number and apoptosis were used.

3.3. Primary cells experiments

To further test established drug combinations on primary leukemia cells, in a long-term setting, the effects of long-term culturing conditions on leukemia cells had to be determined.

3.3.1. Determination of culture conditions that support long-term survival of primary AML blasts

Long-term cultures of primary AML cells have been reportedly difficult to maintain and generally feature specific protocols. Also, “long-term” often refers to different time spans which are not always clearly specified. We refer to long-term as a time span which allows for changes in immunophenotype or in clonal selection in cell culture to occur and be observed. Also, we refer to drug screens which are longer than the 72h golden standard as long-term. Even though other research groups have previously reported long-term ex-vivo survival and expansion of primary AML cells, these studies differ in several key aspects from our approach: (I) The focus of such studies has generally been on adult AML rather than pediatric AML[108–110](II) Generally, leukemia stem cells (characterized as $CD34^+$ and $CD38^-$ cells) are isolated from patient samples and expanded ex-vivo rather than keeping leukemic blasts in culture[109,110] (III) Several models use additional SMIs to facilitate ex-vivo survival. This however, could distort results when assessing drug combination efficacy[109,111] (IV) To model the tumor microenvironment, often co-cultures with bone marrow mesenchymal stromal cells are used, where cytokine concentrations are often variable[112–114]. Therefore, we used fixed, well defined cytokine concentration. (V) Unique and novel scaffold technologies are constantly developed to mimic physiological conditions and while they provide a highly sophisticated replica of the tumor microenvironment, they often feature a unique and complicated design, and are not accessible to many labs and researchers[115].

To study the effects of in vitro long-term cultures on primary AML cells therefore, we compared two culture models: a standard 2D suspension culture and a 3D Methylcellulose based cell culture. Both culture types are routinely used in various permutations of drug screens and constitute a robust and prevalent method to determine drug effects on cancer cells[11,116]. To that end, primary cells, obtained from the CCRI biobank, were sorted after thawing and cultured in the two different culture models (see Figure 7). At several timepoints during the experiments, total cell number and cell viability of primary AML cells were measured.

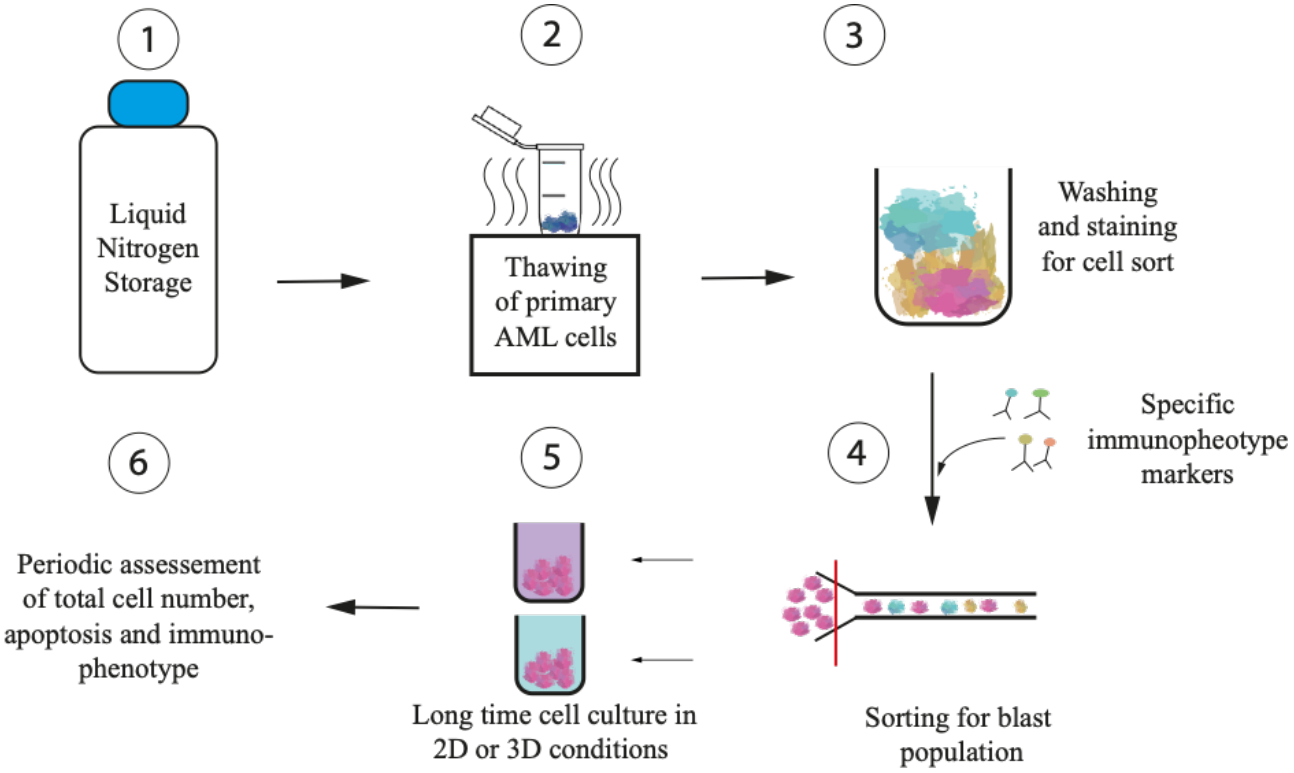

Figure 7: Flowchart of primary cell experiments.

1) Patient samples were obtained from the CCRI BioBank and transferred to the lab on dry ice 2) Samples were then thawed and washed under sterile conditions **3)** Thawed cells (multicolored specks) were then stained with specific immunophenotype markers using data from diagnosis **4)** Cells were sorted for the blast population at the CCRI FACS core unit using a FACS Aria (BD) cell sorter) **5)** Sorted blasts were the subjected to long term culture conditions **6)** Total cell number, apoptosis and immunophenotype were periodically assessed.

3.3.2. Patient samples and preparation of AML cells

Primary cells were obtained from patient samples stored in the CCRI biobank. Samples were selected on two general criteria: (I) Preferentially we decided on patient samples harboring an MLL rearrangement (KMT2A) or having a normal karyotype (NK), since we focused on IR/HR subtypes of AML (II) Also the number of samples frozen of each patient was relevant. We used

only leftover materials stripped from further clinical questions. Sampling as well as subsequent research was covered by appropriate informed consent policies and clearance of study procedures by the involved ethical committees. Samples were either mononuclear cells (MNC) from peripheral blood (PB) or from bone marrow aspirates, stored in liquid nitrogen. Only *de novo* AML samples were considered. The immunophenotype of the blasts was already known from previous diagnostic testing performed in our laboratory and was used for specific sorting of AML blasts (see Figure 4). From each patient, clinical data as well as a complete immunophenotype was available. Samples were thawed under sterile conditions, as previously described. Instead of RPMI, iscove modified dulbeccos media (IMDM) with 5% FCS was used to reconstitute the cells. Samples were thawed under sterile conditions, as previously described. Instead of RPMI, IMDM with 5% FCS was used to reconstitute the cells.

3.3.3. Cell sorting of primary AML cells

After thawing, AML blasts were sorted to remove residua normal, healthy cells. Each sample was therefore stained with a unique set of markers unequivocally identifying the blast population (according to immunophenotype data obtained at diagnosis; see pt. 3.3.2.). For sorting, usually a 3-4 color panel was used (see Table 15).

After thawing and washing, cells were resuspended in 300 µl IMDM 5% FCS. An aliquot of 70 µl was used to determine the cell count on the *Sysmex* (Sysmex Corporation). Cells were then stained with respective antibodies for 15min in the dark. Afterwards, cells were washed with 1x PBS and resuspended in 500 µl IMDM 5% FCS. Before sorting cells were filtered using a tube with a cell-strainer cap (Corning). All steps were performed in a sterile environment.

Cells were then sorted into tubes containing IMDM with 30% FCS. The sorting strategy was later adapted to incorporate a dead/live staining, to exclude dead cells from cultures. A representative gating strategy is depicted in Figure 4.

3.3.4. Comparison of 2D versus 3D culture conditions

After cells were sorted, they were immediately transferred into their respective culture conditions: either IMDM with 30% FCS or StemMACS^{Tm} HSC-CFU media from Miltenyi. Media were prepared before sorting and final cytokine concentrations and exact media composition can be viewed in Table 3. For the long-term cultures, 24-well plates were used. Cells were suspended in 500µl for each well. Cell number per well was adapted to sorting yield, from a minimum of 50k cells/per well to a maximum of 100 cells per well. Cells were then incubated

at 37°C and 5% CO_2. Cytokines and media were not changed for the duration of the experiment.

Table 3: Cytokine concentration for primary cells.

Cytokine	C in ng/ml
SCF	25ng/ml
GM-CSF	10ng/ml
G-CSF	10ng/ml
IL-3	10ng/ml
IL-6	10ng/ml
IFN-γ	10ng/ml
TPO	10ng/ml
SDF-1α (CXCL12)	10ng/ml
FLT-3 Ligand	10ng/ml

Cell viability, total cell number and apoptosis were measured in regular intervals using the assays described previously (see pt. 3.2.). Additionally, a full immunophenotype assessment was performed to detect changes upon cell culture, as well as differences between culturing conditions.

Hence, an immunophenotypic assessment was performed before and after culturing, using a dried format Duraclone^{Tm} (Beckman Coulter) “LAIP”-tube (leukemia associated immunophenotype). The Duraclone^{Tm} tube contains a number of 9 fixed markers and two additional slots (PE, APC) for patient specific “drop-ins” (see Table 4) The “LAIP panel” includes markers for CD (Cluster of Differentiation)15, CD34, CD117, CD33, CD11b, CD14, HLA-DR, CD45KO and CD16. For detailed information on fluorochromes see Table 4. For information on the respective markers see Table 7.

For immunophenotypic analysis, cells were extracted from a well by washing with PBS, transferred into a falcon tube and spun down for 10 min at 300g. Cells were then split and 50k

cells were resuspended in 200 µl IMDM and transferred into a LAIP tube containing all the markers. Markers and cells were then incubated at room temperature for 15 min in the dark. Afterwards, cells were washed 1x with PBS and resuspended in 300 µl IMDM. Cells were then measured on the flow cytometer *LSRII (BD)*. The technical staff of the CCRI set flow cytometer machine settings of the LSRII for cell sorting.

Table 4: Duraclone^{Tm} LAIP-tube flow cytometry panel.

Filter	**530/30**	**576/26**	**610/20**	**695/40**	**780/60**	**660/20**	**780/60**	**712/40**	**450/40**	**525/50**	**655**
Specificity	CD15	Drop-in 1.	CD34	CD117	CD33	Drop-in 2.	CD11b	CD14	HLA-DR	CD45	CD16
Channel	FITC	PE	ECD	PC5.5	PC7	APC	APC-Ax750	APC-Ax700	Pacific Blue	Krome Orange	BV605

4. Materials

4.1. Solutions and Media

Table 5: Solutions and Media.

Medium	Manufacturer
IMDM Glutamax	Sigma-Aldrich Chemie GMBH
RPMI 1640	Sigma-Aldrich Chemie GMBH
Fetal Calf Serum	Gibco
Methylcellulose complete	Miltenyi
Methylcellulose basic	Miltenyi
1x Dulbecco's Phosphate Buffered Saline	Life Technologies
Annexin Binding Buffer	Made in house (0.1M HEPES/NaOH ph7.4, 1.4M NaCL, 25mM$CaCL_2$)
CryoSure DMSO	WAK-Chemie Medical GmbH
2-Mercaptoethanol	Sigma-Aldrich Chemie GMBH
Bovine Serum Albumin	Sigma-Aldrich Chemie GMBH
Cell Titer Glo Assay	Promega
Mycoplasma Test	Lonza

4.2. Lab equipment

Table 6: Lab equipment.

Device	Name	Company
Autoclave	Hiclave HG-80	Amerex Instruments
Oven	WTC Binder	Binder
Laminar Flow Hood 1	Esco class II biosafety cabinet culture plus	Escoglobal
Laminar Flow Hood 2	Esco class II biosafety cabinet culture plus	Escoglobal
Fume Hood	1194. Laborotory Fume Cabinet	Hohenloher
Pipette Controller	Accu-Jet Pro	BRAND GMBH + CO KG
Pipette	VWR Single Channel 10-1000µl	VWR International, LLC.
Multichannel Pipette	Finnpipette™ F2 Multichannel Pipettes	Thermo Scientific™
Cell Counter	Sysmex KX-21N	Sysmex Corporation
Hemocytometer	Bright-Line, Double	Bürker-Türk
Microscope 1	Axiovert 40 C	Carl Zeiss
Microscope 2	Nikon TMS	Nikon
Vortex Mixer	NeoLab 7-2020	neoLab
Centrifuge 1	Heraesus Megafuge 1.OR	Thermo Scientific™
Centrifuge 2	Heraesus Multifuge 1S-R	Thermo Scientific™
Table Centrifuge	VWR Mini Star	VWR International, LLC.
Incubator 1	Heareus HeraCell 150 i CO2 Incubator	Thermo Scientific™
Incubator 2	Heareus HeraCell 150 CO2 Incubator	Thermo Scientific™
Waterbath	Grant T 100 ST12	GRANT Instruments
Plate Reader	EnSpire Multimode Plate Reader	Perkin Elmer, INC
Flow Cytometer 1	BD LSR II	BD Bioscience
Flow Cytometer 2	LSRFortessa	BD Bioscience
Flow Cytometer 3	BD FACS Aria Fusion	BD Bioscience

4.3. Antibodies

Table 7: Antibodies.

Specificity	Conjugate	Clone	Species	Manufacturer	Lot-Nr
7AAD	PERCP		Mouse	Beckman Coulter	41
CD2	PE	LT2	Mouse	Exbio	524149
CD7	PE	MEM-186	Mouse	Exbio	525042
CD11A	PE	HI111	Mouse	Pharmingen	9051974
CD11B	APC-Ax750		Mouse	Beckman Coulter	12
CD13	APC	WM15	Mouse	Exbio	529744
CD14	APC-Ax700	MEM15	Mouse	Exebio	527394
CD15	FITC	MMA	Mouse		6005783
CD16	BV605	3G8	Mouse	Biozym	B266619
CD19	APC	SJ25C1	Mouse		9137867
CD33	PC7		Mouse	Beckman Coulter	31
CD34	ECD	581	Mouse	Beckman Coulter	3
CD45	Krome Orange		Mouse	Beckman Coulter	46
CD56	APC	LT56	Mouse	Exbio	528653
CD56	PE	LT56	Mouse	Exbio	527750
CD117	PC5.5	4B5.B8	Mouse	Pharmingen	8208798
Annexin	FITC		Mouse	BD Horizon	7079902

HLA-DR	Pacific Blue		Mouse		
NG2	PE	7.1	Mouse	Beckman Coulter	28

4.4. Cytokines

Table 8: Cytokines.

Cytokine	Source	Catalog nr.	Lot.nr.	Company
Recombinant Human SCF	E.Coli	300-07	051834	Peprotech
Recombinant Human TPO	E.Coli	100-18	121744	Peprotech
Recombinant Humane IL-6	E.Coli	200-06	041716	Peprotech
Recombinant Human IFN-γ	E.Coli	300-02	121527	Peprotech
Recombinant Human SDF-1α (CXCL12)	E.Coli	300-28A	101492	Peprotech
Recombinant Human G-CSF	E.Coli	300-23	121677	Peprotech
Recombinant Human Flt3-Ligand	E.Coli	300-19	011645	Peprotech
Recombinant Human IL-3	E.Coli	200-03	041413	Peprotech
Recombinant Human GM-CSF	E.Coli	300-03	011830	Peprotech

4.5. Inhibitors

Table 9: Inhibitors.

Product Name	Generic Name	Catalog/Product Code	Batch/Lot nr.	CAS No.	Company
ABT-199	Venetoclax	SC-472285	F1319	1257044-40-8	Santa Cruz
PF-04449913	Glasdegib	S7160	02	1095173-27-5	Selleckchem
SCH727965	Dinaciclib	T1912	T1912-1	779353-01-4	TargetMol
RG-7388	Idasanutlin	S7205	02	1229705-06-9	Selleckchem
INCB018424	Ruxolitinib	S1378	11	941678-49-5	Selleckchem
PKC-412	Midostaurin	T3211	T3211-1	120685-11-2	TargetMol
ASP2215	Gilteritinib	S7754	01	1254053-43-4	Selleckchem
GSK1120212	Trametinib	S2673	08	871700-17-3	Selleckchem
AC220	Quizartinib	S1526	02	950769-58-1	Selleckchem
BMS-354825	Dasatinib	S1021		302962-49-8	Selleckchem
1268524-70-4	JQ1	S7110		1268524-70-4	Selleckchem
PD0332991	Palbociclib	S1579		571190-30-2	Selleckchem
SCH772984	-	S7101		942183-80-4	Eubio
BAY43-9006	Sorafenib	S1040		284461-73-0	Selleckchem

4.6. Cell lines and primary cells

Table 10: Cell lines.

Cell line	Biological source	Relevant Genetic aberration	Cell Type	Growth mode
HL-60	human peripheral blood	MYC oncogene	Promyeloblast	suspension
MV4-11	human peripheral blood	FLT3–ITD^{+}	Macrophage	suspension
THP-1	human peripheral blood	MLL-rearrangement	Monocyte	suspension

4.7. Patient Samples

Table 11: Patient Samples.

Patien ID	Sex	Age	Sample type	AML FAB	Aberration
P1	m	17y4m	BM	M1	NK
P2	f	16y10m	BM	M2	Other
P3	f	1y1m	BM	M5a	KMT2A-MLLT3
P4	m	0y1m	pB	M5	KMT2A-MLLT3
P5	m	1y5m	BM	M0	NUP98-KDM5A
P7	m	17y8m	BM	M2	KMT2A-ELL
P8	f	7y1m	pB	M5a	KMT2A-MLLT1
P9	f	11y0m		M5	KMT2A-MLLT10
P10	f	7y1m	BM	M4	DEK-NUP214

5. Results

5.1. Assessment of current drug application in literature

First, a comprehensive catalogue of the current trends in SMI usage was established (see Table 12). Subsequently, the catalogues potential for inhibitor combinations was assessed, and visualized using a combination matrix (see Figure 8). For details on the selection criteria for SMI and SMI combinations, see Methods pt 3.1.1. and 3.1.2..

5.1.1. Catalogue of selected single agents

Table 12: SMI´s selected for single drug- and combination testing. Main targets are kept in bold characters.

Generic name	Name	Inhibition of:
Dasatinib	BMS-354825	**BCR-ABL**, SRC-Family MKI
Dinaciclib	SCH727965	**CDK2**, **CDK5**, **CDK1** and CDK9
Gilteritinib	ASP2215	**FLT3**, AXL, ALK
Glasdegib	PF-04449913	**Hedgehog**
Idasanutlin	RG-7388	**MDM2**
JQ1	1268524-70-4	**BET**
Midostaurin	PKC-412	**FLT3**, **PKCα**, VEGFR2, C-KIT, PDGFR
Palbociclib	PD0332991	**CDK4**, **CDK6**
Quizartinib	AC220	**FLT3-ITD/KD**, CSF1R/FMS, SCFR/KIT, PDGFR
Ruxolitinib	INCB018424	**JAK1**, **JAK2**, MKI
-	SCH773984	**ERK1, ERK2**
Sorafenib	BAY43-9006	**RAF/MEK/ERK**, VEGFR-2, PDGFR-*BETA*
Trametinib	GSK1120212	**MEK, MAPK/ERK**
Venetoclax	ABT-199	**BCL-2**

The established SMI catalogue comprised 14 agents, most of which had FDA approval. However, several agents with pending FDA approval or targets of interest not covered by any available FDA approved drug were added. Those were: Dinaciclib (which received orphan drug status for chronic lymphocytic leukemia), Idasanutlin (approval status unclear, however preclinical data suggest potent effectiveness in AML when combined with Venetoclax[117]), JQ1 (status pending), Quizartinib (FDA rejected, rejection is being reviewed) and SCH773984 (unspecific ERK inhibitors). If a pathway known or suspected to play a role in pediatric AML did not have a specific inhibitor with known efficacy in adult or pediatric AML, we used inhibitors with known effectiveness in preclinical models or in other cancers. These were: SCH773984 and JQ1[118–121].

5.1.2. Assessment of drug combination potential

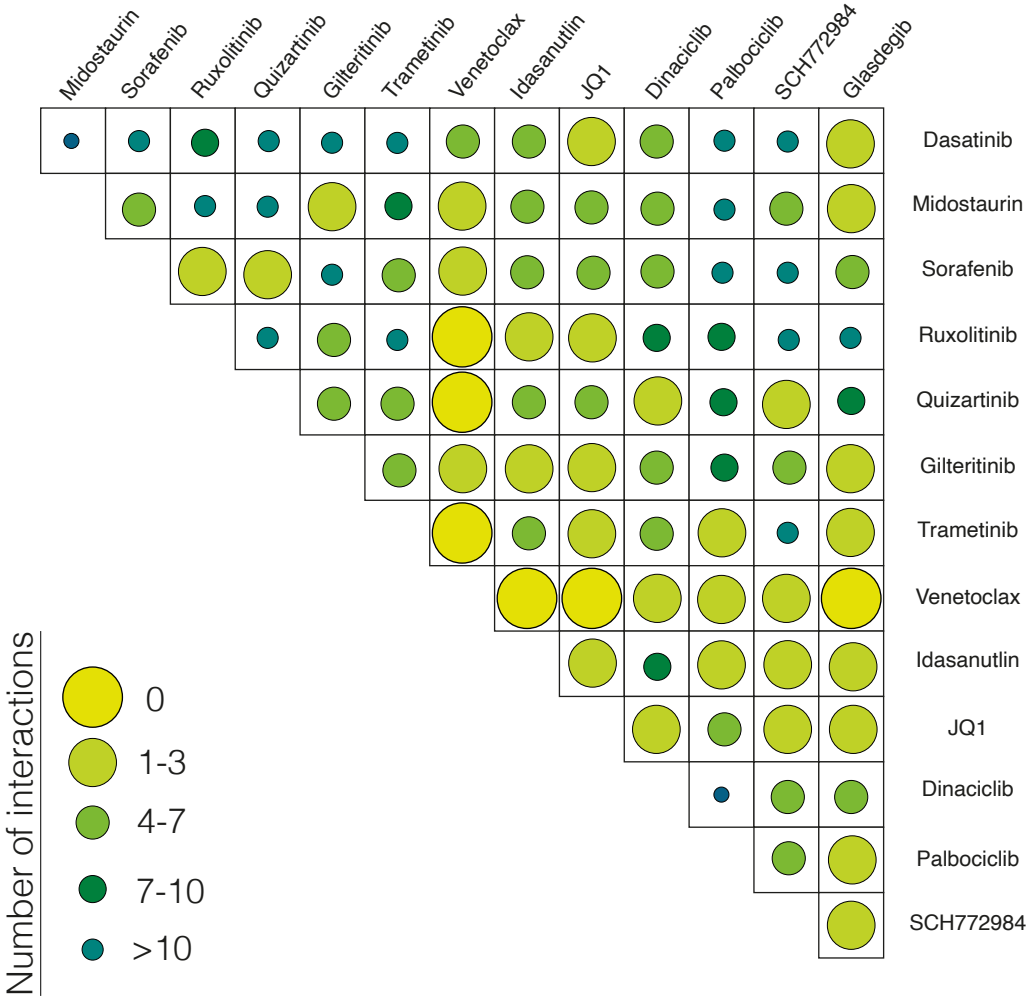

Figure 8: Heuristic combination matrix.

The combination matrix displays the assigned relevance of the combination potential of any given drug combination, based on the non-overlap of their respective pathway targets. Relevance of combinations is indicated by the color and shape of the circle, which is reflective of the number of pathway interactions determined using the online platforms described in pt. 3.1.2.. The number of interactions only refers to the main pathway inhibited by any given drug.

Since the non-overlap of targeted pathways was a decisive factor in determining combination relevance [91], agents targeting similar pathways (e.g. Quizartinib and Midostaurin) or similar cellular processes (e.g. Dinaciclib and Palbociclib) were assigned low in relevance. Also, agents targeting upstream or downstream factors of one another (e.g. Sorafenib and SCH772984) were considered low in relevance. This was important, since the bliss independence model for determining synergy is also based on the minimal interaction assumption[43].

In contrast, high relevance was assigned to agents displaying less interactions (e.g. Venetoclax and Idasanutlin). Notably, the BH-3 mimetic Venetoclax showed little interactions with other pathways according to the tools we used to identify pathway interactions as described in 3.1.2.. This is supported by studies analyzing the mitochondria based apoptotic signaling in cancer cells[122,123]. Also, the combination potential of BH-3 mimetics with standard-of-care an targeted cancer therapies has been described previously by several other research groups[98,123,124].

5.2. Efficacy assessment of single drugs and drug combinations on cell lines

The selected SMIs and potential synergistic SMI combinations were tested using three different AML cell lines as described in Methods pt. 3.2.5.-3.2.7.. To additionally evaluate how generated dose-response curves of single agents compared to existing data, dose-response curves were cross referenced to available data from the PDB dataset if available (see Figure 9).

5.2.1. Single agent IC_{50} assessment on cell lines

Dose-response curves of all agents were then generated for all cell lines using the *Graphpad Prism* software and IC_{50} values determined (see Table 13).

Table 13: IC_{50} values determined through dose-response assay.

The respective IC_{50} values for every cell line, are listed below. Concentrations are in nM.

	HL-60	MV4-11	THP-1
Dasatinib	11018	1148	1708
Dinaciclib	3	2	2
Gilteritinib	289	2	45
Glasdegib	5817	3482	4877
Idasanutlin	226	91	83
JQ1	1498	96	77
Midostaurin	3178	25	397
Palbociclib	652	271	8750
Quizartinib	222	1	8049
Ruxolitinib	23442	2710	17253
SCH772984	212	1	30
Sorafenib	1190	2	1123
Trametinib	2	14	2732
Venetoclax	308	3	138

5.2.2. Cross-validation of dose response data with *PharmacoDB* dataset

To estimate how our generated dose response curves matched data from other labs, we used the open source PDB dataset. We were able to compare our data to dose response curves generated by other labs using the same compounds, experimental setup and AML cell lines. The PDB dataset yielded 5 comparisons of tested drugs for each cell line (see Figure 9). These were: Dasatinib, Dinaciclib, JQ1, Midostaurin and Sorafenib for HL-60; Dasatinib, JQ1, Midostaurin, Quizartinib and Sorafenib for MV4-11; Dasatinib, JQ1, Ruxolitinib, Quizartinib and Sorafenib for THP-1.

Since IC_{50} values are inherently variable, they should always be viewed in the context of curve shape when compared[105,125]. The comparisons showed, that generated dose response curves yielded concordant shapes and IC_{50} values. Although varying, IC_{50} values were found to be in the same range across most comparisons. The greatest divergence in absolute numbers was found in the comparisons of Quizartinib, Ruxolitinib and Sorafenib in THP-1.

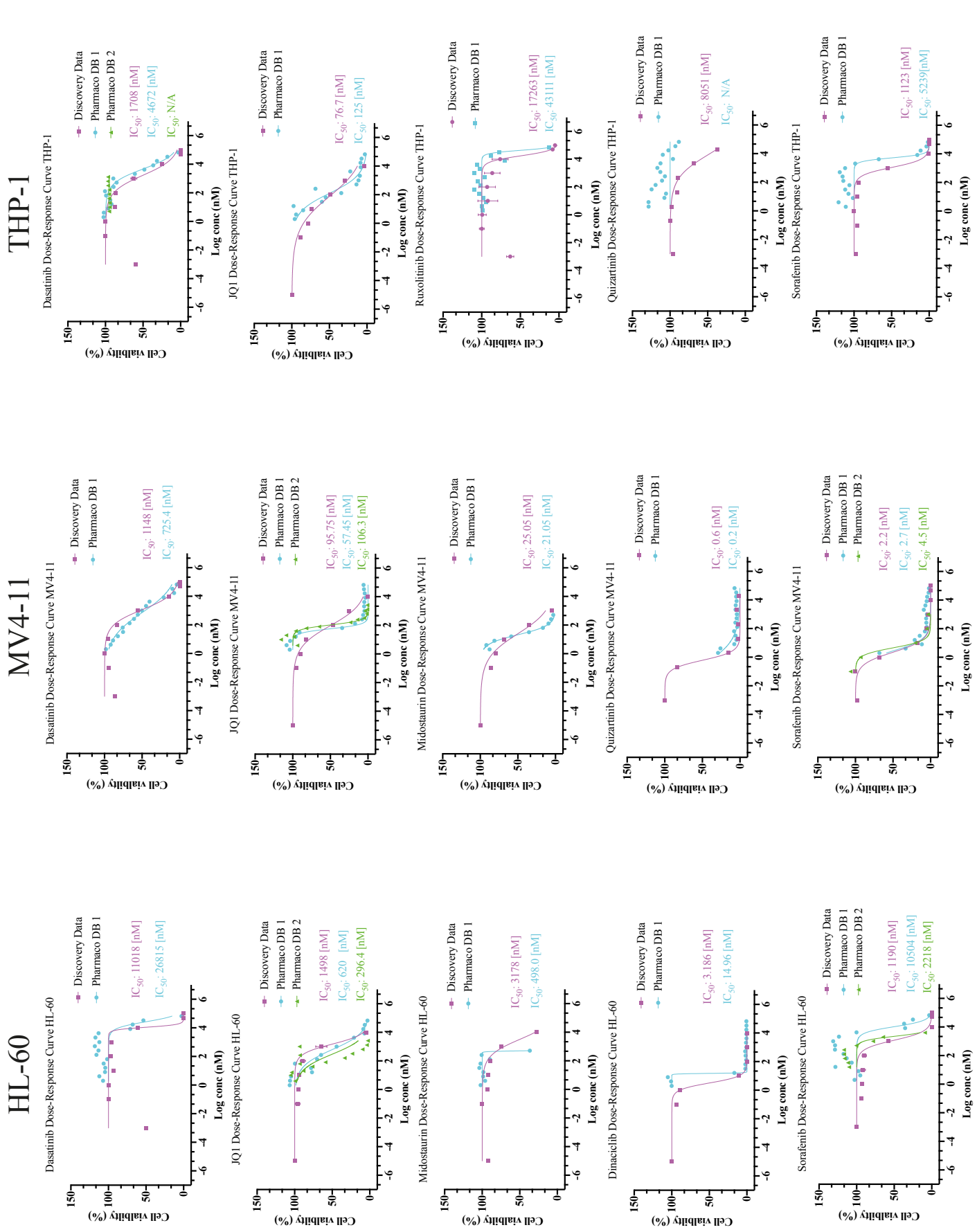

Figure 9: Cross-validation of dose response curves with PharmacoDB dataset.

Dose-response curve data provided by the PDB dataset was compared to generated data using Prism Graphpad. Data for 5 dose response curve comparisons was obtained for all three AML cell lines.

These comparisons provided us with the possibility to countercheck our some of our results with data from other labs. The concordance in curve-shape and IC_{50} values amongst the PDB dataset and our data demonstrated the reproducibility of this assay.

5.2.3. Drug combination testing using AML cell lines

Three AML cell lines were treated with a panel of 15 drug combinations (see Figure 10). These combinations were chosen based on the assigned relevance in the combination matrix in Figure 8. Synergistic effects were quantified according to the bliss independence model (for details see pt.1.2.2. and pt. 3.2.7.). By this metric a positive value designates synergism. Of the 15 tested combinations, 10 included Venetoclax and all combinations showing high deviation from bliss values contained Venetoclax in combination with either a tyrosine kinase (Dasatinib, Quizartinib and Ruxolitinib) or a serine/threonine kinase (Dinaciclib).

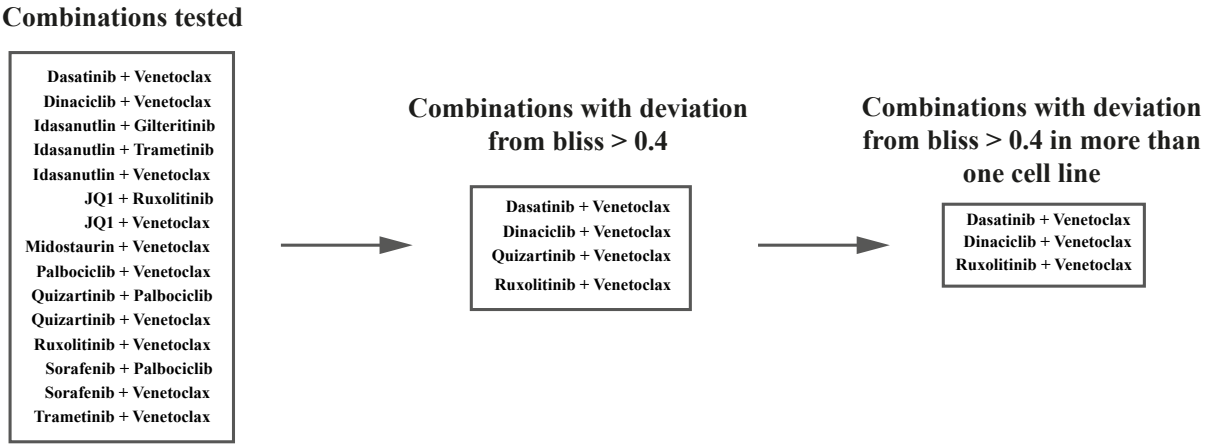

Figure 10: Combinations tested on cell lines.

15 combinations were tested on three AML cell lines. Four of these combinations produced deviation from bliss scores higher than 0.4. Three of the tested combinations were effective in more than one cell line.

The majority of tested combinations showed minor synergistic effects in at least one cell line (see Figure 11). The highest observed value was 0.8 for Dasatinib + Venetoclax in HL-60, while the lowest was -0.1 for Quizartinib + Palbociclib in HL-60. Location parameters of the deviation from bliss values are summed up in Table 14. Three combinations i.e. Dasatinib + Venetoclax, Dinaciclib + Venetoclax and Ruxolitinib + Venetoclax were effective above average in more than one cell line, all with a minimum deviation from bliss of 0.4. None of the combinations showed high deviation from bliss values in all three cell lines (see Table 14).

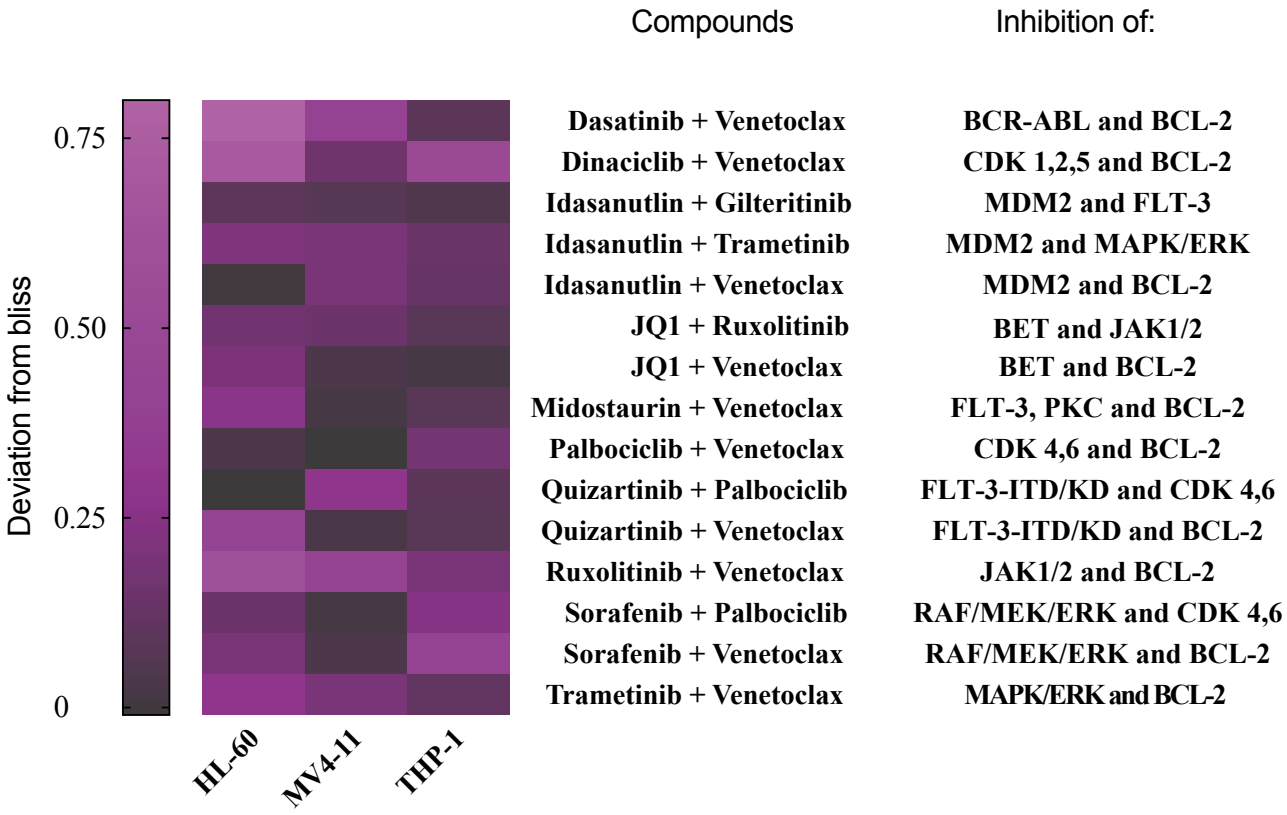

Figure 11: Heatmap of drug combinations.

The heatmap shows the calculated deviation from an additive effect for all 15 combinations: the higher the deviation (bright purple), the higher the observed synergistic effect of a given combination. The heatmap shows only the highest deviation from bliss value for every given drug combination and only of concentrations that were under the C_{max} of both single agents (see pt. 3.2.5.).

Table 14: Location parameters of deviation from bliss values across AML cell lines.

	HL-60	MV4-11	THP-1
Mean	0.3	0.1	0.2
Median	0.2	0.2	0.1
Modus	0.2	0.2	0.08
Highest value	0.8	0.4	0.5
Lowest value	-0.01	-0.01	0.09

To further characterize the effect of combined treatment on AML cell lines, we investigated the cumulative deviation from bliss values of tested concentrations (see Figure 12). This parameter was useful to examine the occurrence of synergy spread over the range of concentrations

tested even if there were no high deviation from bliss values. Considering this parameter, Dasatinib + Venetoclax, Dinaciclib + Venetoclax and Ruxolitinib + Venetoclax were effective over a range of concentrations. The combinations Dasatinib + Venetoclax and Trametinib + Venetoclax were most effective over a wide range of concentrations in HL-60 while Sorafenib + Venetoclax was effective in THP-1. MV4-11 proved to be the most resistant cell line to all tested combinations while.

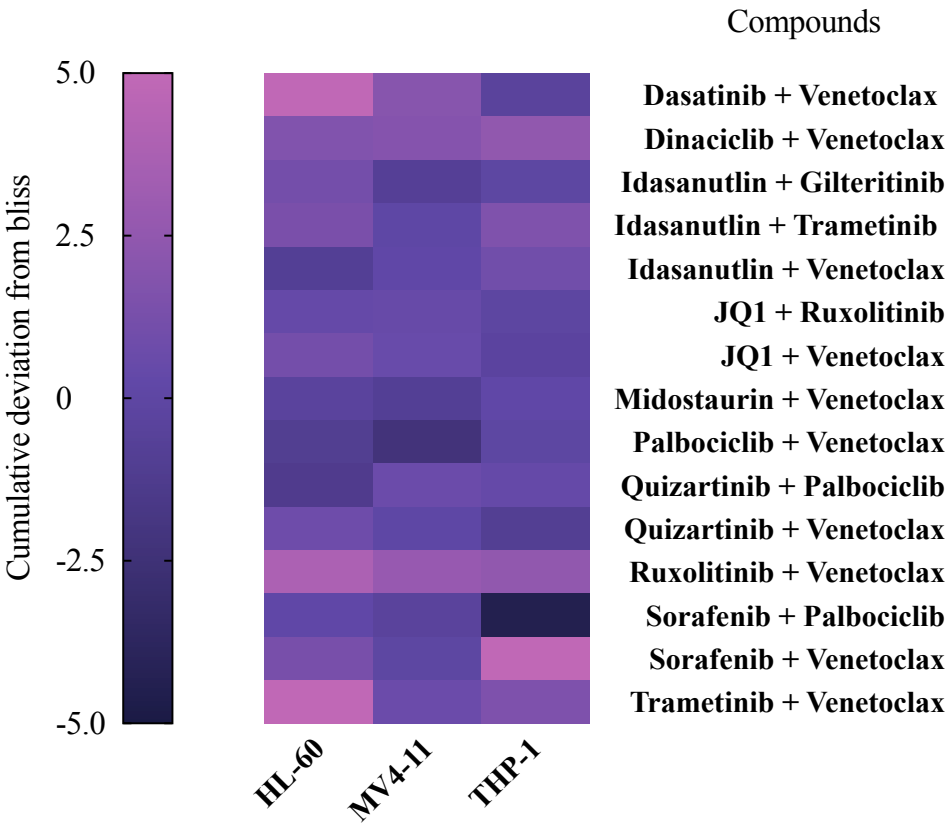

Figure 12: Heatmap of cumulative bliss data.

Deviation from bliss values of tested concentration ranges were aggregated: The more concentration ratios displayed synergistic effects the higher the value. Negative values indicate a collective antagonism of the combination.

5.2.4. Further analysis of drug combinations on HL-60 cell line

Identified combinations with the highest synergistic effects on cell viability, which were Dasatinib + Venetoclax and Ruxolitinib + Venetoclax were further tested on the cell line HL-60. An upscaled setup was used, since more cells were needed to further investigate the effect of combination treatment on cell cycle, apoptosis and cell number using the flow cytometry assays described in pt. 3.2.3. and pt. 3.2.4.. Concentrations were chosen in the same way as they were for the initial combination testing. The well displaying the strongest effect on cell

viability with concentrations under the respective agents C_{max} was then analyzed. Presented experiments have not been repeated at the time of writing and are therefore considered preliminary and statistically not significant.

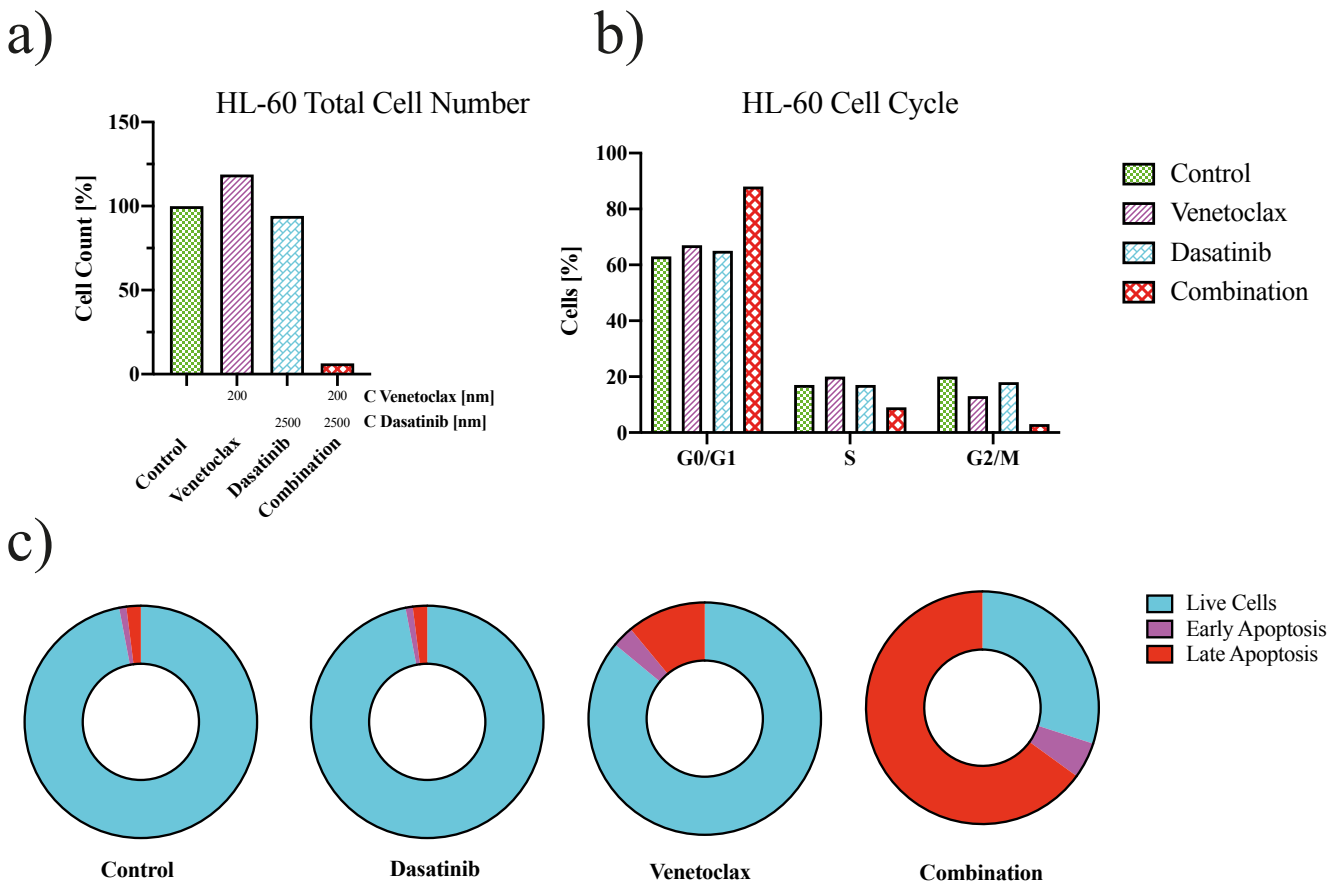

Figure 13: Effects of Venetoclax and Dasatinib on HL-60 cell line.

HL-60 cells were treated with the combination Dasatinib and Venetoclax. Measurements were not repeated **a)** Total cell-count of HL-60 cells of different treatments was determined using Trucount tubes. **b)** HL-60 cells were treated with Venetoclax, Dasatinib or a combination of both drugs for 72h. Cell cycle distribution of cells was determined using Vybrant staining. **c)** Apoptotic cells were detected using 7-AAD and Annexin-V staining.

Compared to the treatment with either Dasatinib or Venetoclax alone, the combination of both drugs was more effective regarding reduction of cell number, induction of cell cycle arrest as well as induction of apoptosis (see Figure 13). Dasatinib and Venetoclax treatment at concentrations 25000 nM and 200 nM respectively, did not cause growth inhibition of cells and relative cell numbers were 94% and 118% of the control. In comparison, the combination led to a decrease in cell number to 6% as compared with the control.

Inhibition of proliferation correlated with G0/G1 arrest in cells treated with the Dasatinib and Venetoclax combination. Percentage of cells in G0/G1 rose to 88% while the fraction of cells

in the G2/M phase dropped to 3%. Cells treated with Dasatinib or Venetoclax alone showed a smaller drop in G2/M fractions, dropping to 13% and 18% respectively, while 20% of cells in control were in the G2/M phase. In addition, there was a 6-fold increase in the number of apoptotic cells upon combined treatment compared to single drug treatments. Cells only treated with Dasatinib showed no increase in apoptotic cells when compared to the control. Venetoclax induced apoptosis in 11% of treated cells.

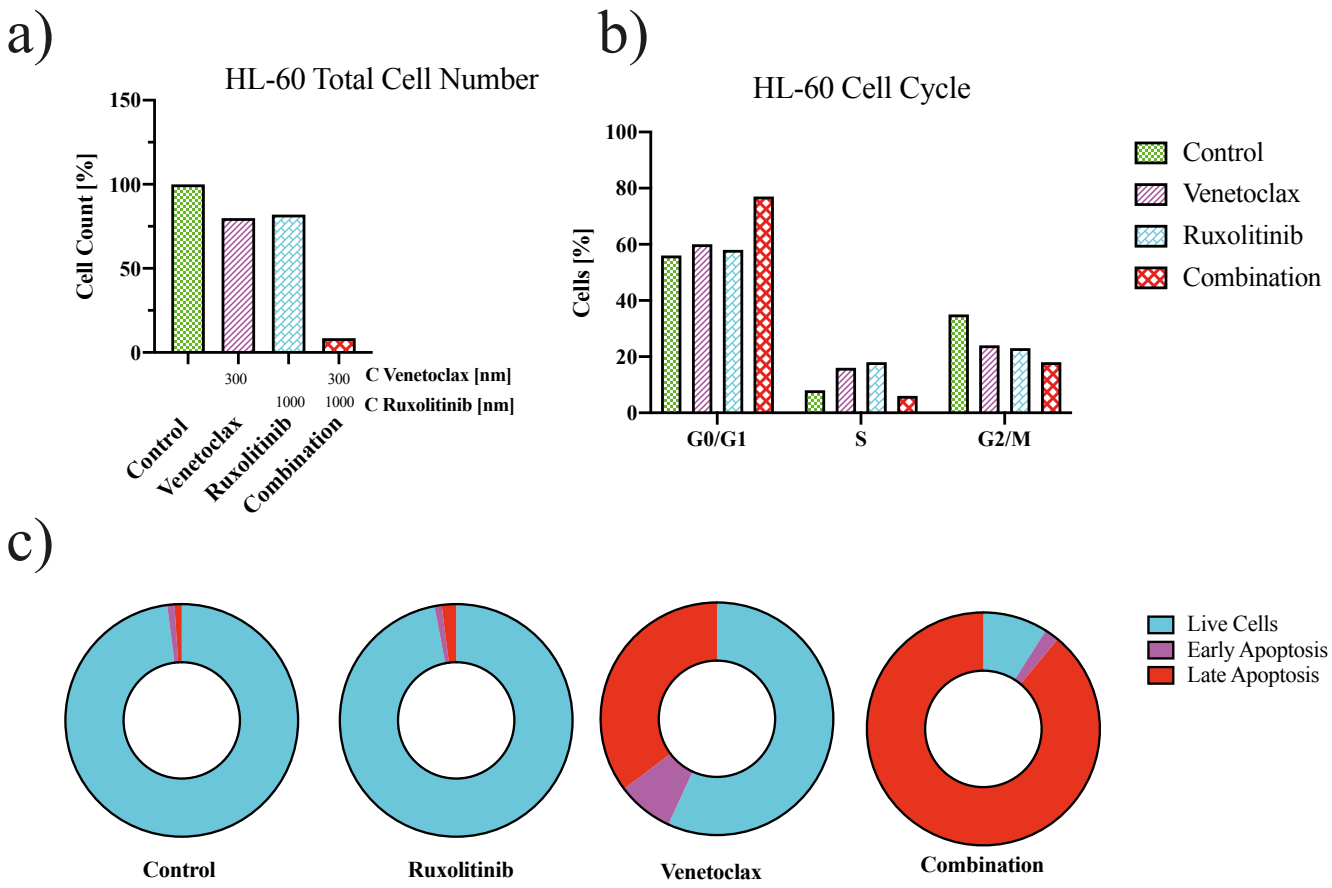

Figure 14: Effects of Venetoclax and Ruxolitinib on HL-60 cell line.

HL-60 cells were treated with the combination Ruxolitinib and Venetoclax. Measurements were not repeated. **a)** Total cell-count of HL-60 cells of different treatments was determined using Trucount tubes. **b)** HL-60 cells were treated with Venetoclax, Ruxolitinib or a combination of both drugs for 72h. Cell cycle distribution of cells was determined using Vybrant staining. **c)** Apoptotic cells were detected using 7-AAD and Annexin-V staining.

The combination of Ruxolitinib and Venetoclax at concentrations 1000nM and 300nM was able to inhibit proliferation of treated cells more potently than cells treated with Ruxolitinib or Venetoclax alone (see Figure 14). While cells treated with either agent alone grew to 88% of the control, combination treatment reduced cell number to 8%.

The reduced cell number of cells treated with the Ruxolitinib and Venetoclax combination is in line with an increase in the cell fraction arrested in the G0/G1 phase from 56 to 77%. In comparison, single agent treatment only slightly raised cell cycle arrest to 60%. Cell fractions in the G2/M phase dropped from 35% in the control, to 23% in cells treated with Ruxolitinib and Venetoclax alone, and to 17% in cells treated with the combination.

The fraction of live cells after combination treatment dropped to 8%. However, while apoptosis was not induced in cells treated with 1000nM of Ruxolitinib alone, cells treated with 300nM of Venetoclax showed induction of apoptosis in 35% of cells.

The combinations Dasatinib + Venetoclax as well as Ruxolitinib +Venetoclax were able to inhibit proliferation of the AML cell line HL-60 more potently than the single agents of the combinations at the concentrations tested. The combination Dasatinib + Venetoclax reduced cell number by 94%. Assessment of cell cycle and apoptosis in cells treated with this combination show, that the combination induced cell cycle arrest as well as apoptosis more potently than Dasatinib and Venetoclax alone and suggest a synergistic relationship that was not quantifiable in this setting. Also, the combination of Ruxolitinib and Venetoclax inhibited cellular proliferation in HL-60. However, the arrest in cell cycle relative to single agent treatment was not as in the Dasatinib+Venetoclax combination, and a larger portion of cells remained in the G2/M phase. Assessment of apoptosis induction in Ruxolitinib+Venetoclax treated HL-60 cells revealed, that only 8% viable cells remained after treatment. This however, seems to be driven by the Venetoclax component of the combination treatment, which induced apoptosis 35% of treated cells. Still, considering the reduction in cell number and arrest in cell cycle the combinations effect seems to be above simple additivity. Taken together, both combinations showed However, these effects are not quantified here and experiments need to be repeated to achieve statistical significance.

5.3. Primary cells

So far, there are only a few reports on successful long-term culture of primary AML cells[108–110]. Most of them are based on co-culture with stromal cells [112–114], where parameters such as cytokine secretion by stromal cells etc. cannot be controlled, or on addition of specific pathway inhibitors[109]. Before assessing the effects of established drug combination on primary cells for clinical translation, we therefore had to establish culturing conditions supporting long-term cell survival of primary AML cells ex-vivo under controlled and standardized conditions. In addition

to cell number and apoptosis, we also monitored immunophenotypic changes of AML cells upon ex-vivo culturing.

In total, we tested ex-vivo long-term survival using AML cells of 9 different patients with different yet common genetic aberrations for long-term survival. 4 of which were also treated with either Ruxolitinib or Venetoclax alone or in combination.

5.3.1. Primary cells and sorting data

As described in pt.3.3.3., patient samples were sorted for the blast population. The number of primary cells frozen at diagnosis was variable and dependent on the availability of residual material after the routine diagnostic work-up. Accordingly, sorting yield also differed from sample to sample and ranged from $2.6x10^5$ to $5.1x10^6$ per vial thawed (see Table 15). Of P4 two vials were thawed and sorting yield was nearly identical at 2.2 $x10^6$ and 2.1 $x10^6$. Consequently, the number of cells seeded per well differed also, depending on the experiment and sorting yield (see Table 15). In samples P1 to P5, Forward Scatter (FSC) and Side Scatter (SSC) were used to exclude debris and dead cells. The rest of samples were additionally stained with a dead/live marker to selectively sort for living cells.

Table 15: Sorting data of primary cells and LAIP drop-ins

Sample ID	Sorted for	LAIP drop-in	Sorting yield	Cells seeded per well
P1	KO: CD45+	APC: CD13 PE: CD56 BV 605: CD16	$1.4x10^6$	25000
P2	KO: CD45+	APC: CD13 PE: CD56 BV 605: CD16	$5.1x10^5$	25000
P3	KO: CD45+ ECD: CD34- PC7: CD33+	APC: CD13 PE: NG2 BV 605: CD16	$1.4x10^6$	100000
P4	KO: CD45+ ECD: CD34- PC7: CD33+	PE: NG2 APC: CD56 BV 605: CD16	$2.1x10^6$	100000
P5	KO: CD45+ ECD: CD34+ PC7: CD33+	PE: CD11A APC: CD13 BV 605: CD16	$3.2\ x10^6$	25000
P7	KO: CD45+ PC7: CD33 + APC: CD 56+ PerCP: 7AAD-	PE: CD7 APC: CD19 BV 605: CD16	$2.6x10^5$	50000
P8	KO: CD45+ ECD CD34+ PerCP: 7AAD-	PE: CD7 APC: CD19 BV 605: CD16	$3.4x10^6$	50000
P9	PerCP: 7AAD- KO: CD45+ ECD CD34-	PE: NG2 APC:CD56 BV 605: CD16	$1.5x10^6$	100000
P10	FITC: CD15- PerCP: 7AAD- PC7: CD33+ Alexa 700: CD14-	PE: CD2 APC: CD13 BV 605: CD16	$4.1x10^6$	100000

5.3.2. Long-term cell cultures of primary AML cells in 2D and 3D conditions

After sorting, cells were immediately transferred into their respective culturing conditions and proliferation, apoptosis and potential differentiation were monitored. Two approaches were assessed and compared. The two approaches were: I) standard 2D suspension culture, or II) 3D methylcellulose based cell culture. With exception of methylcellulose, all other components of the cell culture medium were identical to be able to determine the 3D effect on survival and growth of AML cells (see Table 3). We then kept sorted blasts in culture and periodically assessed cell viability. There was no endpoint defined for the culturing of blasts, rather we maintained cell culturing until a drop in cell viability was observed or until no wells were available for further measurements. Samples were thawed and cultured in succession rather than in parallel, so decisions on culturing could be made on a sample by sample basis.

Samples P1-P4 were cultured in both 2D and 3D conditions, to directly compare the effects on primary AML cells (see Figure 15). The fraction cells in sample P4 used for the comparison was contaminated after sorting and did not yield results. In samples P1-P3 primary AML cells cultured in 3D conditions showed a higher percentage of viable cells at time points 3,7 and 14 days than cells in 2D conditions as well as a higher cell count. The percentage of live cells in 3D conditions was not stable, but varied over time in all three samples. At day 14 samples P1, P2 and P3 maintained 60%, 84% and 63% viable cells respectively. 2D culturing conditions negatively affected cell number and number of live cells in primary cells and samples P2 and P3 contained exclusively cells in early or late stage apoptosis from day 3 onward. Cells from Sample P1 maintained 17% live cells on day and 5% live cells at day 14 in 2D conditions.

While 3D conditions were able to support viability in patient samples cellular proliferation was not observed in samples P1 and P2. Only cells in sample P3 cultured in 3D conditions were able to proliferate and consequently showed an increase in cell number. In contrast, sample P1 only gradually increased cell number at day 14 after an initial decrease and cells in sample P2 showed a steady drop in cell number.

Since 2D conditions did not support ex-vivo survival or proliferation of primary AML cells in samples P1-P3, we continued primary cell experiments in 3D methylcellulose medium. In following samples, untreated controls were used to assess cell number and viability after long-term cell culture. Hence, the last measurement reflects the last time point at which viable cells could be obtained from wells and does not reflect the maximum time span cells could theoretically be cultured (see Table 16). The average time of these last measurements was 13 days.

Considering the fractions of viable cells after the last measuring point, long-term survival in 3D conditions was observed in all patient samples. However, proliferation, induction of apoptosis and cell viability varied across samples (see Table 16). Samples P3, P4, P8, and P10 showed the strongest ex-vivo expansion with an 14-, 14,-, 6-, and 10-fold increase in cell number and were able to maintain viable cells at 63%, 60%, 56% and 85% at days 14, 14, 14, and 9 respectively. Other samples showed a lesser increase in total cell number over time (P5 and P9, 1.5- and 3.3-fold respectively). However, on average 67% of primary cells cultured in 3D conditions were viable at the time point of last measurement.

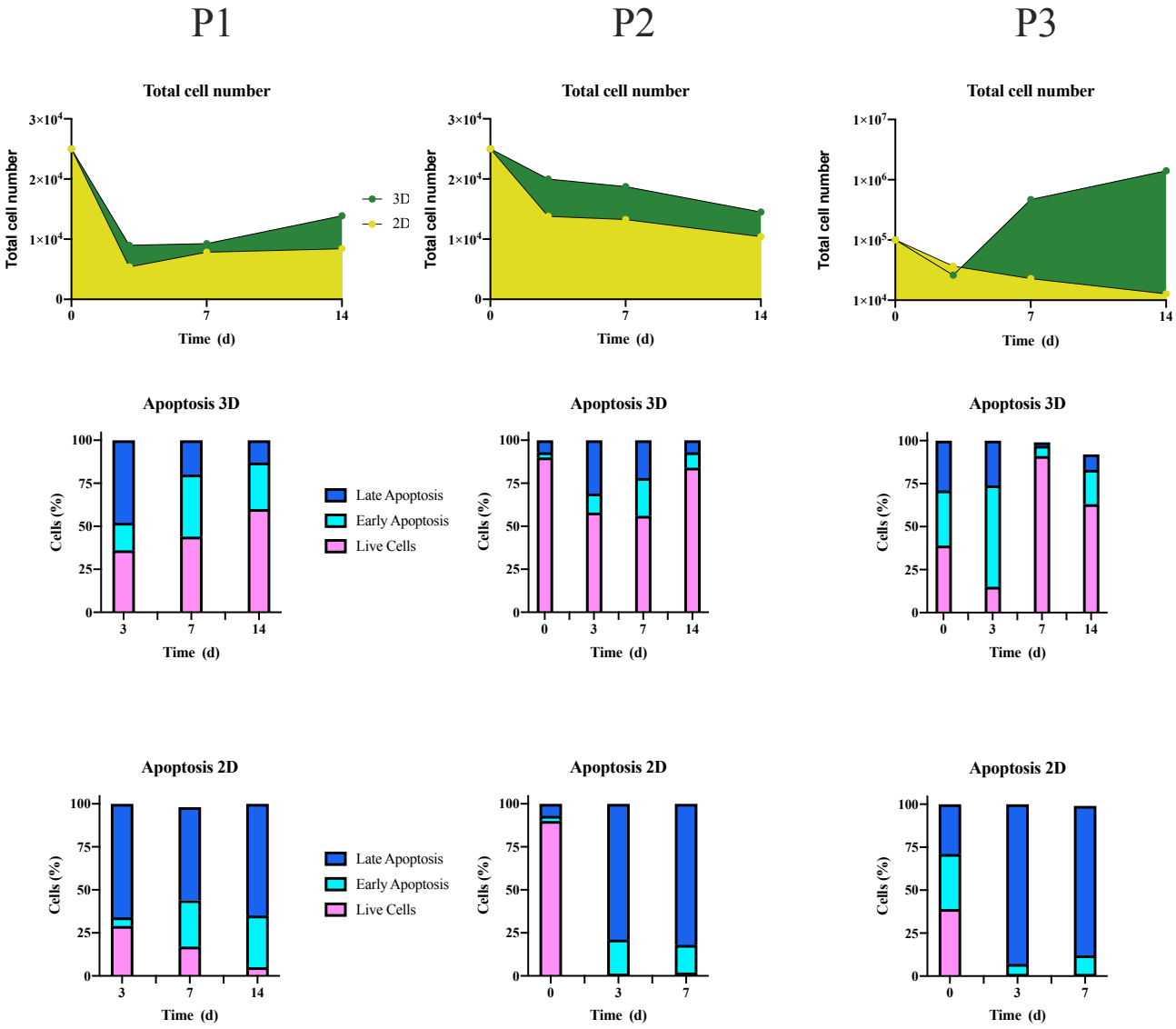

Figure 15: Comparison of 2D versus 3D culturing conditions of samples P1, P2 and P3.

Cells of samples P1, P2 and P3 were cultured in 2D and 3D conditions, which otherwise featured the same components. Half of the cells of each sample was cultured in 2D conditions, the other in 3D conditions. Total cell number was determined using Trucount tubes. Apoptotic cells were detected by Annexin V/7AAD staining.

Three of the four strong proliferating samples cultured in 3D conditions (P3, P4, P8) harbored a KMT2A fusion events and one (P10) harbored a DEK-NUP214 fusion. Additionally, we observed that all patient samples harboring different KMT2A fusion events (P3, P4, P8 and P9; P7 excluded due to contamination) were capable of ex-vivo expansion, with a minimum of a 3.3-fold (P9) and a maximum of a 14-fold (P3 and P4) increase in cell number. Patient samples showing the strongest ex-vivo expansion harbored genetic aberrations which are classified as either as IR or HR. However, a bigger cohort size also including LR patients will be necessary to determine if these findings reach statistical significance. Also, we observed that used cytokine concentrations used (see Table 3), supported long-term *ex vivo* maintenance and proliferation, even though they are 50% lower than concentrations used by other research groups focusing on long-term *ex vivo* cultures of primary AML cells [108,109].

Table 16: Long term survival and expansion of primary AML cells in 3D culturing conditions.

Sample ID	last measurement after seeding in days	Cells seeded per well	x-fold increase/decrease at last measuring point	fraction of live cells at last measuring point
P1	14	25000	0.55	60%
P2	14	25000	0.58	84%
P3	14	100000	14	63%
P4	14	100000	14	60%
P5	24	25000	1.5	97%
P7	Contaminated	50000	-	-
P8	14	50000	6	56%
P9	9	100000	3.3	34%
P10	9	100000	10	85%
Average	14	60625	6	67%

5.3.3. Effects of long-term culturing conditions on the immunophenotype of primary AML cells

Determining immunophenotypic stability in long-term cultures was important for two main reasons: I) AML blasts are usually in differentiation arrest and therefore any phenotypical changes are of interest II) Differentiated cells may react differently to combination treatment then leukemic blasts. Therefore, we aimed to assess immunophenotype pre- and post-long-

term culture. However, a constant assessment of immunophenotype after either treated or untreated long-term cell cultures was not achieved, due to problems like contamination, insufficient cell number or incomplete phenotyping. Immunophenotype tracking therefore, was incomplete and did not yield data in the majority of samples.

The samples kept in culture for the longest amount of time providing immunophenotypic data at different time points, were P4 with immunophenotype assessment at days 0, 7, and 14 and P5 with immunophenotype assessment at day 0, 17 and 24. As described in pt.3.3.2. and 3.3.3., cells were sorted after thawing and cultured in 3D medium with normal cytokine concentrations (see Table 3). Primary AML cells in sample P4 showed immunophenotypic changes indicating a monocytic differentiation over time. Monocytic maturation markers CD11b and CD14 showed increased expression on cells suggesting culturing conditions induced cellular differentiation (see Figure16)[126–128]. In contrast however, cellular expansion was ongoing at the last time point and cells were still proliferating at day 14 (see Figure 18). At day 14 single populations were difficult to distinguish and full phenotype assessment of sample P4 at all time points was not achieved.

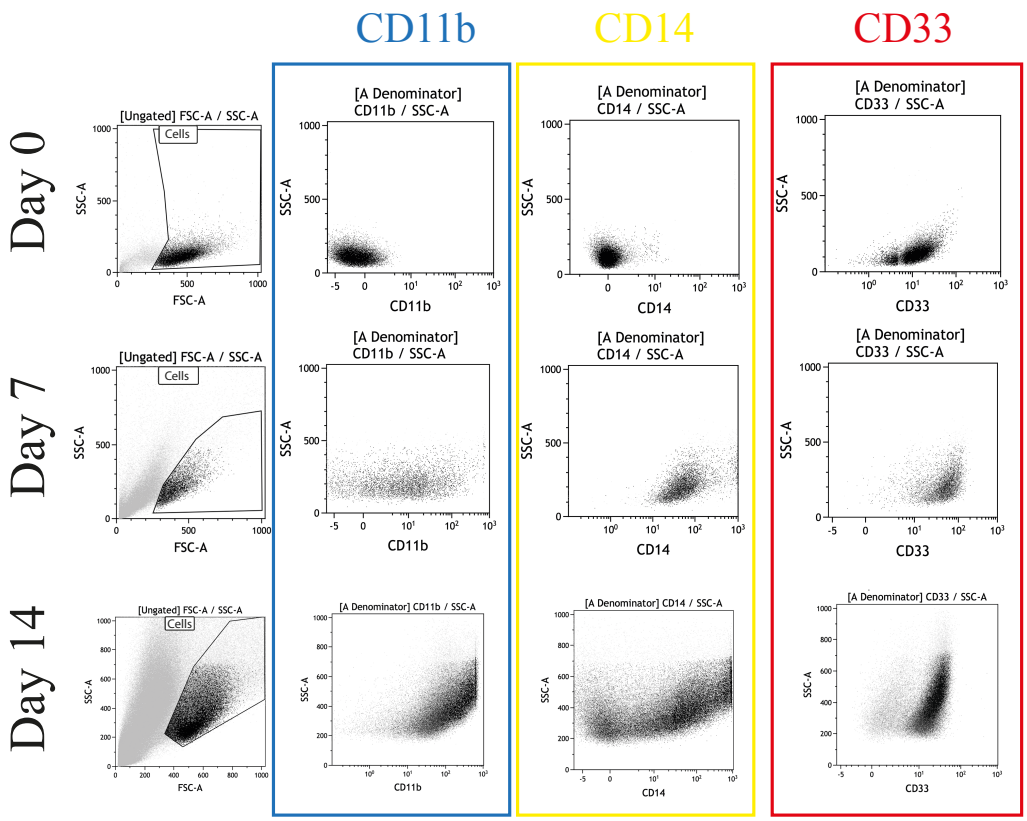

Figure 16: Immunophenotype tracking in long-term cell culture in sample P4.

Dot plots show selected markers of LAIP analysis of primary cells on day 0, 17 and 24. Markers CD11b, CD14 and CD33 are framed in their respective colors blue, yellow and red.

Primary cells of Sample P5 were kept in culture for 24 days and immunophenotype was assessed on day 0, 17 and 24 (see Figure 17). Three markers could be categorically traced at these three time points: CD11a, CD14 and CD34. Changes in the expression pattern of these three markers indicate an impartial monocyte differentiation at day 24. Expression of CD14 increased at day 24, while associated monocyte maturation marker markers CD11a and the stem cell associated marker CD34 remained unchanged (see Figure17). Considering these markers therefore, blasts of sample P5 showed a partial monocytic differentiation, however other definitive markers were not traceable across all time points[126–128].

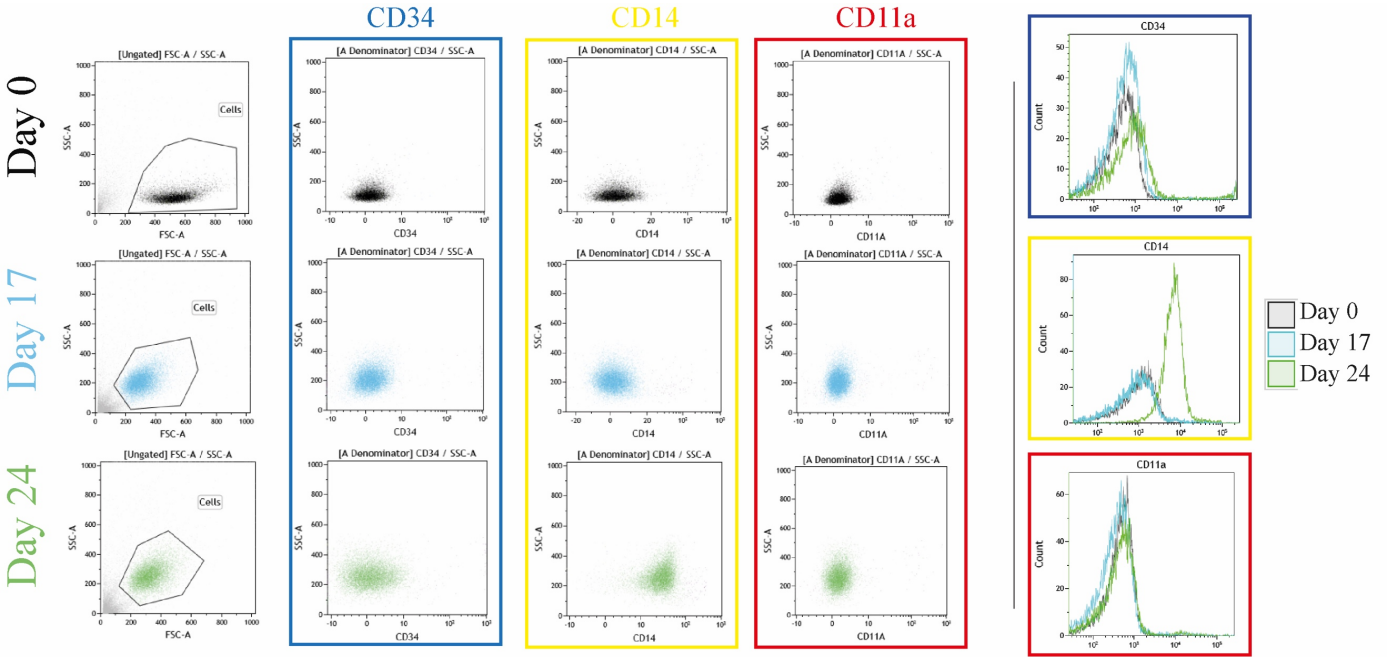

Figure 17: Immunophenotype tracking in long-term cell culture in sample P5.

Dot plots show selected markers of LAIP analysis of primary cells on day 0, 17 and 24. Markers CD11a, CD14 and CD34 are framed in their respective colors red, yellow and blue. Histograms on the right show shifts in marker expressions occurring over timer.

The *ex vivo* maintenance of primary AML cells induced partial differentiation in at least two samples but remained inconclusive for other samples. However, despite the immunophenotypic changes, both samples (P4 and P5) displayed proliferative activity across all assessed time points. Monocytic differentiation has been reported previously in *ex vivo* long-term cultures of adult primary AML cells and it has been suggested that cellular differentiation *ex vivo* may have clinical relevance[108,129]. However, a bigger cohort size is needed to elucidate if information on *ex vivo* cellular differentiation or changes in immunophenotype in long-term cultures is of relevance for clinical decision making in pediatric AML.

5.3.4. Impact of lowering GM-CSF concentrations in sample P4

Cytokine concentrations for *ex vivo* maintenance and expansion of primary AML cells are highly variable across different research groups, even though effects on AML cells can differ drastically depending on the exact composition and concentrations of cytokines. It has been demonstrated, that the cytokine GM-CSF is crucial for *ex vivo* maintenance of primary AML cells and is therefore included in many *ex vivo* AML cultures[130,131]. The role of GM-CSF in the differentiation of *ex vivo* cultured AML cells has not yet been established beyond its importance in *ex vivo* maintenance, since *ex vivo* studies on primary AML cells often focus on 72h drug screens without immunophenotype assessment. However, GM-CSF is a known driver of *in vivo* monocyte maturation and induces cellular differentiation of myeloid precursor cells *ex vivo* in a dose dependent manner[132–134].

Since differentiated cells might react differently to drug exposure than the original leukemic blasts we tested whether I) our cell culture conditions promote differentiation of AML cells and II) whether this can be avoided by reduction of GM-CSF concentrations without affecting AML cell proliferation and viability. To that end we reduced GM-CSF concentrations in sample P4 from 10nm to 1nM (10-fold) and 0.5nM (20-fold). Only cells cultured in standard cytokine concentrations (see Table 3) and the 10-fold reduction were measured, since the 20-fold reduction only yielded dead cells when inspected under the microscope. Cells cultured in 3D conditions with a 10-fold reduction of GM-CSF did not contain a viable cell fraction according to AnnexinV/7AAD staining (see Figure 18). This was concordant with the drop in total cell number which was reduced to 60% of the seeding number at day 3 and 80% at day 7. In contrast, cells cultured in 3D conditions with cytokine conditions according to Table 3 showed viable cell fractions at all measurement points and showed and 14-fold increase in cell number at day 14.

The experiment was performed exclusively with AML cells of sample P4, which showed that *ex vivo* maintenance and proliferation was not supported by a GM-CSF concentration of 1nM. Other samples were not subjected to lower cytokine concentrations and therefore this has to be considered as preliminary data. A higher number of samples will be needed to determine what range of GM-CSF concentration is supportive of *ex* vivo maintenance and proliferation and whether different concentrations trigger immunophenotypic changes across different genetic subtypes. Also, the effects of varying cytokine concentrations in general need to be addressed in future studies.

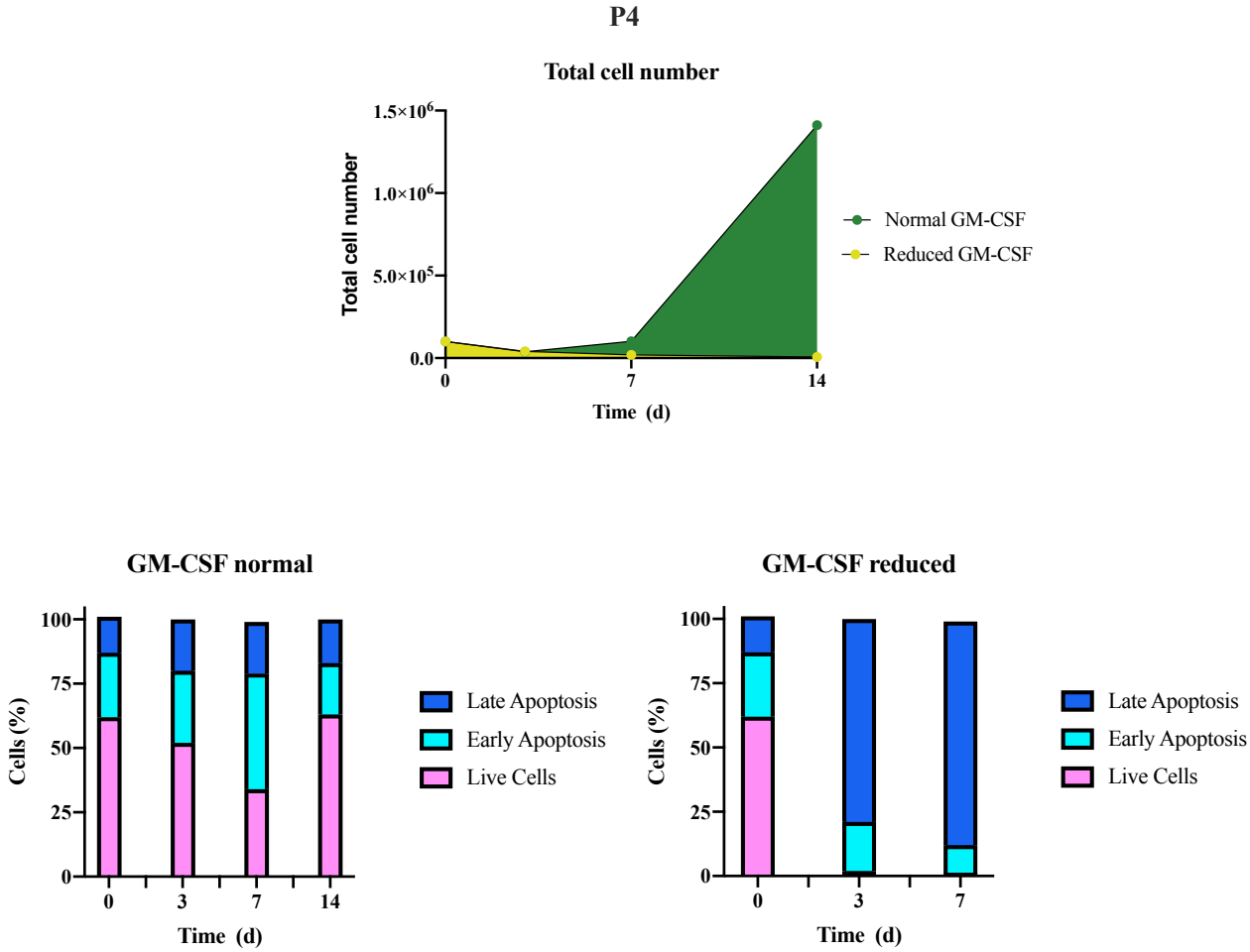

Figure 18: Reduction of GM-CSF in long-term cell cultures of primary cells in sample P4.

Primary cells were seeded after sorting in 3D methylcellulose medium with standard cytokine concentrations, except for GM-CSF which was reduced 10- and 20-fold. Total cell number and viability was assessed at day 3, 7 and 14 after seeding of cells cultured with the standard GM-CSF concentration and the 10-fold reduced concentration.

5.3.5. Validation of drug combination on primary cells

Due to a limiting number of cells obtained from some patients, we could not perform all the experiments with all of the samples. Therefore, we tested the efficacy of the combination Ruxolitinib and Venetoclax in single concentration combinations on samples from five different patients. Also, the combination of Ruxolitinib and Venetoclax was favoured over the Dasatinib and Venetoclax combination, since Ruxolitinib targets the JAK/STAT axis, which is known to be upregulated in pediatric AML[28]. Single drug concentrations were chosen based on results from cell line experiments as well as C_{max} values from clinical studies performed on adult patients. Cells of samples P5, P7, P8, P9 and P10 were sorted, and cultured in 3D Methylcellulose for at least 9 days, as described in pt.3.3.. . Again, AML samples were thawed

and sorted in succession. Cell number and apoptosis were assessed at different time points for all patient samples. P7 did not yield results due to the contamination of one of the wells.

AML cells of sample P5 were treated with a concentration of 500nM Ruxolitinib and 100 nM Venetoclax (see Figure 19). Untreated cells of sample P5 did not show strong proliferation in the assessed period (see Table 16). Cell number of the control and Ruxolitinib treated cells, increased by 60% over 17 days and cell viability was not affected in these cells. In contrast, Venetoclax treated cells were impaired in cellular proliferation and cell number increased by 6%. Consequently, cellular proliferation of AML cells treated with the combination at these concentrations was impaired as well. However, the combination did not induce apoptosis at tested concentrations.

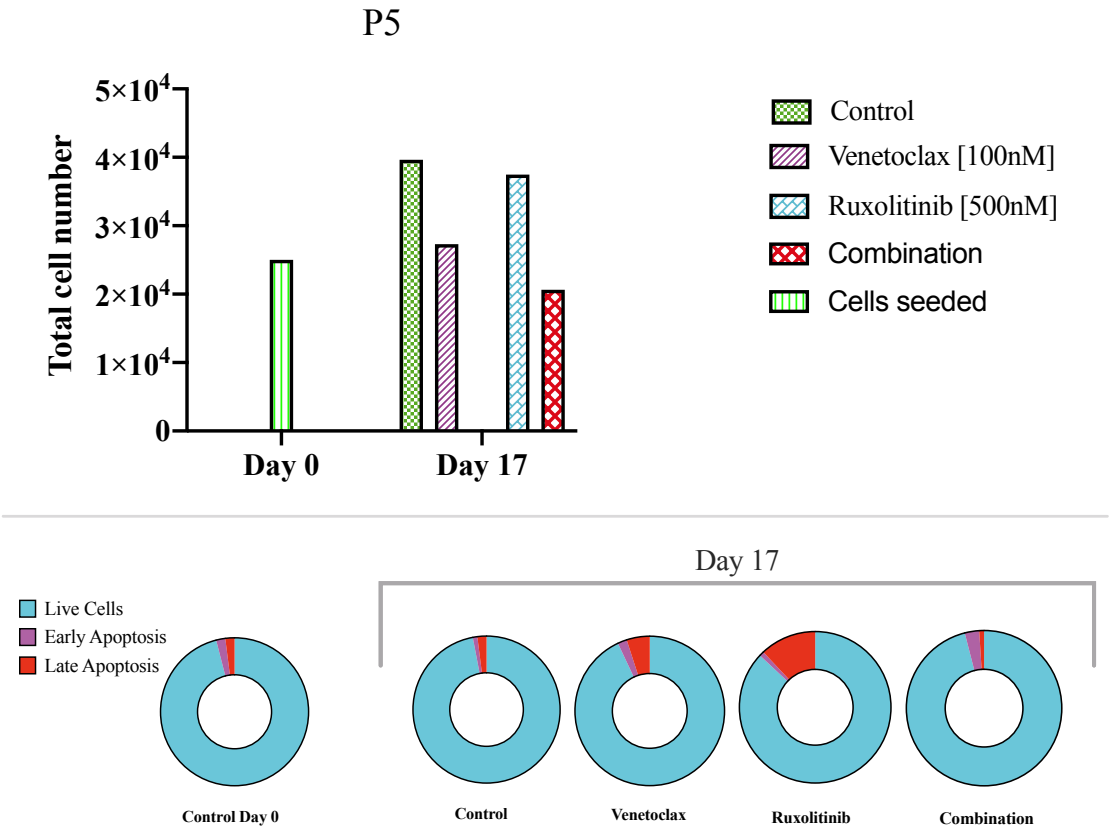

Figure 19: Cell number and cell viability of P5 when treated with Ruxolitinib + Venetoclax after 17 days.

Sorted blasts were treated with Ruxolitinib + Venetoclax and cultured for 17 days. Bar chart shows total cell number of samples, while circles graphs indicate cell viability. Measurements were not repeated.

Due to the low response of cells in sample P5 to the drug combination, following samples were subsequently treated with higher doses of each drug. Single drug concentrations were kept

under the C_{max} value of both drugs. Cells of samples P8, P9 and P10 were treated at concentrations 200nM Venetoclax and 1000nM Ruxolitinib.

Cells in sample P8 treated with the combination showed a decline in cell number to 20% of the initial seeding number at day 7 (see Figure 20). Although cells treated with the combination recovered in terms of cell number at day 14, relative cell viability in these cells decreased to 35%. Compared to the control, total cell number of combination treated cells dropped to 26% total, and 15% considering live cells (cells 7AAD and Annexin V negative) in samples at day 14. Cells treated with Ruxolitinib or Venetoclax alone, showed a 4- and 6-fold increase in cell number at day 14 as well as 86% and 83% viable cells.

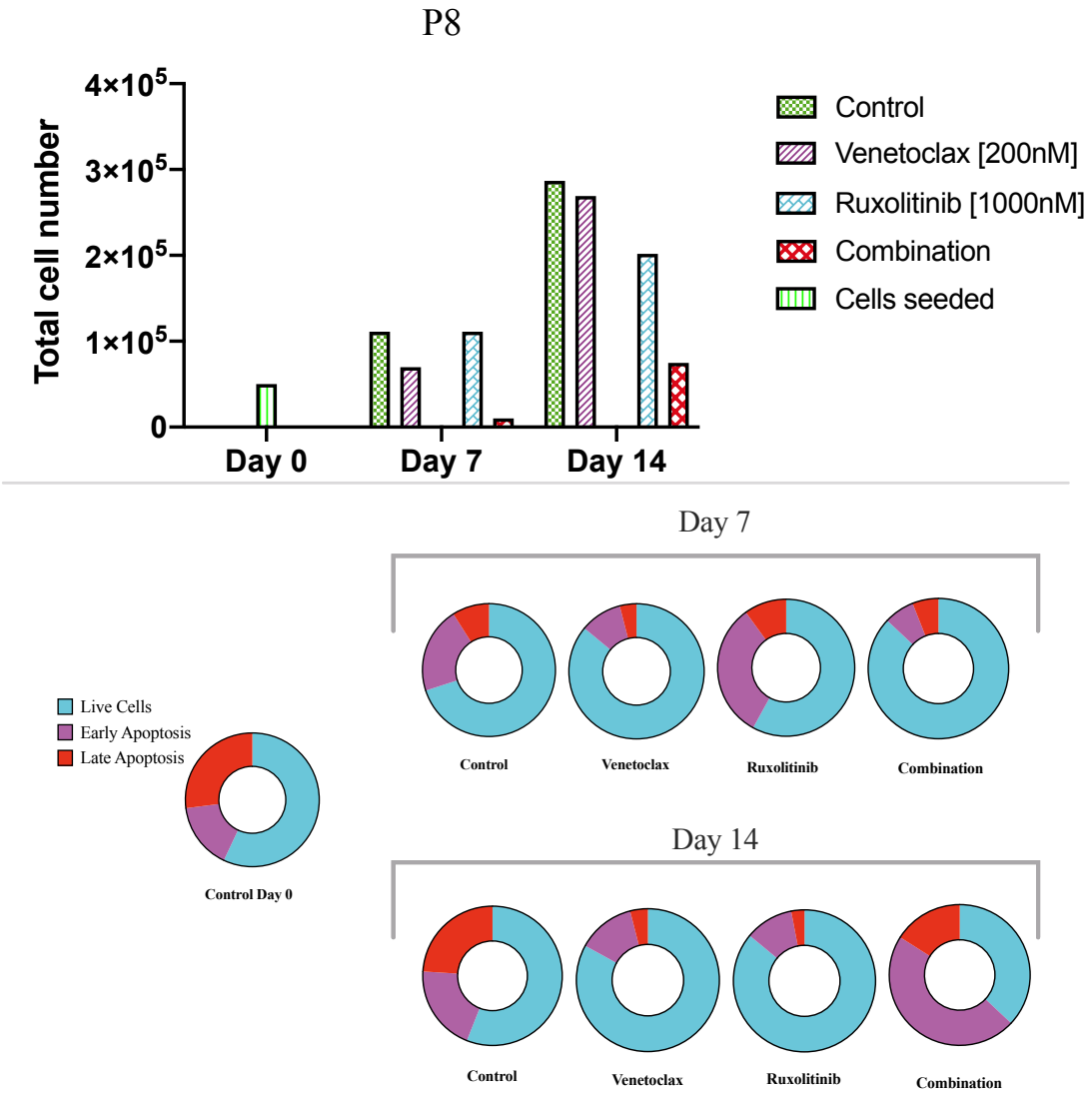

Figure 20: Cell number and cell viability of P8 when treated with Ruxolitinib + Venetoclax after day 7 and 14.

Sorted blasts were treated with Ruxolitinib + Venetoclax and cultured for 14 days. Bar chart shows total cell number of samples, while circles graphs indicate cell viability. Measurements were not repeated.

Cells of samples P9 and P10 were also treated with the combination Ruxolitinib and Venetoclax at concentrations 1000nM and 200nM respectively (see Figure 21). Viability and cell count were assessed at day 9 in both samples.

Although total cell number increased over time, untreated cells, as well as cells treated with Ruxolitinib or Venetoclax alone, had a live cell count of 31%,32% and 25% respectively. Total cell count after combination treatment was 19% of the control. Considering live cell count only, the combination treatment contained 2.4% viable cells compared with the control. Ruxolitinib and Venetoclax treated cells contained viable cell fractions of 72% and 73% respectively, when normalized to the controls live cell count.

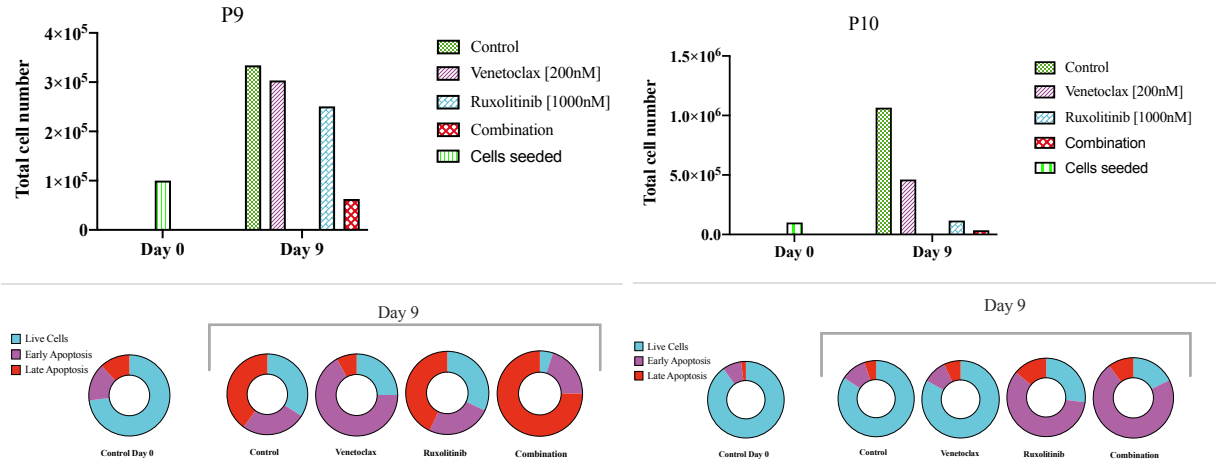

Figure 21: Cell number and cell viability of sample P9 and P10 on day 9 after combination treatment.

Sorted blasts were treated with Ruxolitinib + Venetoclax and cultured for 9 days. The bar charts show the total cell number of cells of samples P9 and P10, while circle graphs indicate cell viability of cells in these samples. Measurements were not repeated.

Compared to other samples, P10 had the strongest proliferating control but proofed to be more susceptible to single agent treatment and consequently also to combination treatment. Venetoclax treated cells were inhibited in proliferation and grew only to 42% of control but increased 4-fold when compared to the seeding number. Ruxolitinib treatment alone completely inhibited proliferation and reduced the viable cell fraction to 27%. Combination treated cells showed a decrease in total cell number to 3% when compared to the control at day 9 and contained a viable cell fraction of 19%.

The combination of Ruxolitinib and Venetoclax was tested on four patient samples, three of which were treated with the same concentrations. The effect of combination treatment and single agent treatment on primary AML cells varied across all tested samples (see Figure 22)

and did not display unambiguous synergism at tested concentrations. Considering the mean value only the observed effect of combination treatment on total cell number and live cell fractions is stronger than an additive effect. On average, Ruxolitinib and Venetoclax treatment alone reduced total cell number to 68% and 76% of the control, while the average effect of combination treatment reduced total cell number to 21%. Considering live cells only, combination treated cells were reduced to 1% of the control while Ruxolitinib and Venetoclax alone reduced live cells to 63% and 60% respectively.

Taking into account the high standard deviation and variable sensitivities to combination treatment of primary AML cells, the combination Ruxolitinib and Venetoclax had a greater effect on total cell count and live cell count of primary AML cells than a simple additive effect would suggest. However, a higher number of patient samples needs to be screened for sensitivity to this particular combination at a wider range of concentrations to unequivocally determine synergistic effects and quantify said effects.

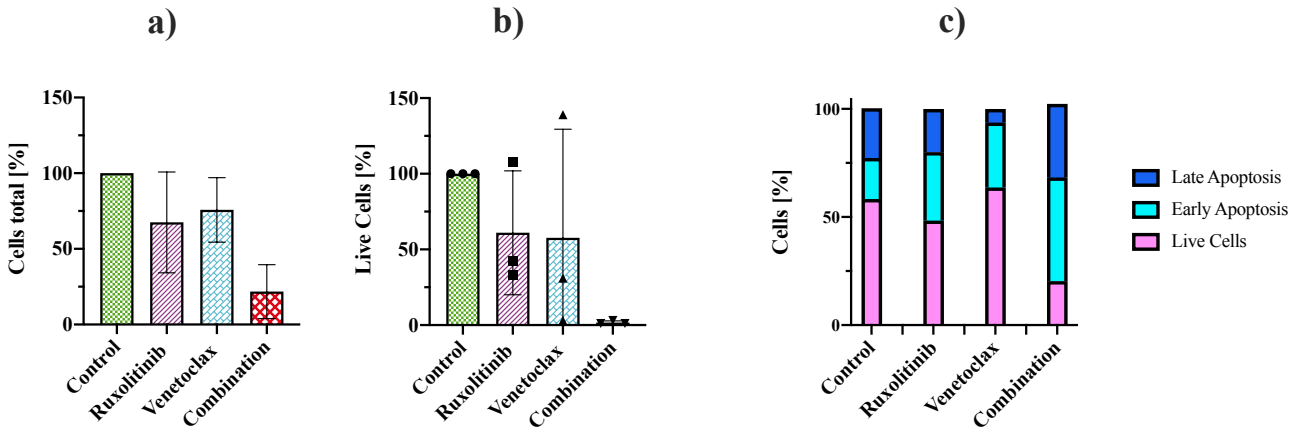

Figure 22: Sensitivity of patient samples P8, P9 and P10 to Ruxolitinib and Venetoclax combination treatment.

a) Total cell count of primary AML cells after treatment with Ruxolitinib and Venetoclax combination at 1000nM and 200nM as well as after single drug treatment determined by using Trucount tubes **b)** Live cell count of primary AML cells after treatment with Ruxolitinib and Venetoclax combination at 1000nM and 200nM as well as after single drug treatment through AnnexinV/7AAD staining **c)** Apoptosis assessment of primary AML cells after Ruxolitinib and Venetocalx treatment through AnnexinV/7AAD staining.

6. Summary of experiments and results

This small-scale study highlights the potential benefits and pitfalls of a long-term, multi parameter screening platform for drugs and drug combinations in pediatric AML cells *ex vivo* and demonstrates how a functional approach could identify previously unknown susceptibilities of leukemic AML blasts to combinations of pathway inhibitors. Additionally, its emphasize is on combinations of FDA approved single agents to accelerate the process of clinical translation of novel findings. Generated data provides insights into long-term *ex vivo* survival and maintenance of pediatric AML cells and demonstrates that innovations in pediatric AML therapy may profit greatly from functional multi parameter drug screen studies. Due to the small sample size, these results are considered preliminary data and further investigations will be necessary to confirm and consolidate these findings.

To identify drug combinations of agents with FDA approval, we first screened cell lines for susceptibility to combinations from a preselection of agents and quantified synergistic effects by using the bliss-independence model. We demonstrate the plausibility of combining agents that target nonoverlapping pathways, thus excluding combinations containing agents targeting the same pathway, same type of target (e.g. TK), feedback loops and up- and downstream effectors of each other. Cell lines with varying genetic aberrations relevant in AML carcinogenesis were therefore treated with combinations of drugs that were chosen based on a minimum of interaction on a molecular level. In total, we tested 15 different combinations, three of which were effective in at least two cell lines: Dasatinib + Venetoclax, Dinaciclib + Venelocalx and Ruxolitinib + Venetoclax. None of the combinations displayed significant antagonistic effects, while all combinations showed at least mild synergistic effects or additive effects in at least one cell line. The two combinations displaying the strongest synergistic effect by our metrics were Dasatinib + Venetoclax and Ruxolitinib + Venetoclax. Both combinations were able to reduce cell proliferation and induce apoptosis in HL-60 at lower concentrations than either agent alone. The combination Dasatinib + Venetoclax blocked cellular proliferation in HL-60 and induced apoptosis at concentrations 2500nM Dasatinib and 200nM Venetoclax, while remaining cells entered G0/G1phase. Also, the combination Ruxolitinib + Venetoclax was effective in reducing viable cell number at concentrations 1000nM and 200nM respectively in the cell line HL-60.

In parallel we assessed culturing conditions for long-term survival of primary AML cells *ex vivo*. To that end we used sorted AML blasts from 9 different patient samples with genetic aberrations stratifying them as IR or HR patients. When compared, 3D methylcellulose medium was superior to the corresponding 2D suspension culture model in supporting *ex vivo* maintenance and expansion of primary AML cells across samples P1 to P3. Also, 3D methylcellulose supported long-term *ex vivo* proliferation or at least survival across all patient samples, with a 6-fold increase in cell number on average and a live cell fraction of 67% on the last measured time point. The average days of primary AML cells kept in culture for all samples was 14 days and culturing conditions supported cellular survival and proliferation up to 24 days. In samples P4 and P5 we could show, that 3D culturing conditions triggered changes in immunophenotype of AML blasts after long-term culturing. Although the changes in immunophenotype indicate a partial monocyctic differentiation, the immunophenotype was incomplete and cells did not stop proliferating. A constant assessment of immunophenotype over the whole duration of the experiments was not achieved in the majority of patient samples, due to problems like contamination, insufficient cell number or incomplete immunophenotype.

In this setup, the effects of established drug combinations on primary AML cells could be monitored in a longer time frame and thus adding information depth on blast sensibility or resistance to a given agent over time. Therefore, we then proceeded to assess the efficacy of the established combination Ruxolitinib + Venetoclax in primary cells. We assessed effectiveness of this combination in four different patient samples. Although the effect of single agent and combination treatment on AML cells varied across patients, on average the effect on total cell number and live cell number suggests a stronger response than a simple additive effect.

The long-time setup with multi parameter readouts (i.e. total cell count and apoptosis) demonstrated, that the initial results obtained after a 72h drug screen, may not be entirely reflective of the actual cellular response, as demonstrated by the combinations effect on cells of sample P8 (see Figure 20). However, to unequivocally determine the combinations validity and its magnitude a higher number of patient samples needs to be screened for sensitivity to this particular combination at a wider range of concentrations.

7. Discussion

7.1. Identifying drug combinations based on nonoverlapping of targeted pathways

The value of using drug combinations of two or three agents in cancer therapy has been well established[94,135–137]. Given the vast heterogeneity in pediatric AML and the lack of novel FDA approved agents for its therapy, combination testing represents a convenient method to identify novel treatment options with agents already used in therapy for other cancers[58,84]. Choosing drug combinations of agents targeting different pathways and from different classes, has so far aided the search for drug combinations in preclinical studies[21,91,94]. This is also in accordance with the method we used to detect synergy between agents: the bliss independence model. Since the bliss independence model assumes that two given substances operate independent of one another at a molecular level and each one contributing to the end result independently, it was preferable to using e.g. isobolograms [19,38,43].

Cell lines are currently used as a robust preclinical model to assess the efficacy of novel drugs. However, different cell lines are almost certain to produce different results. Also, sample number of primary cells is limited due to the low incident rate of pediatric AML[49,50]. Therefore, we initially tested our combinations on three different AML cell lines and proceeded with drugs showing synergistic effects in more than one cell line. Combinations including the BH-3 mimetic Venetoclax were abundant, since the majority of other agents do not directly interfere with apoptosis induction[123]. The majority of combinations showed synergistic effects in at least one cell line. Of the 15 combinations tested, three combinations were effective in at least two cell lines with deviation from bliss values over 0.4: Dasatinib + Venetoclax, Dinaciclib + Venelocalx and Ruxolitinib + Venetoclax.

Even though only a few combinations showed prominent synergistic effects in AML cell lines, it is likely that combinations displaying lesser effects in this setup may be successful in a clinical setting as well. Depending on future applications, it might be sufficient to use a combination, which displays synergistic effect over a wider range of concentrations (such as Sorafenib + Venetoclax and Trametinib + Venetoclax) rather than a combination showing a peak in synergy at a specific concentration (see Figure 23)[38,43]. E.g. the combination of BCL-2 Inhibitor Venetoclax and the MEK inhibitor Trametinib did not show high *deviation from bliss* values,

rather it produced intermediate results over a wider range of tested concentrations. Considering the obstacles and pitfalls of clinical translation, it is important to be aware of parameters such as the synergistic effects happening at certain concentrations and pharmacokinetic data (e.g. C_{max} and AUC) when available in preclinical models. These should be considered to exclude combinations of agents which would not be able to reach the specific concentrations required to act in a synergistic manner[92,102,103,138].

To that end, we displayed the sum of *deviation from bliss* values of all tested concentrations in a heatmap to visualize which combinations displayed sub-additive effects over a wider range of concentrations. The combinations Dasatinib + Venetoclax, Dinaciclib + Venetoclax and Ruxolitinib + Venetoclax displayed synergistic effects over a wider range of concentrations than other combinations. Notably, this parameter is only suitable to roughly capture the range of tested concentrations at which a given combination is effective in the used setup.

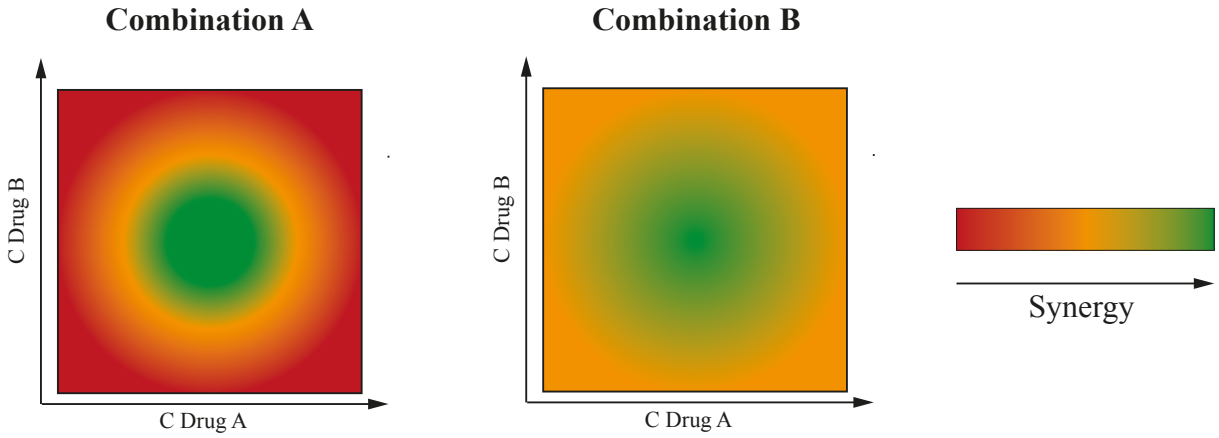

Figure 23: Hypothetical synergy dynamics.

Drug combinations can display two different effects in terms of synergy. The hypothetical Combination A shows a high deviation from bliss value at a specific concentration range, whereas Combination B produced intermediate values but over a wider range of concentrations.

In this study we established, that combinations including the BH-3 mimetic Venetoclax and a relative unspecific TKI produced the highest effects in AML cell lines such as the combination of the TKI inhibitor Dasatinib or the Janus-associated kinase inhibitor Ruxolitinib in combination with Venetoclax. Due to the metrics we used to determine agents for combinations (i.e. targeting nonoverlaping pathways), there was a bias for combinations including the BH-3 mimetic Venetoclax since it inhibits a mitochondrial pathway rather than a pathway localized in the cytoplasm[123,139]. Kurtz et.al. report similar findings for a variety of hematopoietic malignancies occurring in adults[91].

In concordance with our findings, a clinical trial currently in the recruitment phase will investigate the potency of the BH-3 mimetic Venetoclax with the MEK inhibitor Cobimetinib adult AML (ClinicalTrials.gov ID code NCT02670044). Notably, we used Trametinib (a MEK-MAPK/ERK inhibitor) rather than Cobimetinib, confirming the feasibility of targeting these pathways. Off-note, combinations reported to have superior effects in similar preclinical models by other groups (e.g. Idasanutlin + Venetoclax), could not be replicated using our approach[117].

We certainly overlooked several important combinations due to a variety of factors such as: selection bias, synergy definition model and operator errors. However, since combinations of SMI have largely remained unexplored so far in pediatric AML, these findings warrant further analysis of established combinations. Future studies will focus on validating multiple combinations and the effect of the combinations on the activation status of certain signaling molecules as well as the duration of pathway inhibition. Another important aspect is, whether functional drug combination screens in pediatric AML will identify combinations that precisely target products of genetic aberrations as well as whether similar combinations are effective in the adult form of AML and vice versa.

7.2. Long-term cell culture of primary AML cells

Ex vivo expansion and long-term survival of pediatric AML cells and AML cells in general are rarely reported and often feature specific and particular protocols and complex systems. There is considerable inter laboratory variation and publications do not always disclose relevant culturing parameters. The current methodological landscape for long-term culturing of AML cells includes: the expansion of leukemic stem-cells with a specific phenotype rather than the bulk of leukemic blasts; usage of SMI to inhibit certain pathways to maintain long-term *ex vivo* survival of AML cells, co-cultures with bone marrow mesenchymal stromal cells and unique and novel scaffold technologies mimicking physiological conditions[108,108,109,113,115]. Due to the multiplicity of approaches, there is no standard protocol or even a standard definition of the time span referred to as “long-term”. Therefore, we compared two systems which are readily available. Also, we considered “long-term” cultures comprising a time span in which cellular processes such as immunophenotype maturation, proliferation and clonal selection can be observed if present.

3D methylcellulose medium supplemented with defined cytokines proved to be better suited for long-term *ex vivo* expansion and survival of primary AML cells than the corresponding 2D suspension culture model. Compared to cytokine concentrations found in literature for similar studies, we used concentrations 50% lower than other research groups[108]. Nevertheless, we were able to culture and extract usable data from primary cells up to 24 days and found that used conditions were still able to support *ex vivo* survival and also proliferation in the majority of tested samples.

A significant drawback of methylcellulose medium is its semi solid state, which requires precise handling from the operators perspective. The long-term cultures also increase the risk of contamination. Also, when considering upscaling and automation the semi solid state poses a considerable challenge and cost factor.

Usage of specific cytokines to sustain *ex vivo* cancer cell cultures and their concentrations are still subject to discussion and there is significant inter laboratory divergence. Especially considering long-term cell cultures, there is the possibility of cellular differentiation triggered by present cytokine. On the other hand, cell cultures without cytokines have not been reported to support long-term survival of AML cells *ex vivo* at all. It has been demonstrated that requirements for *ex vivo* maintenance are variable in terms of basic cytokine requirements[131,140,141]. This is probably reflective of the fact that there is a high intra patient heterogeneity concerning the tumor microenvironment and cytokine concentrations *in vivo*[108,142,143]. However, these complex dynamics are hard to capture and replicate *ex vivo* and using composite culturing systems, such as co-cultures of bone marrow mesenchymal stromal cells, do not clarify which cytokines are important and which could be omitted. This was highlighted by the fact that a 10-fold reduction in GM-CSF levels did not support cell survival in cells of sample P4 and emphasized the necessity of assessing cytokine sensitivity in multiple patient samples in future studies.

Since samples tested exclusively consisted of IR and HR patient cells, we could not unequivocally conclude whether *ex vivo* growth characteristics corresponded with a specific risk group or carry any prognostic value. AML cells of IR and HR patient samples differed in terms of proliferation and size of live cell fractions after long-term culture, however, among the four strongest proliferating samples, three harbored KMT2A fusion event. To ultimately determine whether *ex vivo* growth and survival characteristics reflect the molecular landscape of pediatric AML or whether it can be linked to disease outcome, a bigger cohort size including LR patients will be necessary. Also, we observed partial differentiation patterns in two samples

during long-term cultures. However, the cells in these samples still kept proliferating. Other research groups have observed similar results in adult AML cells with double the concentration of cytokines and linked the capacity of long-term in vitro survival or AML cells to adverse disease outcomes regardless of cellular differentiation[108,129]. The experimental setup and procedures presented in this thesis provide the benefit of being able to monitor multiple parameters from long-term cell cultures, however a higher number samples needs to be analyzed to statistically validate observed results.

7.3. Drug combinations in primary cells

The long-term setup for the assessment of drug combination efficacy in AML cells has the potential to answer several important questions regarding drug efficacy and clinical translation such as: I) Does the drug combination induce cellular differentiation over time in *ex vivo* or *in vivo* conditions? II) How durable is the effect of the combination on AML cells? III) How long are targeted agents able to inhibit their respective target and signaling pathways? IV) Which cellular processes important to carcinogenesis are affected? V) Considering the same parameters, are there differences in efficacy of drug combinations on AML cells between long-term and short-term studies? VI) Will SMI combinations effective in adult AML display the same efficacy in pediatric AML? The scale and layout of this study allows for addressing some key points regarding these issues.

Of the identified combinations effective in cell lines, we validated the efficacy of the combination Ruxolitinib + Venetoclax on cells of four different patient samples. Ruxolitinib is a known inhibitor of JAK1 and 2 and consequently reduces STAT signaling, which was shown to be upregulated in pediatric AML cells[28,144,145]. Therefore, this combination was of particular interest for this study. Since we used single concentrations a quantitative assessment of synergy was not possible, however the combination did indicate that the effect on total cell number and cell viability was stronger than an additive effect. The significance of combinations containing Venetoclax and a broader TKI has been previously described by Kurtz et.al.. However, these results were obtained using adult hematopoietic cancer cells and were also performed only in a 72h drug screen[91]. Further investigations in this matter will be necessary to identify whether this combination is equally effective in adult and pediatric AML[146]. Results presented here however are preliminary data, and more primary AML cells with a variety of genetic aberrations need to be tested for sensitivity to this combination at a wider range of concentrations to obtain results with statistical significance.

Sample P8 can be used as a representative example of how long-term drug screens can augment current screening efforts. In this case, cells were cultured for 17 days and results differed based on the time point at which apoptosis and cell number were assessed. This underscores the importance of investigating not only important parameters such as apoptosis and cell viability but also the also the duration of growth and pathway inhibition. Especially in preclinical studies, the evaluation of additional parameters can bolster the efforts a new drug or drug combination to withstanding the rigorous selection process implemented by the clinical

In this study, we have demonstrated that leukemic blasts are able to survive in long-term cultures under specific conditions, and that this system can be used for the evaluation of cellular response to exogenous perturbations. The necessity for long-term screening platforms is self-evident, when considering the complete lack thereof in scientific publications. Nevertheless, data generated from long-term platforms has the potential of yielding important insights regarding the effects on novel drug combinations on cancer cells in a therapy relevant time frame and augmenting existing disease models[108]. In this regard, it is also important to prospectively collect patient samples specifically for this type of functional screening.

8. Conclusion and outlook

The continuous efforts undertaken to further identify genetic heterogeneity in pediatric AML have identified a number of actionable and potentially actionable targets[52,58]. However, these findings have so far, been unable to produce targeted therapies for this disease, let alone specific subtypes thereof[11,16]. Aside from explorative tyrosine kinase inhibitors, innovation in treatment options for pediatric AML has been negligible. Additionally, the use of investigational FLT-3 inhibitors still faces the challenge of nondurable responses as well as the development of resistances during the course of therapy[84,147]. Therefore, we hypothesized that a long-term functional phenotype-driven drug sensitivity assay using novel drug combinations of promising FDA-approved drugs may yield critical insights into potential novel options for targeted therapy.

Considering the vast improvements to therapies in other cancers, it is warranted to say that the molecular vulnerabilities of pediatric AML have not been fully utilized so far and input from functional platforms is still marginal[15]. We demonstrated the feasibility of using a functional screening platform to assess sensibility of AML cells to novel drug combinations and the benefits of extending the duration of such experiments to obtain novel insight into AML blast behavior upon exposure to therapy. Such a functional long-term screening platform also carries the potential to create a framework to assess numerus novel parameters in a format that is realizable in most laboratories. For instance, there are still plenty of unexplored experiments to further assess vulnerabilities from a functional standpoint which can be performed in this framework such as: dynamic BH-3 profiling, patient-derived xenograft models and innovative drug screening models[11,16]. Our experiments demonstrated, that by extending the time frame of a standard experiment, novel insight could be obtained regarding sensitivities to novel drug combinations. If implemented at diagnosis, results obtained from this long-term assay could influence clinical decision making for patients with poor or no response to standard treatment and relapsed patients by elucidating blast specific vulnerabilities to specific agents over time. If cell death does not occur in blasts, it still crucial to know, what the cancer cell will do and what it´s impact on patient survival or recovery will be. Also, this system would offer the opportunity to mimic patient specific reactions, such as cytokine spikes, to give clues on dosage and timing of drug administration.

Since a functional screen uses exogenous perturbations of AML cells, this process is highly advantageous when assessing aberrant information flow through cellular signaling pathways and how these are impacted by targeted drugs[90]. Another important aspect of using long-term

assays is to determine the duration of pathway inhibition, which for most drugs is an unknown parameter. Using methods such as phospho-profiling, inhibition duration and alternative signaling after drug exposure can be elucidated and this information can be applied to refine combination treatment.

The general use of exogenous perturbations has so far been the starting point of virtually every new substance on the market and in clinics. Hence, determining cellular sensitivities by using functional platforms, is a highly iterative process and factors such as automation and upscaling are decisive factors of a platforms long-term performance. From this perspective, the semi solid state of methylcellulose as used in our experiments is at a disadvantage since its viscosity poses a challenge to conventional pumps designed for liquid medium and investments in novel designs for such systems are warranted.

Since the molecular landscape in pediatric AML is a highly dynamic one, it is important to implement novel therapeutic strategies and combination therapy has shown to be incremental for future innovations in cancer therapy[148]. Currently, development of drug combinations is transitioning from an empirical to a more targeted approach[149–151]. The undertaking of choosing drug combinations so far has been often based on a trial and error approach which warranted highly iterative process. In contrast, if the number of agents for combinations is limited to FDA approved drugs, the number of possible combinations is smaller and favorable pharmacokinetic and –dynamic data can be incorporated in the decision-making process. Our findings suggest, that using FDA approved drugs greatly accelerates the process of clinical translation since identified combinations such as Dasatinib+Venetoclax and Ruxolitinib+Venetoclax can readily be implemented in therapy.

Although the number of FDA approved SMIs is steadily increasing, there is still a plethora of pathway molecules that lack a specific inhibitor and cumulative information obtained from functional screenings and structural information of SMIs could be used to be implemented in machine learning-based programs to identify suitable combinations as well as predicting structural analogs of inhibitors to steer their efficacy[139,152–155]

Universal targeted cancer therapy is as of yet, an elusive concept[11]. Current scientific knowledge has highlighted the discrepancy between identifying the underlying genetic causes of pediatric AML and the lack of correspondent therapeutic advances. This thesis aimed to address the possibility of using FDA approved drugs to establish effective combinations and set a framework for a long-term drug screening platform. Although preliminary data is

presented here, some key aspects have been highlighted regarding long-term drug screens of novel drug combinations as well as the potential of this platform to improve therapeutic options in pediatric AML in the future.

9. References

1. Ferlay, J. *et al.* Estimating the global cancer incidence and mortality in 2018: GLOBOCAN sources and methods. *Int. J. Cancer* **144**, 1941–1953 (2019).
2. Bray, F. *et al.* Global cancer statistics 2018: GLOBOCAN estimates of incidence and mortality worldwide for 36 cancers in 185 countries. *CA. Cancer J. Clin.* **68**, 394–424 (2018).
3. Bray, F., Ren, J.-S., Masuyer, E. & Ferlay, J. Global estimates of cancer prevalence for 27 sites in the adult population in 2008. *Int. J. Cancer* **132**, 1133–1145 (2013).
4. Tarver, T. Cancer Facts & Figures 2012. American Cancer Society (ACS): *Atlanta, GA: American Cancer Society, 2012. 66 p., pdf. Available from. J. Consum. Health Internet* **16**, 366–367 (2012).
5. Vogelstein, B. *et al.* Cancer Genome Landscapes. *Science* **339**, 1546–1558 (2013).
6. Hanahan, D. & Weinberg, R. A. Hallmarks of Cancer: The Next Generation. *Cell* **144**, 646–674 (2011).
7. Tricoli, J. V. *et al.* Biologic and clinical characteristics of adolescent and young adult cancers: Acute lymphoblastic leukemia, colorectal cancer, breast cancer, melanoma, and sarcoma: Biology of AYA Cancers. *Cancer* **122**, 1017–1028 (2016).
8. Sweet-Cordero, E. A. & Biegel, J. A. The genomic landscape of pediatric cancers: Implications for diagnosis and treatment. *Science* **363**, 1170–1175 (2019).
9. Steliarova-Foucher, E., Stiller, C., Lacour, B. & Kaatsch, P. International Classification of Childhood Cancer, third edition. *Cancer* **103**, 1457–1467 (2005).
10. Campbell, B. B. *et al.* Comprehensive Analysis of Hypermutation in Human Cancer. *Cell* **171**, 1042-1056.e10 (2017).
11. Letai, A. Functional precision cancer medicine—moving beyond pure genomics. *Nat. Med.* **23**, 1028–1035 (2017).
12. Druker, B. J. *et al.* Efficacy and Safety of a Specific Inhibitor of the BCR-ABL Tyrosine Kinase in Chronic Myeloid Leukemia. *N. Engl. J. Med.* **344**, 1031–1037 (2001).
13. Tsherniak, A. *et al.* Defining a Cancer Dependency Map. *Cell* **170**, 564-576.e16 (2017).
14. Lawrence, M. S. *et al.* Discovery and saturation analysis of cancer genes across 21 tumour types. *Nature* **505**, 495–501 (2014).
15. PCAWG Drivers and Functional Interpretation Working Group *et al.* Pathway and network analysis of more than 2500 whole cancer genomes. *Nat. Commun.* **11**, 729 (2020).
16. Friedman, A. A., Letai, A., Fisher, D. E. & Flaherty, K. T. Precision medicine for cancer with next-generation functional diagnostics. *Nat. Rev. Cancer* **15**, 747–756 (2015).
17. Jain, N. & O'Brien, S. Targeted therapies for CLL: Practical issues with the changing treatment paradigm. *Blood Rev.* **30**, 233–244 (2016).

18. Lo-Coco, F. *et al.* Retinoic Acid and Arsenic Trioxide for Acute Promyelocytic Leukemia. *N. Engl. J. Med.* **369**, 111–121 (2013).
19. Wu, P., Nielsen, T. E. & Clausen, M. H. Small-molecule kinase inhibitors: an analysis of FDA-approved drugs. *Drug Discov. Today* **21**, 5–10 (2016).
20. Fedorov, O., Müller, S. & Knapp, S. The (un)targeted cancer kinome. *Nat. Chem. Biol.* **6**, 166–169 (2010).
21. Roskoski, R. Properties of FDA-approved small molecule protein kinase inhibitors: A 2020 update. *Pharmacol. Res.* **152**, 104609 (2020).
22. Manning, G. The Protein Kinase Complement of the Human Genome. *Science* **298**, 1912–1934 (2002).
23. Scott, D. E., Bayly, A. R., Abell, C. & Skidmore, J. Small molecules, big targets: drug discovery faces the protein–protein interaction challenge. *Nat. Rev. Drug Discov.* **15**, 533–550 (2016).
24. Arkin, M. R., Tang, Y. & Wells, J. A. Small-Molecule Inhibitors of Protein-Protein Interactions: Progressing toward the Reality. *Chem. Biol.* **21**, 1102–1114 (2014).
25. Li, B., Rong, D. & Wang, Y. Targeting Protein-Protein Interaction with Covalent Small-Molecule Inhibitors. *Curr. Top. Med. Chem.* **19**, 1872–1876 (2019).
26. Walz, C. *et al.* Essential role for Stat5a/b in myeloproliferative neoplasms induced by BCR-ABL1 and JAK2V617F in mice. *Blood* **119**, 3550–3560 (2012).
27. Vainchenker, W. & Constantinescu, S. N. JAK/STAT signaling in hematological malignancies. *Oncogene* **32**, 2601–2613 (2013).
28. Schumich, A. *et al.* Phospho-Profiling Linking Biology and Clinics in Pediatric Acute Myeloid Leukemia: *HemaSphere* 1 (2019) doi:10.1097/HS9.0000000000000312.
29. Eyre, T. A. *et al.* Efficacy of venetoclax monotherapy in patients with relapsed, refractory mantle cell lymphoma after Bruton tyrosine kinase inhibitor therapy. *Haematologica* **104**, e68–e71 (2019).
30. Mokhtari, R. B. *et al.* Combination therapy in combating cancer. *Oncotarget* **8**, (2017).
31. Döhner, H. *et al.* Diagnosis and management of acute myeloid leukemia in adults: recommendations from an international expert panel, on behalf of the European LeukemiaNet. *Blood* **115**, 453–474 (2010).
32. Oran, B. & Weisdorf, D. J. Survival for older patients with acute myeloid leukemia: a population-based study. *Haematologica* **97**, 1916–1924 (2012).
33. Shafer, D. & Grant, S. Update on rational targeted therapy in AML. *Blood Rev.* **30**, 275–283 (2016).
34. Sasine, J. P. & Schiller, G. J. Emerging strategies for high-risk and relapsed/refractory acute myeloid leukemia: Novel agents and approaches currently in clinical trials. *Blood Rev.* **29**, 1–9 (2015).

35. Walasek, A. The new perspectives of targeted therapyin acute myeloid leukemia. *Adv. Clin. Exp. Med.* **28**, 271–276 (2019).
36. Pagliarini, R., Shao, W. & Sellers, W. R. Oncogene addiction: pathways of therapeutic response, resistance, and road maps toward a cure. *EMBO Rep.* **16**, 280–296 (2015).
37. Luo, J., Solimini, N. L. & Elledge, S. J. Principles of Cancer Therapy: Oncogene and Non-oncogene Addiction. *Cell* **136**, 823–837 (2009).
38. Chou, T.-C. Theoretical Basis, Experimental Design, and Computerized Simulation of Synergism and Antagonism in Drug Combination Studies. *Pharmacol. Rev.* **58**, 621–681 (2006).
39. Chou, T.-C. Preclinical *versus* clinical drug combination studies. *Leuk. Lymphoma* **49**, 2059–2080 (2008).
40. Long, G. V. *et al.* Combined BRAF and MEK inhibition versus BRAF inhibition alone in melanoma. *N. Engl. J. Med.* **371**, 1877–1888 (2014).
41. Chou, T.-C. Drug Combination Studies and Their Synergy Quantification Using the Chou-Talalay Method. *Cancer Res.* **70**, 440–446 (2010).
42. Goldoni, M. & Johansson, C. A mathematical approach to study combined effects of toxicants in vitro: Evaluation of the Bliss independence criterion and the Loewe additivity model. *Toxicol. In Vitro* **21**, 759–769 (2007).
43. Foucquier, J. & Guedj, M. Analysis of drug combinations: current methodological landscape. *Pharmacol. Res. Perspect.* **3**, e00149 (2015).
44. Cheson, B. D. *et al.* Report of the National Cancer Institute-sponsored workshop on definitions of diagnosis and response in acute myeloid leukemia. *J. Clin. Oncol.* **8**, 813–819 (1990).
45. Campo, E. *et al.* The 2008 WHO classification of lymphoid neoplasms and beyond: evolving concepts and practical applications. *Blood* **117**, 5019–5032 (2011).
46. Reilly, J. T. Pathogenesis of acute myeloid leukaemia and inv(16)(p13;q22): a paradigm for understanding leukaemogenesis? *Br. J. Haematol.* **128**, 18–34 (2005).
47. De Kouchkovsky, I. & Abdul-Hay, M. 'Acute myeloid leukemia: a comprehensive review and 2016 update'. *Blood Cancer J.* **6**, e441–e441 (2016).
48. Shallis, R. M., Wang, R., Davidoff, A., Ma, X. & Zeidan, A. M. Epidemiology of acute myeloid leukemia: Recent progress and enduring challenges. *Blood Rev.* **36**, 70–87 (2019).
49. Pession, A. *et al.* Results of the AIEOP AML 2002/01 multicenter prospective trial for the treatment of children with acute myeloid leukemia. *Blood* **122**, 170–178 (2013).
50. Spix, C., Frank, M., Grabow, D. & Kaatsch, P. Die Langzeitüberlebenden-Kohorte des Deutschen Kinderkrebsregisters – Datenlage und Response-Verhalten. *63 Jahrestag. Dtsch. Ges. Für Med. Inform.* Biometrie und Epidemiologie e.V. (GMDS) (2018) doi:10.3205/18GMDS118.

51. Creutzig, U. *et al.* Diagnosis and management of acute myeloid leukemia in children and adolescents: recommendations from an international expert panel. *Blood* **120**, 3187–3205 (2012).
52. Zwaan, C. M. *et al.* Collaborative Efforts Driving Progress in Pediatric Acute Myeloid Leukemia. *J. Clin. Oncol.* **33**, 2949–2962 (2015).
53. Rasche, M. *et al.* Successes and challenges in the treatment of pediatric acute myeloid leukemia: a retrospective analysis of the AML-BFM trials from 1987 to 2012. *Leukemia* **32**, 2167–2177 (2018).
54. Creutzig, U. *et al.* Favorable outcome in infants with AML after intensive first- and second-line treatment: an AML-BFM study group report. *Leukemia* **26**, 654–661 (2012).
55. Stevens, R. F., Hann, I. M., Wheatley, K., Gray, R. G. & on behalf of the MRC Childhood Leukaemia Working Party. Marked improvements in outcome with chemotherapy alone in paediatric acute myeloid leukaemia: results of the United Kingdom Medical Research Council's 10th AML trial. *Br. J. Haematol.* **101**, 130–140 (1998).
56. Tomizawa, D. *et al.* Appropriate dose reduction in induction therapy is essential for the treatment of infants with acute myeloid leukemia: a report from the Japanese Pediatric Leukemia/Lymphoma Study Group. *Int. J. Hematol.* **98**, 578–588 (2013).
57. Balgobind, B. V. *et al.* Integrative analysis of type-I and type-II aberrations underscores the genetic heterogeneity of pediatric acute myeloid leukemia. *Haematologica* **96**, 1478–1487 (2011).
58. Bolouri, H. *et al.* The molecular landscape of pediatric acute myeloid leukemia reveals recurrent structural alterations and age-specific mutational interactions. *Nat. Med.* **24**, 103–112 (2018).
59. Mercher, T. & Schwaller, J. Pediatric Acute Myeloid Leukemia (AML): From Genes to Models Toward Targeted Therapeutic Intervention. *Front. Pediatr.* **7**, 401 (2019).
60. Farrar, J. E. *et al.* Genomic Profiling of Pediatric Acute Myeloid Leukemia Reveals a Changing Mutational Landscape from Disease Diagnosis to Relapse. *Cancer Res.* **76**, 2197–2205 (2016).
61. Mrózek, K., Heinonen, K. & Bloomfield, C. D. Clinical importance of cytogenetics in acute myeloid leukaemia. *Best Pract. Res. Clin. Haematol.* **14**, 19–47 (2001).
62. Swerdlow, S. *et al. WHO classification of Tumors of Haematopoietic and Lymphoid Tissues. Lyon: IARC (2008).*
63. Bennett, J. M. *et al.* Proposals for the Classification of the Acute Leukaemias French-American-British (FAB) Co-operative Group. *Br. J. Haematol.* **33**, 451–458 (1976).
64. Walter, R. B. *et al.* Significance of FAB subclassification of "acute myeloid leukemia, NOS" in the 2008 WHO classification: analysis of 5848 newly diagnosed patients. *Blood* **121**, 2424–2431 (2013).

65. Vardiman, J. W. *et al.* The 2008 revision of the World Health Organization (WHO) classification of myeloid neoplasms and acute leukemia: rationale and important changes. *Blood* **114**, 937–951 (2009).

66. Arber, D. A. *et al.* The 2016 revision to the World Health Organization classification of myeloid neoplasms and acute leukemia. *Blood* **127**, 2391–2405 (2016).

67. Maassen, A. *et al.* Validation and proposals for a refinement of the WHO 2008 classification of myelodysplastic syndromes without excess of blasts. *Leuk. Res.* **37**, 64–70 (2013).

68. Döhner, H., Weisdorf, D. J. & Bloomfield, C. D. Acute Myeloid Leukemia. *N. Engl. J. Med.* **373**, 1136–1152 (2015).

69. Ossenkoppele, G. J., Janssen, J. J. W. M. & van de Loosdrecht, A. A. Risk factors for relapse after allogeneic transplantation in acute myeloid leukemia. *Haematologica* **101**, 20–25 (2016).

70. Röllig, C. *et al.* Long-Term Prognosis of Acute Myeloid Leukemia According to the New Genetic Risk Classification of the European LeukemiaNet Recommendations: Evaluation of the Proposed Reporting System. *J. Clin. Oncol.* **29**, 2758–2765 (2011).

71. Buldini, B. *et al.* Prognostic significance of flow-cytometry evaluation of minimal residual disease in children with acute myeloid leukaemia treated according to the AIEOP-AML 2002/01 study protocol. *Br. J. Haematol.* **177**, 116–126 (2017).

72. Theunissen, P. *et al.* Standardized flow cytometry for highly sensitive MRD measurements in B-cell acute lymphoblastic leukemia. *Blood* **129**, 347–357 (2017).

73. Buldini, B., Maurer-Granofszky, M., Varotto, E. & Dworzak, M. N. Flow-Cytometric Monitoring of Minimal Residual Disease in Pediatric Patients With Acute Myeloid Leukemia: Recent Advances and Future Strategies. *Front. Pediatr.* **7**, 412 (2019).

74. Rubnitz, J. E. *et al.* Minimal residual disease-directed therapy for childhood acute myeloid leukaemia: results of the AML02 multicentre trial. *Lancet Oncol.* **11**, 543–552 (2010).

75. Loken, M. R. *et al.* Residual disease detected by multidimensional flow cytometry signifies high relapse risk in patients with de novo acute myeloid leukemia: a report from Children's Oncology Group. *Blood* **120**, 1581–1588 (2012).

76. Creutzig, U. *et al.* Randomized trial comparing liposomal daunorubicin with idarubicin as induction for pediatric acute myeloid leukemia: results from Study AML-BFM 2004. *Blood* **122**, 37–43 (2013).

77. Ritter, J., Creutzig, U. & Schellong, G. Treatment results of three consecutive German childhood AML trials: BFM-78, -83, and -87. AML-BFM-Group. *Leukemia* **6 Suppl 2**, 59–62 (1992).

78. Kaspers, G. J. L. *et al.* Improved Outcome in Pediatric Relapsed Acute Myeloid Leukemia: Results of a Randomized Trial on Liposomal Daunorubicin by the International BFM Study Group. *J. Clin. Oncol.* **31**, 599–607 (2013).

79. Creutzig, U., Dworzak, M. & Reinhardt, D. Akute myeloische Leukämie – AML – im Kindes- und Jugendalter. *AWMF Online* (2019).
80. Kolb, H.-J. Graft-versus-leukemia effects of transplantation and donor lymphocytes. *Blood* **112**, 4371–4383 (2008).
81. Niewerth, D., Creutzig, U., Bierings, M. B. & Kaspers, G. J. L. A review on allogeneic stem cell transplantation for newly diagnosed pediatric acute myeloid leukemia. *Blood* **116**, 2205–2214 (2010).
82. Reinhardt, D., Von Neuhoff, C., Sander, A. & Creutzig, U. Prognostische Relevanz genetischer Aberrationen der akuten myeloischen Leukämie bei Kindern und Jugendlichen. *Klin. Pädiatr.* **224**, 372–376 (2012).
83. Sander, A. *et al.* Consequent and intensified relapse therapy improved survival in pediatric AML: results of relapse treatment in 379 patients of three consecutive AML-BFM trials. *Leukemia* **24**, 1422–1428 (2010).
84. Lonetti, A., Pession, A. & Masetti, R. Targeted Therapies for Pediatric AML: Gaps and Perspective. *Front. Pediatr.* **7**, 463 (2019).
85. Stone, R. M. *et al.* Midostaurin plus Chemotherapy for Acute Myeloid Leukemia with a *FLT3* Mutation. *N. Engl. J. Med.* **377**, 454–464 (2017).
86. Cooper, T. M. *et al.* A Phase I Study of Quizartinib Combined with Chemotherapy in Relapsed Childhood Leukemia: A Therapeutic Advances in Childhood Leukemia & Lymphoma (TACL) Study. *Clin. Cancer Res.* **22**, 4014–4022 (2016).
87. Johnson, D. B., Smalley, K. S. M. & Sosman, J. A. Molecular Pathways: Targeting NRAS in Melanoma and Acute Myelogenous Leukemia. *Clin. Cancer Res.* **20**, 4186–4192 (2014).
88. Place, A. E. *et al.* Phase I trial of the mTOR inhibitor everolimus in combination with multi-agent chemotherapy in relapsed childhood acute lymphoblastic leukemia. *Pediatr. Blood Cancer* **65**, e27062 (2018).
89. Pession, A., Lonetti, A., Bertuccio, S., Locatelli, F. & Masetti, R. Targeting Hedgehog pathway in pediatric acute myeloid leukemia: challenges and opportunities. *Expert Opin. Ther. Targets* **23**, 87–91 (2019).
90. Yaffe, M. B. Why geneticists stole cancer research even though cancer is primarily a signaling disease. *Sci. Signal.* **12**, eaaw3483 (2019).
91. Kurtz, S. E. *et al.* Molecularly targeted drug combinations demonstrate selective effectiveness for myeloid- and lymphoid-derived hematologic malignancies. *Proc. Natl. Acad. Sci.* **114**, E7554–E7563 (2017).
92. Spilker, M. E. *et al.* Found in Translation: Maximizing the Clinical Relevance of Nonclinical Oncology Studies. *Clin. Cancer Res.* **23**, 1080–1090 (2017).
93. Liu, Y., Sun, J. & Zhao, M. ONGene: A literature-based database for human oncogenes. *J. Genet. Genomics* **44**, 119–121 (2017).

94. Kurtz, S. E. *et al.* Dual inhibition of JAK1/2 kinases and BCL2: a promising therapeutic strategy for acute myeloid leukemia. *Leukemia* **32**, 2025–2028 (2018).
95. Chang, E. *et al.* The combination of FLT3 and DNA methyltransferase inhibition is synergistically cytotoxic to FLT3/ITD acute myeloid leukemia cells. *Leukemia* **30**, 1025–1032 (2016).
96. Cerami, E. G. *et al.* Pathway Commons, a web resource for biological pathway data. *Nucleic Acids Res.* **39**, D685–D690 (2011).
97. Cotto, K. C. *et al.* DGIdb 3.0: a redesign and expansion of the drug–gene interaction database. *Nucleic Acids Res.* **46**, D1068–D1073 (2018).
98. Tyner, J. W. *et al.* Functional genomic landscape of acute myeloid leukaemia. *Nature* **562**, 526–531 (2018).
99. Collins, S. The HL-60 promyelocytic leukemia cell line: proliferation, differentiation, and cellular oncogene expression. *Blood* **70**, 1233–1244 (1987).
100. Bosshart, H. & Heinzelmann, M. THP-1 cells as a model for human monocytes. *Ann. Transl. Med.* **4**, 438–438 (2016).
101. Quentmeier, H., Reinhardt, J., Zaborski, M. & Drexler, H. G. FLT3 mutations in acute myeloid leukemia cell lines. *Leukemia* **17**, 120–124 (2003).
102. Stroh, M., Duda, D. G., Takimoto, C. H., Yamazaki, S. & Vicini, P. Translation of Anticancer Efficacy From Nonclinical Models to the Clinic. *CPT Pharmacomet. Syst Pharmacol* **3**, e128 (2014).
103. Batchelor, H. K. & Marriott, J. F. Paediatric pharmacokinetics: key considerations: Paediatric pharmacokinetics. *Br. J. Clin. Pharmacol.* **79**, 395–404 (2015).
104. Lundholt, B. K., Scudder, K. M. & Pagliaro, L. A Simple Technique for Reducing Edge Effect in Cell-Based Assays. *J. Biomol. Screen.* **8**, 566–570 (2003).
105. Sebaugh, J. L. Guidelines for accurate EC50/IC50 estimation. *Pharm. Stat.* **10**, 128–134 (2011).
106. Chou, T.-C. & Talalay, P. Quantitative analysis of dose-effect relationships: the combined effects of multiple drugs or enzyme inhibitors. *Adv. Enzyme Regul.* **22**, 27–55 (1984).
107. Chou, T.-C. The combination index (CI < 1) as the definition of synergism and of synergy claims. *Synergy* **7**, 49–50 (2018).
108. Brenner, A. K. *et al.* The Capacity of Long-Term in Vitro Proliferation of Acute Myeloid Leukemia Cells Supported Only by Exogenous Cytokines Is Associated with a Patient Subset with Adverse Outcome. *Cancers* **11**, 73 (2019).
109. Pabst, C. *et al.* Identification of small molecules that support human leukemia stem cell activity ex vivo. *Nat. Methods* **11**, 436–442 (2014).
110. Hatfield, K. J., Reikvam, H. & Bruserud, Ø. Identification of a subset of patients with acute myeloid leukemia characterized by long-term *in vitro* proliferation and altered cell cycle regulation of the leukemic cells. *Expert Opin. Ther. Targets* **18**, 1237–1251 (2014).

111. Bhavanasi, D. *et al.* Signaling mechanisms that regulate ex vivo survival of human acute myeloid leukemia initiating cells. *Blood Cancer J.* **7**, 636 (2017).
112. Bruserud, Ø., Gjertsen, B. T., Foss, B. & Huang, T.-S. New Strategies in the Treatment of Acute Myelogenous Leukemia (AML): In Vitro Culture of AML Cells-The Present Use in Experimental Studies and the Possible Importance for Future Therapeutic Approaches. *Stem Cells* **19**, 1–11 (2001).
113. Ito, S. *et al.* Long term maintenance of myeloid leukemic stem cells cultured with unrelated human mesenchymal stromal cells. *Stem Cell Res.* **14**, 95–104 (2015).
114. van Gosliga, D. *et al.* Establishing long-term cultures with self-renewing acute myeloid leukemia stem/progenitor cells. *Exp. Hematol.* **35**, 1538–1549 (2007).
115. Bianco, J. E. R. *et al.* Characterization of a novel decellularized bone marrow scaffold as an inductive environment for hematopoietic stem cells. *Biomater. Sci.* **7**, 1516–1528 (2019).
116. Vu, L. P. *et al.* Functional screen of MSI2 interactors identifies an essential role for SYNCRIP in myeloid leukemia stem cells. *Nat. Genet.* **49**, 866–875 (2017).
117. Lehmann, C., Friess, T., Birzele, F., Kiialainen, A. & Dangl, M. Superior anti-tumor activity of the MDM2 antagonist idasanutlin and the Bcl-2 inhibitor venetoclax in p53 wild-type acute myeloid leukemia models. *J. Hematol. Oncol.J Hematol Oncol* **9**, 50 (2016).
118. Bryant, K. L. *et al.* Combination of ERK and autophagy inhibition as a treatment approach for pancreatic cancer. *Nat. Med.* **25**, 628–640 (2019).
119. Kang, C., Kim, C.-Y., Kim, H. S., Park, S.-P. & Chung, H.-M. The Bromodomain Inhibitor JQ1 Enhances the Responses to All- *trans* Retinoic Acid in HL-60 and MV4-11 Leukemia Cells. *Int. J. Stem Cells* **11**, 131–140 (2018).
120. Jha, S. *et al.* Dissecting Therapeutic Resistance to ERK Inhibition. *Mol. Cancer Ther.* **15**, 548–559 (2016).
121. Weisberg, E. *et al.* Evaluation of ERK as a therapeutic target in acute myelogenous leukemia. *Leukemia* **34**, 625–629 (2020).
122. Certo, M. *et al.* Mitochondria primed by death signals determine cellular addiction to antiapoptotic BCL-2 family members. *Cancer Cell* **9**, 351–365 (2006).
123. Merino, D. *et al.* BH3-Mimetic Drugs: Blazing the Trail for New Cancer Medicines. *Cancer Cell* **34**, 879–891 (2018).
124. Aldoss, I. *et al.* Efficacy of the combination of venetoclax and hypomethylating agents in relapsed/refractory acute myeloid leukemia. *Haematologica* **103**, e404–e407 (2018).
125. Kalliokoski, T., Kramer, C., Vulpetti, A. & Gedeck, P. Comparability of Mixed IC50 Data – A Statistical Analysis. *PLoS ONE* **8**, e61007 (2013).
126. Wickramasinghe, S., Porwit, A. & Erber, W. Normal bone marrow cells. in *Blood and Bone Marrow Pathology* 19–44 (Elsevier, 2011). doi:10.1016/B978-0-7020-3147-2.00002-X.

127. Naeim, F., Nagesh Rao, P., Song, S. X. & Phan, R. T. Principles of Immunophenotyping. in *Atlas of Hematopathology* 29–56 (Elsevier, 2018). doi:10.1016/B978-0-12-809843-1.00002-4.
128. Gorczyca, W. *et al.* Immunophenotypic Pattern of Myeloid Populations by Flow Cytometry Analysis. in *Methods in Cell Biology* vol. 103 221–266 (Elsevier, 2011).
129. Brenner, A. K. *et al.* Patients with acute myeloid leukemia can be subclassified based on the constitutive cytokine release of the leukemic cells; the possible clinical relevance and the importance of cellular iron metabolism. *Expert Opin. Ther. Targets* **21**, 357–369 (2017).
130. Dhami, S. P. S., Kappala, S. S., Thompson, A. & Szegezdi, E. Three-dimensional ex vivo co-culture models of the leukaemic bone marrow niche for functional drug testing. *Drug Discov. Today* **21**, 1464–1471 (2016).
131. Hatfield, K., Ryningen, A., Corbascio, M. & Bruserud, Ø. Microvascular endothelial cells increase proliferation and inhibit apoptosis of native human acute myelogenous leukemia blasts. *Int. J. Cancer* **119**, 2313–2321 (2006).
132. Sun, L. *et al.* GM-CSF Quantity Has a Selective Effect on Granulocytic vs. Monocytic Myeloid Development and Function. *Front. Immunol.* **9**, 1922 (2018).
133. Chao, M. P. *et al.* Human AML-iPSCs Reacquire Leukemic Properties after Differentiation and Model Clonal Variation of Disease. *Cell Stem Cell* **20**, 329-344.e7 (2017).
134. Van Overmeire, E. *et al.* M-CSF and GM-CSF Receptor Signaling Differentially Regulate Monocyte Maturation and Macrophage Polarization in the Tumor Microenvironment. *Cancer Res.* **76**, 35–42 (2016).
135. Keith, C. T., Borisy, A. A. & Stockwell, B. R. Multicomponent therapeutics for networked systems. *Nat. Rev. Drug Discov.* **4**, 71–78 (2005).
136. Palmer, A. C. & Sorger, P. K. Combination Cancer Therapy Can Confer Benefit via Patient-to-Patient Variability without Drug Additivity or Synergy. *Cell* **171**, 1678-1691.e13 (2017).
137. Tomska, K. *et al.* Drug-based perturbation screen uncovers synergistic drug combinations in Burkitt lymphoma. *Sci. Rep.* **8**, 12046 (2018).
138. Liston, D. R. & Davis, M. Clinically Relevant Concentrations of Anticancer Drugs: A Guide for Nonclinical Studies. *Clin. Cancer Res.* **23**, 3489–3498 (2017).
139. Tang, J. *et al.* Target Inhibition Networks: Predicting Selective Combinations of Druggable Targets to Block Cancer Survival Pathways. *PLoS Comput. Biol.* **9**, e1003226 (2013).
140. Bruserud, Ø., Gjertsen, B. T. & von Volkman, H. L. *In Vitro* Culture of Human Acute Myelogenous Leukemia (AML) Cells in Serum-Free Media: Studies of Native AML Blasts and AML Cell Lines. *J. Hematother. Stem Cell Res.* **9**, 923–932 (2000).
141. Bruserud, O., Frostad, S. & Foss, B. In Vitro Culture of Acute Myelogenous Leukemia Blasts: A Comparison of Four Different Culture Media. *J. Hematother.* **8**, 63–73 (1999).

142. Binder, S., Luciano, M. & Horejs-Hoeck, J. The cytokine network in acute myeloid leukemia (AML): A focus on pro- and anti-inflammatory mediators. *Cytokine Growth Factor Rev.* **43**, 8–15 (2018).

143. Niyongere, S. *et al.* Heterogeneous expression of cytokines accounts for clinical diversity and refines prognostication in CMML. *Leukemia* **33**, 205–216 (2019).

144. Ajayi, S. *et al.* Ruxolitinib. in *Small Molecules in Hematology* (ed. Martens, U. M.) vol. 212 119–132 (Springer International Publishing, 2018).

145. Aittomäki, S. & Pesu, M. Therapeutic Targeting of the JAK/STAT Pathway. *Basic Clin. Pharmacol. Toxicol.* **114**, 18–23 (2014).

146. Fernandez, E. *et al.* Factors and Mechanisms for Pharmacokinetic Differences between Pediatric Population and Adults. *Pharmaceutics* **3**, 53–72 (2011).

147. Sexauer, A. N. & Tasian, S. K. Targeting FLT3 Signaling in Childhood Acute Myeloid Leukemia. *Front. Pediatr.* **5**, 248 (2017).

148. Al-Lazikani, B., Banerji, U. & Workman, P. Combinatorial drug therapy for cancer in the post-genomic era. *Nat. Biotechnol.* **30**, 679–692 (2012).

149. Basu, A. *et al.* An Interactive Resource to Identify Cancer Genetic and Lineage Dependencies Targeted by Small Molecules. *Cell* **154**, 1151–1161 (2013).

150. Garnett, M. J. *et al.* Systematic identification of genomic markers of drug sensitivity in cancer cells. *Nature* **483**, 570–575 (2012).

151. Barretina, J. *et al.* The Cancer Cell Line Encyclopedia enables predictive modelling of anticancer drug sensitivity. *Nature* **483**, 603–607 (2012).

152. NCI DREAM Community *et al.* A community effort to assess and improve drug sensitivity prediction algorithms. *Nat. Biotechnol.* **32**, 1202–1212 (2014).

153. Behinaein, B., Rudie, K. & Sangrar, W. Petri Net Siphon Analysis and Graph Theoretic Measures for Identifying Combination Therapies in Cancer. *IEEE/ACM Trans. Comput. Biol. Bioinform.* **15**, 231–243 (2018).

154. Benard, B., Gentles, A. J., Köhnke, T., Majeti, R. & Thomas, D. Data mining for mutation-s pecific targets in acute myeloid leukemia. *Leukemia* **33**, 826–843 (2019).

155. Lo, Y.-C., Rensi, S. E., Torng, W. & Altman, R. B. Machine learning in chemoinformatics and drug discovery. *Drug Discov. Today* **23**, 1538–1546 (2018).